EFFECTS OF PRECIPITATION RECHARGE AND ARTIFICIAL DISCHARGE ON SALT WATER-FRESH WATER INTERFACE MOVEMENT IN SELÇUK SUB-BASIN: CLIMATIC INDICATIONS

A THESIS SUBMITTED TO
THE GRADUATE SCHOOL OF NATURAL AND APPLIED SCIENCES
OF
MIDDLE EAST TECHNICAL UNIVERSITY

BY

GÖKBEN AYKANAT

IN PARTIAL FULFILLMENT OF THE REQUIREMENTS
FOR
THE DEGREE OF MASTER OF SCIENCE
IN
GEOLOGICAL ENGINEERING

FEBRUARY 2011

Approval of the thesis:

EFFECTS OF PRECIPITATION RECHARGE AND ARTIFICIAL DISCHARGE ON SALT WATER-FRESH WATER INTERFACE MOVEMENT IN SELÇUK SUB-BASIN: CLIMATIC INDICATIONS

submitted by **GÖKBEN AYKANAT** in partial fulfillment of the requirements for the degree of **Master of Science in Geological Engineering Department, Middle East Technical University** by,

Prof. Dr. Canan Özgen _____
Dean, Graduate School of **Natural and Applied Sciences**

Prof. Dr. M. Zeki Çamur _____
Head of Department, **Geological Engineering**

Prof. Dr. M. Zeki Çamur
Supervisor, **Geological Engineering Dept., METU** _____

Examining Committee Members:

Prof. Dr. Hasan Yazıcıgil _____
Geological Engineering Dept., METU

Prof. Dr. M. Zeki Çamur _____
Geological Engineering Dept., METU

Prof. Dr. Nurkan Karahanoğlu _____
Geological Engineering Dept., METU

Prof. Dr. Serdar Bayarı _____
Hydrogeological Engineering Dept., HÜ

Dr. Koray K. Yılmaz _____
Geological Engineering Dept., METU

Date: 09.02.2011

I hereby declare that all information in this document has been obtained and presented in accordance with academic rules and ethical conduct. I also declare that, as required by these rules and conduct, I have fully cited and referenced all material and results that are not original to this work.

Name, Last name : Gökben AYKANAT

Signature :

ABSTRACT

EFFECTS OF PRECIPITATION RECHARGE AND ARTIFICIAL DISCHARGE ON SALT WATER-FRESH WATER INTERFACE MOVEMENT IN SELÇUK SUB-BASIN: CLIMATIC INDICATIONS

Aykanat, Gökben

M.Sc., Department of Geological Engineering

Supervisor: Prof. Dr. M. Zeki Çamur

February 2011, 108 pages

Fluctuations in temperature and precipitation amounts due to climate change influence recharge rate of groundwater. Any variations in the amount of precipitation recharge and artificial discharge directly affect groundwater level and so the salt water intrusion rate in the aquifers, which are in contact with sea water. The purpose of this study is to determine the overall historical precipitation recharge trend in Selçuk sub-basin and to detect whether there is a decrease or increase in recharge amounts due to climate change since 1100 BC. Besides, it covers assessing the future position of the salt water-fresh groundwater interface as a result of possible fluctuations in climate and artificial discharge. For this purpose, numerical density

dependent cross sectional groundwater flow with solute transport model was conducted using finite element approach. At first, current salt water-fresh water interface and artificial discharge related head changes in the aquifer were determined. Backward modeling was utilized to obtain concentration distribution in the year 1976 representing the last stage of the undisturbed period. Then, progradation of salt water-fresh water interface since 1100 BC to 1976 was modeled using calibrated parameters and current recharge value. As a result of sea-regression model simulations (1100 BC-1976) less degree of salt water intrusion than that of currently detected in the area was obtained. The result suggests that overall recharge amount in the last 3076 years must have been less than that of 1976. Moreover, future (2010-2099) position of the interface and head changes under the influence of both climate change and increasing water demand were determined. Future model simulations indicate that salt water-fresh water interface moves farther landward. However this movement is mostly due to increasing discharge amount rather than that of climatic changes.

Key words: Salt water intrusion, density dependent numerical modeling, Selçuk sub-basin, climate change

ÖZ

SELÇUK ALT-HAVZASINDAKİ YAĞIŞ BESLENİMİ VE YAPAY BOŞALIMIN TUZLU SU-YERALTI SUYU ARAYÜZEYİ HAREKETİNE ETKİLERİ: İKLİMSEL BELİRTİLER

Aykanat, Gökben

Yüksek Lisans, Jeoloji Mühendisliği Bölümü

Tez Yöneticisi: Prof. Dr. M. Zeki Çamur

Şubat 2011, 108 sayfa

Sıcaklık ve yağış miktarındaki iklim değişikliğine bağlı dalgalanmalar yeraltı suyunun beslenim oranını etkilemektedir. Yağış beslenimi ve yapay boşalım miktarındaki değişimler, yeraltı suyu seviyesine ve böylece deniz suyu ile temas halinde bulunan akiferlerdeki tuzlu su girişim oranına doğrudan tesir etmektedir. Bu çalışmanın amacı Selçuk alt-havzasındaki genel tarihsel yağış besleniminin eğilimini belirlemek ve MÖ 1100 den itibaren iklim değişikliğinden dolayı beslenim miktarında artış ya da azalış olup olmadığını saptamaktır. Ayrıca amaç, iklimdeki ve yapay boşalımdaki olabilecek dalgalanmalar sonucunda tuzlu su-yeraltı suyu arayüzeyinin gelecekteki konumunun incelenmesini kapsamaktadır. Bu sebeple,

sonlu eleman yaklaşımı kullanılarak sayısal yoğunluk-bağımlı kesitsel yer altı suyu akım ve iyon taşınım modeli geliştirilmiştir. İlk olarak, akiferdeki güncel tuzlu su-yer altı suyu arayüzeyi ve yapay boşalıma bağlı hidrolik yük değişimi belirlenmiştir. Bozulmamış sürecin son aşamasını temsil eden 1976 yılındaki konsantrasyon dağılımını elde etmek için ters modellemeden yararlanılmıştır. Sonra, kalibre edilmiş değişkenler ve güncel beslenim değeri kullanılarak MÖ 1100 den 1976 ya kadar tuzlu su-yer altı suyu arayüzeyinin ilerlemesi modellenmiştir. Regresyon (deniz gerilemesi) modeli simülasyonları sonucunda (MÖ 1100-1976) alanda günümüzde belirlenenden daha az derecede tuzlu su girişimi olmuş olması gerektiği belirlenmiştir. Bu sonuç son 3076 yıldaki genel beslenim miktarının 1976 dan daha az olması gerektiğine işaret etmektedir. Bunlara ek olarak, hem iklim değişimi hem de su talebindeki artışın etkisi altındaki arayüzeyin gelecekteki (2010-2099) durumu ve hidrolik yük değişimi belirlenmiştir. Gelecek model simülasyonu tuzlu su-yeraltı suyu arayüzeyinin karaya doğru daha fazla hareket edeceğini göstermiştir. Fakat bu hareket çoğunlukla iklimsel değişikliklerden ziyade artan boşalım miktarından dolayıdır.

Anahtar kelimeler: Tuzlu su girişimi, yoğunluk-bağımlı sayısal modelleme, Selçuk alt-havzası, iklim değişikliği

To the Chance of My Life,

My Family

ACKNOWLEDGMENTS

I would like to express my sincere gratitude to my supervisor Prof. Dr. M. Zeki Çamur for his guidance, criticism, advice and encouragements throughout this study.

I would like to express my very special thanks to my family members for their love before anything else; my father Hüsnü Aykanat for his full confidence and advice, my mother Malike Aykanat for her endless support, encouragements and being with me during sleepless nights, my brother Umut Aykanat for being in my life with his beautiful heart and my sister Bilge Aykanat for her endless patience, support and being my source of happiness.

I am thankful to my friend Ceren Bora for her support during this study and friendship in every part of my life, and my esteemed colleague Tuğba Lale for her encouragements and help during the working life.

Finally, I wish to express my deepest gratitude to the chance of my life, Emre Avcıoğlu, for his endless care, love and belief in me. Without his support, encouragement and guidance this work would not have been completed. His presence makes the life livable.

TABLE OF CONTENTS

ABSTRACT iv

ÖZ vi

ACKNOWLEDGMENTS ix

TABLE OF CONTENTS x

LIST OF TABLES xv

LIST OF FIGURES xvii

CHAPTERS

1. INTRODUCTION 1

1.1. Purpose and Scope 1

2. LITERATURE REVIEW 5

2.1. Climate Change 5

2.1.1. Effects of Climate Change on Groundwater Recharge 8

2.2. Salt Water Intrusion 11

2.2.1. Sharp Interface Approach 11

2.2.2. Disperse Interface Approach 14

3. STUDY AREA 17

3.1. Physiography 17

3.2. Climate 18
3.3. Geomorphology 23
3.4. Geology 24
3.4.1. Regional Geology 24
3.4.2. Local Geology 25
3.5. Hydrogeology 31
3.5.1. Water Bearing Units 31
3.5.2. Hydraulic Parameters 32
3.5.3. Recharge 34
3.5.4. Discharge 34
3.6. Hydrochemistry 35
4. MODELING AND METHODOLOGY 39
4.1. Modeling 39
4.1.1. Introduction 39
4.1.2. Model Development Processes 40
4.1.2.1. Hydrogeologic Characterization 40
4.1.2.2. Model Conceptualization 41
4.1.2.3. Model Selection 41
4.1.2.4. Model Design 42
4.1.2.5. Model Calibration 43

4.1.2.6. Sensitivity Analysis 44
4.1.2.7. Presentation of Results 44
4.1.3. Numerical Modeling of Density Dependent Groundwater Flow and Solute Transport 44
4.2. Methodology 48
4.2.1. Pre-Pumping Period Areal Model 48
4.2.2. Pre-Pumping Period Cross Sectional Model 49
4.2.3. Pumping Period Cross Sectional Model 49
4.2.4. Sea-Regression Period Cross Sectional Model 49
4.2.5. Climate Controlled Future Period Cross Sectional Model 49
5. AREAL FLOW MODEL 51
5.1. Conceptual Model 51
5.2. Discretization and Boundary Conditions 51
5.3. Model Parameters 52
5.4. Calibration and Results 52
6. CROSS SECTIONAL SATURATED FLOW MODELS 54
6.1. Conceptual Model 55
6.2. Discretization and Boundary Conditions 56
6.3. Model Parameters 57
6.4. Pre-Pumping Period Cross Sectional Model 58

6.4.1. Initial conditions 59
6.4.2. Calibration 59
6.4.3. Results 61
6.5. Pumping Period Cross Sectional Model 63
6.5.1. Initial Conditions 64
6.5.2. Calibration 64
6.5.3. Results 66
6.6. Sea-Regression Period Cross Sectional Model 70
6.6.1. Model Parameters 71
6.6.2. Discretization and Boundary Conditions 72
6.6.3. Initial Conditions 73
6.6.4. Results 74
6.6.5. Sensitivity Analysis 78
6.7. Climate-Controlled Future Period Cross Sectional Model 83
6.7.1. Model Parameters 84
6.7.1.1. Recharge 84
6.7.1.2. Discharge 86
6.7.2. Initial Conditions 87
6.7.3. Results 87
7. RESULTS AND DISCUSSION 93

8. CONCLUSIONS AND RECOMMENDATIONS 99

8.1. Conclusions 99

8.2. Recommendations 100

REFERENCES 102

LIST OF TABLES

TABLES

Table 3. 1. Well data of Selçuk Sub-basin 33
Table 5. 1. Observed and simulated head values of the areal model 53
Table 6. 1. Parameters used in cross sectional models 58
Table 6. 2. Calibrated and observed pressure and head values 59
Table 6. 3. Discharge values in different time periods 64
Table 6. 4. Observed and calculated head and pressure values in 2002 of the pumping period 65
Table 6. 5. Head values of steady state and 2009 in meters 67
Table 6. 6. Precipitation recharge amounts for the sea-regression period models (for domain see Figure 6.9) 72
Table 6. 7. Average progradation velocity of shoreline for each period 74
Table 6. 8. Head values of pre-pumping period and sea-regression period in meters 74
Table 6. 9. Minimum and maximum values of permeability and recharge in Selçuk sub-basin. 79
Table 6. 10. Observed and calculated head values (meter) for Cases I, II, III and IV. 79
Table 6. 11. Prediction of the IPCC models for future changes in temperature and precipitation (D,J,F,M,A,M,J,J,A,S,O and N refer to the first letters of the months) 83
Table 6. 12. Estimated mean future precipitation and temperature values for A1FI model 85
Table 6. 13. Estimated mean future precipitation and temperature values for B1 model 85
Table 6. 14. Annual recharge values for three future time periods 86

Table 6. 15. Discharge value for time periods 86
Table 6. 16. Comparison of head values in 2009 and in 2099 for both A1FI and B1 models (in meters). 87

LIST OF FIGURES

FIGURES

Figure 1. 1. Location map of Küçük Menderes River Basin and Selçuk Sub-basin... 4
Figure 2. 1. Estimate of Earth's annual global mean energy balance (Wm^{-2})(Kiehl and Trenberth, 1997)..... 6
Figure 2. 2. Hydrostatic condition of the Ghyben-Herzberg relation 12
Figure 2. 3. Flow pattern near a beach (modified from Glover, 1959). 14
Figure 2. 4. Circulation of salt water from the sea to the zone of diffusion and back to the sea (Cooper, 1959). 15
Figure 3. 1.Elevation map of the Selçuk sub-basin (modified from Yazıcıgil et al, 2000a)..... 17
Figure 3. 2. Average (1964-2009) monthly temperature values in Selçuk station 19
Figure 3. 3. Annual (1964-2009) temperature values in Selçuk station..... 19
Figure 3. 4. Average (1964-2009) monthly precipitation values in Selçuk station ... 20
Figure 3. 5. Annual (1964-2009) precipitation values in Selçuk station 21
Figure 3. 6. Average (1964-2009) monthly evaporation values in Selçuk station..... 22
Figure 3. 7. Average (1964-2006) monthly relative humidity values in Selçuk station 23
Figure 3. 8. Geomorphological map of the Küçük Menderes River delta (Gökçen et al., 1990)..... 24
Figure 3. 9. Geological map of Küçük Menderes River Basin (Yazıcıgil et al.,2000b) 27
Figure 3. 10. Generalized columnar section of Küçük Menderes River Basin (after Yazıcıgil et al.,2000b)..... 28
Figure 3. 11. Geological map of Selçuk Sub-basin (after Yazıcıgil et al.,2000b) 29

Figure 3. 12. Geological cross sections along A-A' and B-B' (after Yazıcıgil et al.,2000b) 30
Figure 3. 13. Locations of the wells in Selçuk Sub-basin 31
Figure 3. 14. Discharge for irrigation need per km^2 in Selçuk Sub-basin (Nippon, 1999) 35
Figure 3. 15. Electrical conductivity (EC) measurements of 2002 in wells 54131 and 54132 (Hassan, 2004) 37
Figure 3. 16. Total dissolved solids (TDS) estimated from EC measurements of 2002 in well 54131 38
Figure 5. 1. Discretization and boundary conditions of the areal model 52
Figure 5. 2. Steady state groundwater pressure distribution in the study area 53
Figure 6. 1. Position of the cross sectional line 54
Figure 6. 2. Discretization and boundary conditions of cross sectional model 57
Figure 6. 3. Comparison of the areal and pre-pumping model head values along the cross section line 61
Figure 6. 4. Pressure distribution in the pre-pumping period 62
Figure 6. 5. Concentration distribution in the pre-pumping period 62
Figure 6. 6. Observed versus simulated concentrations in well 54131 for the year of 2002 in the pumping period 66
Figure 6. 7. Concentration distribution of the pumping period from 1976 to 1990 [a) 1976-1977, b) 1978-1988, c) 1989-1990] 68
Figure 6. 8. Concentration distribution of the pumping period from 1991 to 2009 [d) 1991-2002 and e) 2003-2009] 69
Figure 6. 9. Locations of the shorelines used in the sea-regression period model runs (modified from Gökçen et al.,1990) 71
Figure 6. 10. Boundary conditions for the period of pre-1100 BC 73
Figure 6. 11. Salt water-fresh water interface change from 1100 BC to 100 AD [a) pre-1100 BC, b) 1100 BC-100 BC, c) 100 BC-100 AD] 76

Figure 6. 12. Salt water-fresh water interface change from 100 AD to 1976 [d) 100 AD-300 AD and e) 300 AD-1976]..... 77
Figure 6. 13. Comparison of TDS values obtained from the sea-regression and pre-pumping period runs at the location of well 54131..... 78
Figure 6. 14. Sea-regression period result in 1976 for Case II (min recharge-max permeability) 81
Figure 6. 15. Comparison of TDS values of Case II with those of estimated in 1976 at the location of well 54131. 81
Figure 6. 16. Sea-regression period result in 1976 for Case IV (max recharge-max permeability) 82
Figure 6. 17. Comparison of TDS values of Case IV with those of estimated in 1976 at the location of well 54131..... 82
Figure 6. 18. Average (1964-1990) precipitation and temperature data of Selçuk Sub-basin. 84
Figure 6. 19. Concentration distribution at the end of the period 2010-2039 [a) A1FI model and b) B1 model]..... 88
Figure 6. 20. Concentration distribution at the end of the period 2039-2069 [a) A1FI model and b) B1 model]..... 89
Figure 6. 21. Concentration distribution at the end of the period 2069-2099 [a) A1FI model and b) B1 model]..... 90
Figure 6. 22. Concentration (kg/kg) distribution in pumping areas of Cooperative I and II according to A1FI model 91
Figure 6. 23. Concentration (kg/kg) distribution in pumping areas of Cooperative I and II according to B1 model..... 92
Figure 7. 1. Reconstructed April-June precipitation totals and June-August temperature anomalies (Büntgen et al., 2011) 97

CHAPTER 1

INTRODUCTION

Groundwater is the major source of fresh water throughout the world. It mainly supplies water for domestic, agricultural and industrial needs. Therefore, any variations in the demand for groundwater due to population growth, increase in agricultural and industrial activities can affect available groundwater amount. However, groundwater amount is not only affected by the increase in demand but also affected by factors that decrease groundwater resources such as climate change. Contamination of groundwater resources is another reason that limits the availability.

Climate change and its expected impacts on the Earth and consequently on human life have become the main concern of the scientists lately. Lots of researches have been conducted to predict both the trend of the climate change and its possible effects on the Earth. One of the effects of the climate change is on groundwater recharge. Global changes in the temperature and precipitation amounts directly influence the recharge rate. Although groundwater is the major source of fresh water in the world, there have been few researches on the potential effects of climate change on it.

1.1. Purpose and Scope

The purpose of this study is to determine the overall historical recharge trend (since 1100 BC) in Selçuk sub-basin and to detect whether there is a decrease or increase in recharge amounts due to climate change since then. Besides, it covers assessing the

future position of the salt water-fresh water interface as a result of possible fluctuations in climate and artificial discharge.

For this purpose, Selçuk sub-basin, which is one of the sub-basins of Küçük Menderes River Basin, was selected as the study area. Küçük Menderes River Basin is located in the Aegean Region in western Turkey. It is bounded by mountains at north, south and east and Aegean Sea at west. It has four sub-basins called Bayındır-Torbalı, Ödemiş-Tire, Kiraz and Selçuk.

Selçuk sub-basin is located in the southwest part of the Küçük Menderes River Basin, in provincial boundaries of İzmir. The sub-basin is surrounded by Aegean Sea in southwest and mountains in other directions. Selçuk sub-basin is situated between 4197000-420700 North latitudes and 522000-536000 East longitudes (Figure 1.1).

The western Anatolia is exposed to the progradational processes since the end of the last Glacial Period over large distances (Erinç, 1978). The aquifer of Selçuk Sub-basin formed during this process is in contact with the sea water since the beginning of the formation. Recent findings indicate that a salt water intrusion problem is present in the western side of the aquifer (Yazıcıgil et al., 2000a, Hassan, 2004, and Çamur and Yazıcıgil, 2005).

Scope of this study covers following topics:

- Determination of the steady state head distribution of the aquifer using two dimensional areal flow model.
- Determination of the salt water-fresh water interface in the aquifer at the end of the pre-pumping, undisturbed, period (pre-1976)
- Determination of the salt water-fresh water interface and artificial discharge related head changes in the aquifer for the pumping period (1976-2009)
- Prediction of the progradation of salt water-fresh water interface since 1100 BC to 1976 (end of pre-pumping period)

- Prediction of the future (2010-2099) position of the interface under the influence of both climate change and increasing water demand

using a density dependent cross sectional groundwater flow with solute transport model.

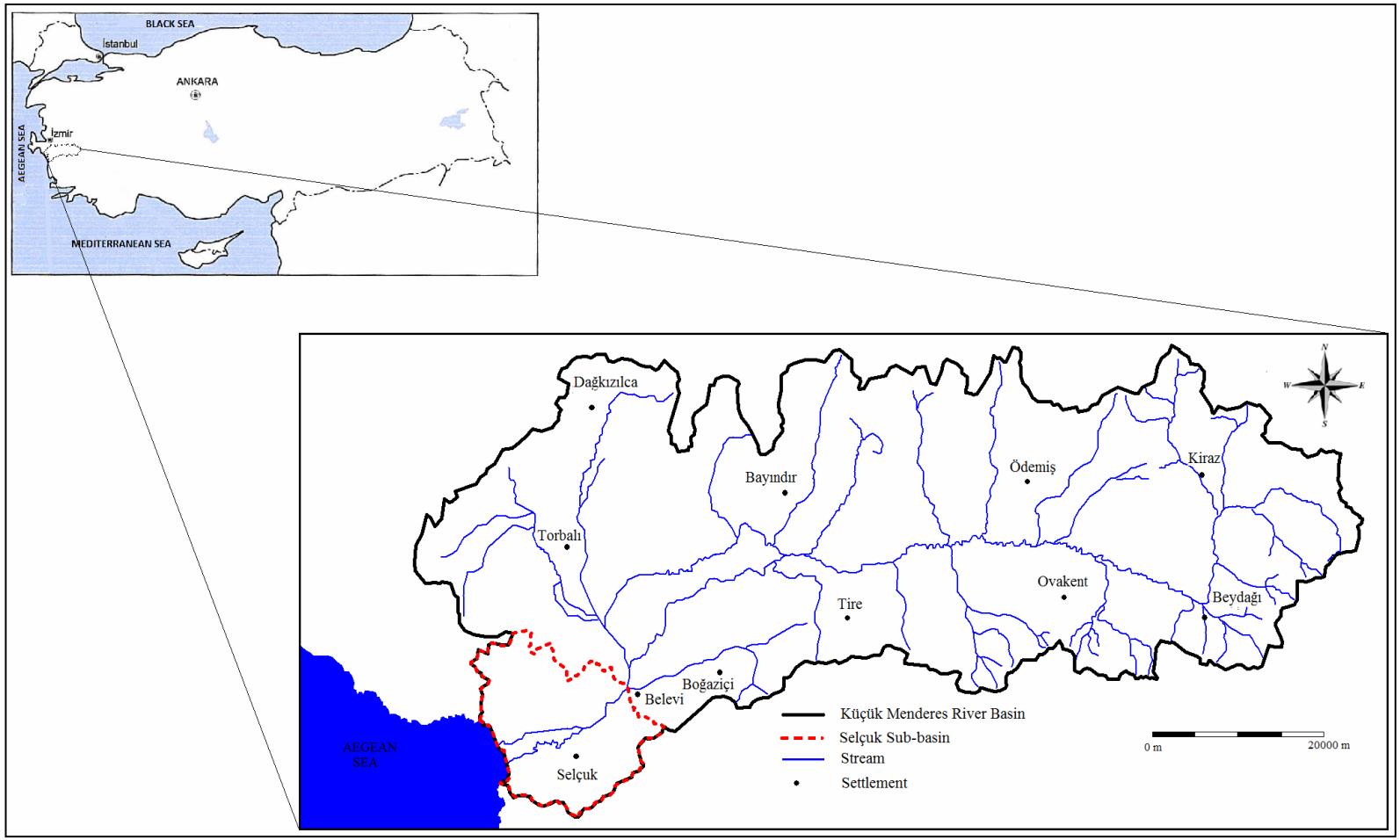

Figure 1. 1. Location map of Küçük Menderes River Basin and Selçuk Sub-basin

CHAPTER 2

LITERATURE REVIEW

2.1. Climate Change

Climate change is defined as “statistically significant variation in either the mean state of the climate or in its variability, persisting for an extended period (typically decades or longer)” (IPCC, Intergovernmental Panel on Climate Change, 2001). The energy for weather and climate comes from the Sun. This solar radiation is received by the Earth. About a third of the sunlight that reaches the top of the atmosphere is reflected back to the space and the rest of it is reflected by different components of the climate system such as clouds, small particles in the atmosphere, ocean, ice, land and biota. The energy absorbed from solar radiation is balanced by outgoing radiation from the Earth and atmosphere. This terrestrial radiation takes the form of long-wave invisible infrared energy. According to IPCC report (2001) climate can be affected by any factor that changes the radiation received from the Sun or lost to the space, or that alters the redistribution of energy within the atmosphere or between the atmosphere, land, and ocean (Figure 2.1).

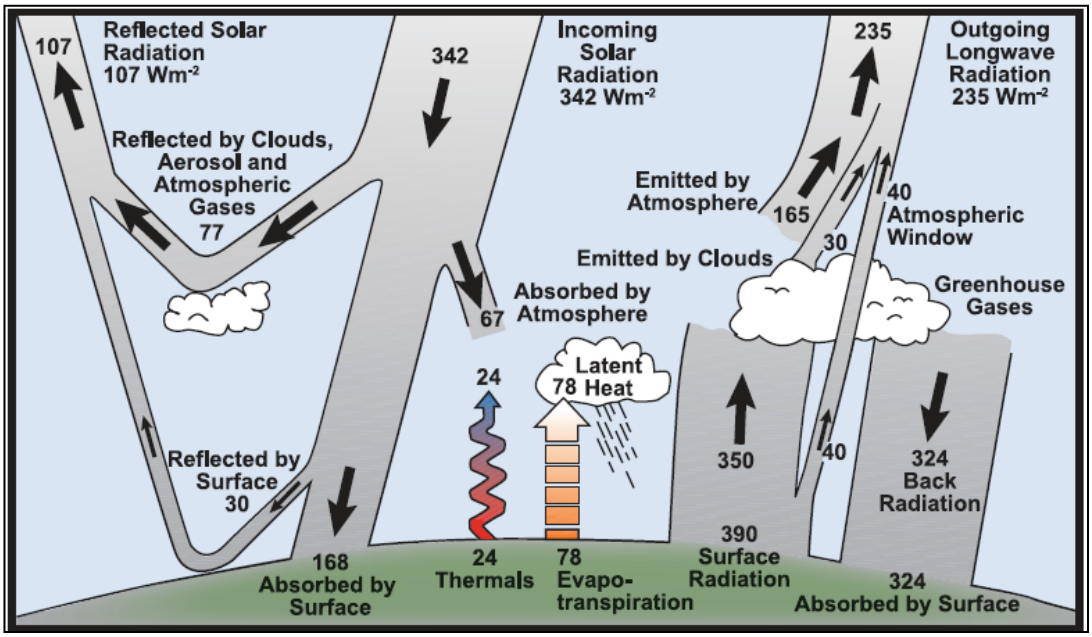

Figure 2. 1. Estimate of Earth's annual global mean energy balance (Wm^{-2})(Kiehl and Trenberth, 1997)

There are several factors that are responsible for the climate change. One of these factors is change in the amount of seasonal distribution of solar radiation reaching to the surface due to the orbital changes of the Earth. Milankovitch, who is an astronomer, mentioned about the changes in Earth's eccentric orbit and periodic variations both in inclination of the Earth's axis and in its axis of rotation. He attempted to explain regular cycle of cold periods during Pleistocene using these variations (Behringer, 2010). Moreover, Sun's output energy is effective in climate change. It varies by small amounts (0.1 %) over Sun's 11-year activity cycle (National Research Council, 1994). These variations cause increase or decrease in Earth's climate. Besides, in the seventeenth century, the relation between heat balance and sunspots (huge magnetic storms on Sun's surface) were revealed by telescopes: a reduction or absence of sunspots generally went with the cooling periods on earth (Behringer, 2010).

Another factor that affects climate change is plate tectonics. Behringer (2010) has also mentioned that plate tectonics play an important role in the genesis of ice ages. Early continental drift caused changes in ocean currents and in wind direction and precipitation patterns due to the formation of mountains. These processes also affected sea levels and land to water ratio. Moreover, when the land masses reach to the poles, they prevent the flow of sea water at these coldest places and thus ice is formed. The snow and ice cover lead to reflection of more sunlight and to increase in cooling.

Variations in Earth's reflectivity also influence climate change. The Earth's reflectivity mainly changes due to the variations in cloudiness, snow and ice cover, vegetation cover and land use. For example, if a snow cover melts, reflectivity of the surface decreases and more sunlight is absorbed by the ground, so the temperature tends to increase (http://www.aph.gov.au).

Volcanic eruptions also induce climate change. When large quantities of gases and particles reach to the stratosphere, climate is affected over great distances because these small particles, called aerosols, can reflect and absorb radiation.

Changes in the temperature of the Earth's surface can cause variations in ocean currents. These variations can bring about important changes in climate from region to region, because ocean currents directly affect the distribution of heat around the Earth.

The other effective factor is greenhouse gases. Some gases, such as carbon dioxide, water vapor, methane, chlorofluorocarbon and nitrogen dioxide, are able to change the energy balance of the Earth by absorbing long-wave radiation emitted from the Earth. Re-emission of long-wave radiation back to the Earth's surface increases quantity of heat energy. As a result, a reduced proportion of carbon dioxide causes cooling while an increased proportion warming (Behringer, 2010).

Lastly, it is stated by IPCC (1990) that, the climate has its own natural variability on all timescales and changes occur without any external influence.

2.1.1. Effects of Climate Change on Groundwater Recharge

Groundwater is the major source of fresh water. It plays a vital role in drinking water and agriculture. Therefore, any effect of climate change on groundwater is important. Groundwater will less directly and more slowly impacted by climate change than surface waters. This is due to the fact that surface waters can be resupplied in a shorter time and reflection of drought and floods are quickly seen. However, groundwater will be affected much slower. Only after a long time period of droughts will show decreasing trend in groundwater level (BGR, 2008). Therefore, prolonged observations are needed.

Climate change will influence groundwater recharge rates, i.e., the renewable groundwater resource and groundwater levels (Cruz et al., 2007). Localized groundwater recharge can occur from discrete bodies of surface water. Over large areas of land, it takes place if infiltration of precipitation through the soil can percolate beyond the reach of evapotranspiration (Peck et al., 1988). Therefore, any change in these parameters due to climate change will affect recharge. There are several predictions about the effects of climate change on recharge.

Hardy (2003) mentioned that warming will accelerate oceanic evaporation and thus it will increase average of global precipitation. He claimed that regional and seasonal changes may occur, so that in higher latitudes large increases in precipitation, soil moisture and runoff will be seen due to the moist air penetration, except summer, and precipitation will decrease at lower latitudes (5^0-30^0).

According to BGR (Federal Institute for Geosciences and Natural Resources, 2008) report, increase in rainfall may decrease groundwater recharge in humid areas due to the exceeded infiltration capacity of soil while heavy rains and thus, surface runoff may increase. However in semi-arid and arid areas increased rainfall may increase

recharge because only high-intensity rainfalls can infiltrate fast enough before evaporating. Direct infiltration of precipitation and dissolution channels may replenish bedrock aquifers and alluvial aquifers may mainly recharged by floods in semi-arid areas (Al-Sefry et al., 2004).

Furthermore, Grabrecht et al. (2006) stated that gradual warming because of the long-term climate change will increase evapotranspiration. It is mentioned in BGR (2008) that higher temperatures will cause higher evaporation and plant transpiration rate and thus, soils will dry. This will lead to higher losses of soil moisture and groundwater recharge in hot and arid areas.

Intergovernmental Panel on Climate Change (Cruz et al., 2007) examined the effects of climate change for each continent and reported some assumptions about future trends. In climate controlled future period part of this study, projections of IPCC on possible increase in surface air temperature and percent change in precipitation, which are area-averaged and seasonal, in West Asia were used. Two models, namely SRES (Special Report on Emission Scenarios) A1FI (high future emission trajectory) and B1 (low future emission trajectory) were published from IPCC. Precipitation and temperature values for the periods 2010-2039, 2040-2069 and 2070-2099 were predicted with respect to data obtained between the years 1961 and 1990 (Table 2.1). According to this data, projections of temperature for the 21st century that are based on Atmosphere-Ocean General Circulation Models show a notable increase in warming over the temperature observed in the 20th century. Moreover, seasonal decrease and increases in precipitation for the 21st century varies in different places.

Table 2.1. Projected changes in surface air temperature and precipitation for sub-regions of Asia (Cruz et al. 2007)

Sub-regions	Season	2010 to 2039				2040 to 2069				2070 to 2099			
		Temperature °C		Precipitation %		Temperature °C		Precipitation %		Temperature °C		Precipitation %	
		A1FI	B1	A1FI	B1	A1FI	B1	A1FI	B1	A1FI	B1	A1FI	B1
North	DJF	2.94	2.69	16	14	6.65	4.25	35	22	10.45	5.99	59	29
Asia	MAM	1.69	2.02	10	10	4.96	3.54	25	19	8.32	4.69	43	25
(50.0N-67.5N;	JJA	1.69	1.88	4	6	4.20	3.13	9	8	6.94	4.00	15	10
40.0E-170.0W)	SON	2.24	2.15	7	7	5.30	3.68	14	11	8.29	4.98	25	15
Central	DJF	1.82	1.52	5	1	3.93	2.60	8	4	6.22	3.44	10	6
Asia	MAM	1.53	1.52	3	-2	3.71	2.58	0	-2	6.24	3.42	-11	-10
(30N-50N;	JJA	1.86	1.89	1	-5	4.42	3.12	-7	-4	7.50	4.10	-13	-7
40E-75E)	SON	1.72	1.54	4	0	3.96	2.74	3	0	6.44	3.72	1	0
West	DJF	1.26	1.06	-3	-4	3.1	2.0	-3	-5	5.1	2.8	-11	-4
Asia	MAM	1.29	1.24	-2	-8	3.2	2.2	-8	-9	5.6	3.0	-25	-11
(12N-42N;	JJA	1.55	1.53	13	5	3.7	2.5	13	20	6.3	2.7	32	13
27E-63E)	SON	1.48	1.35	18	13	3.6	2.2	27	29	5.7	3.2	52	25
Tibetan	DJF	2.05	1.60	14	10	4.44	2.97	21	14	7.62	4.09	31	18
Plateau	MAM	2.00	1.71	7	6	4.42	2.92	15	10	7.35	3.95	19	14
(30N-50N;	JJA	1.74	1.72	4	4	3.74	2.92	6	8	7.20	3.94	9	7
75E-100E)	SON	1.58	1.49	6	6	3.93	2.74	7	5	6.77	3.73	12	7
East	DJF	1.82	1.50	6	5	4.18	2.81	13	10	6.95	3.88	21	15
Asia	MAM	1.61	1.50	2	2	3.81	2.67	9	7	6.41	3.69	15	10
(20N-50N;	JJA	1.35	1.31	2	3	3.18	2.43	8	5	5.48	3.00	14	8
100E-150E)	SON	1.31	1.24	0	1	3.16	2.24	4	2	5.51	3.04	11	4
South	DJF	1.17	1.11	-3	4	3.16	1.97	0	0	5.44	2.93	-16	-6
Asia	MAM	1.18	1.07	7	8	2.97	1.81	26	24	5.22	2.71	31	20
(5N-30N;	JJA	0.54	0.55	5	7	1.71	0.88	13	11	3.14	1.56	26	15
65E-100E)	SON	0.78	0.83	1	3	2.41	1.49	8	6	4.19	2.17	26	10
South-East	DJF	0.86	0.72	-1	1	2.25	1.32	2	4	3.92	2.02	6	4
Asia	MAM	0.92	0.80	0	0	2.32	1.34	3	3	3.83	2.04	12	5
(10S-20N;	JJA	0.83	0.74	-1	0	2.13	1.30	0	1	3.61	1.87	7	1
100E-150E)	SON	0.85	0.75	-2	0	1.32	1.32	-1	1	3.72	1.90	7	2

2.2. Salt Water Intrusion

Salt water intrusion is a special case of groundwater contamination. It happens due to the movement of saline water into fresh water aquifers. Salt water intrusion essentially occurs in all coastal aquifers, where fresh water and sea water are in a hydraulic continuity. When fresh water level drops due to any reasons a resulting decrease in hydrostatic pressure occurs. This causes intrusion of sea water into fresh water in the aquifer.

There are two types of modeling approaches which have been used to represent the salt water intrusion. The first approach claims that a sharp interface exists between salt water and fresh water. The other approach is based on the presence of a transition zone of mixed salt and fresh water.

2.2.1. Sharp Interface Approach

According to this approach fresh water and salt water are two completely immiscible fluids. Therefore an abrupt interface exists between them. There is no transition zone between them.

The first approximation about the depth of the salt water in coastal aquifers was developed by two independent investigators; Ghyben (1989) and Herzberg (1901). They determined the relationship between depth to sea water below sea level in a coastal aquifer and the height of fresh water above sea level (Figure 2.2). The analytical explanation of this principle is known as Ghyben-Herzberg formula.

$$z = \frac{\rho_f}{\rho_s - \rho_f} h_f \tag{2.1}$$

where;

z is depth to the interface below mean sea level

h_f is water table elevation above mean sea level

ρ_f is fresh water density = 1000 kg/m^3

ρ_s is salt water density = 1025 kg/m^3

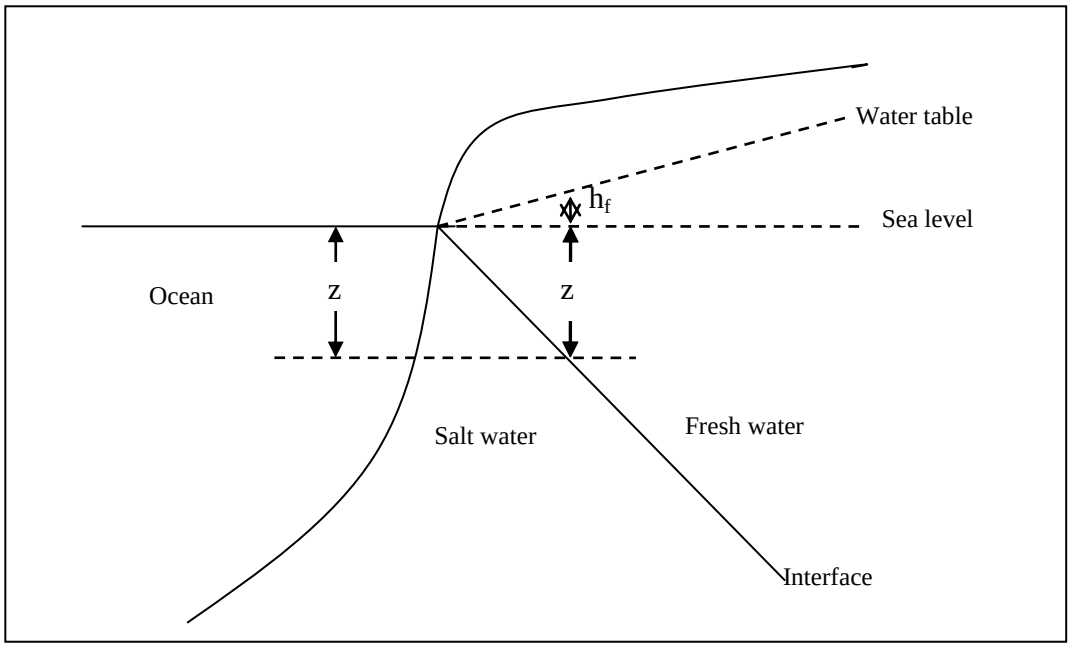

Figure 2. 2. Hydrostatic condition of the Ghyben-Herzberg relation

Although the difference in densities of fresh and salt water is small, this equation infers that there is a 40 m of fresh water below sea level for every meter of fresh water above sea level.

$$z = 40h_f \tag{2.2}$$

Because in this approach there is no discharge from the fresh water to the sea, another approach is demonstrated by Glover (1959). It is found by Glover that, under steady flow conditions, a sharp interface is formed between fresh and salt water. Because salt water has greater density, along the interface the pressure of the static salt water is counterbalanced by the pressures that drive the fresh water seaward. The

fresh water escapes through a gap between this interface and the shoreline (Figure 2.3). Increase in the fresh water flow widens the gap. The interface between the fresh water and sea water was plotted using following expression.

$$z^2 = \frac{2Q'x\rho_f}{K(\rho_s-\rho_f)} + \left[\frac{Q'\rho_f}{K(\rho_s-\rho_f)}\right]^2 \quad (2.3)$$

where;

z is the depth below sea level to the interface

x is the distance measured positive inland from the shoreline

Q' is fresh water flow per unit length of shoreline

K is hydraulic conductivity

The width of the gap, x_o, through which the fresh water escapes to the sea was formulated as seen below;

$$x_0 = -\frac{Q'}{2K(\rho_s-\rho_f)} \quad (2.4)$$

Moreover, Henry (1959) derived theoretical equations for the shape and location of the interface, boundary velocities and several boundary conditions.

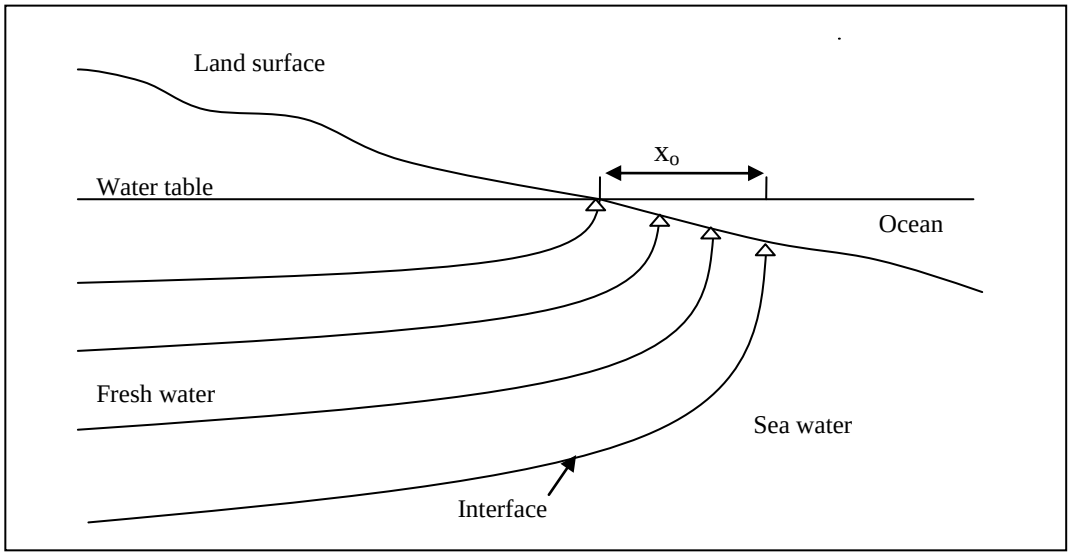

Figure 2. 3. Flow pattern near a beach (modified from Glover, 1959).

2.2.2. Disperse Interface Approach

Salt water and fresh water are essentially miscible fluids. Thus, contact zone between these two fluids becomes a transition zone caused by hydrodynamic dispersion (see Figure 2.4). Density of the mixed water changes from density of fresh water to density of sea water (Bear, Verruijit, 1987).

A hypothesis was developed by Cooper (1959) to state the mixing zone and continuous sea water circulations observed in field studies. He suggested that salt water is not static where zone of diffusion exists. He assumed that salt water flows in a cycle from seafloor into the zone of diffusion in a coastal aquifer and back to the sea (Figure 2.4).

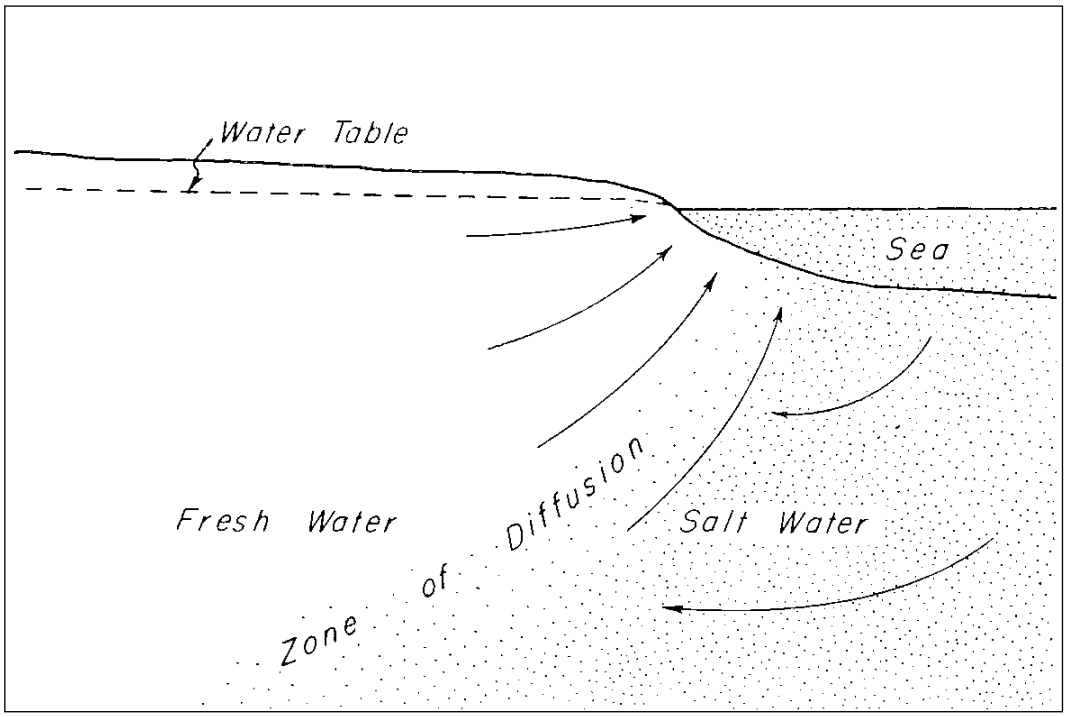

Figure 2. 4. Circulation of salt water from the sea to the zone of diffusion and back to the sea (Cooper, 1959).

Kohout (1964) studied Biscayne aquifer of the Miami; Florida. He concluded that as fresh water head of the aquifer is high after heavy recharge, water of the aquifer moves seaward expelling salt water from the aquifer. When head decreases, salt water in the lower part of the aquifer flows inland into the zone of diffusion. Then it moves upward and returns to the sea.

As mentioned by Reilly et al. (1985), since 1965 number of papers on salt water intrusion has increased greatly and specialized topics were dealt with. Two dimensional cross sectional analysis, two dimensional areal analysis, three dimensional analysis, upconing applications and numerical methods were performed on salt water intrusion during these studies.

Numerical salt water intrusion models have been developed for areal and cross sectional simulations. Voss (1984) developed SUTRA that models movement of the

fluid and solute or energy transport in a subsurface environment. Merritt (1994) constructed groundwater flow model using the SWIP code. Koch and Zhang (1998) modeled saltwater seepage from coastal brackish channel in Florida. Voss and Koch (2001) simulated saltwater upconing due to groundwater pumping in Germany. SEAWAT-2000 model was developed for the simulation of three-dimensional, variable density, transient groundwater flow in porous media by Guo and Langevin (2002).

CHAPTER 3

STUDY AREA

3.1. Physiography

Selçuk sub-basin is one of the sub-basins of Küçük Menderes River Basin. It is surrounded by Aegean Sea in the southwest and mountains in other directions. The relief map of the study area is given in Figure 3.1. The elevation in the area changes between 0 and 500 meters. The sub-basin is connected to the other sub-basins by a narrow passage passing from the northeast part of the sub-basin trough Belevi. The main drainage system in Selçuk sub-basin is Küçük Menderes River.

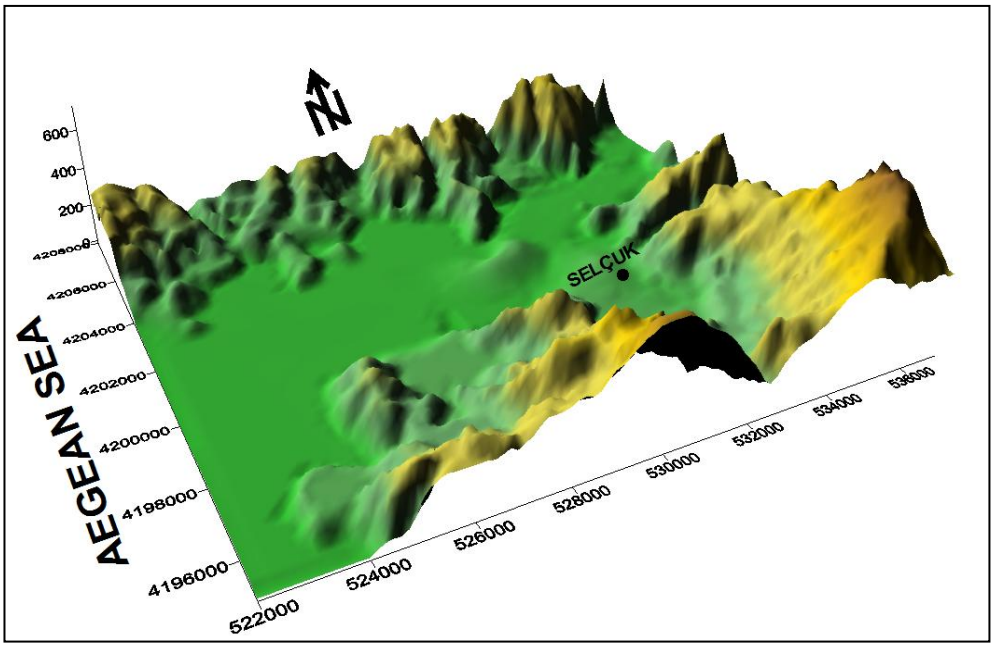

Figure 3. 1.Elevation map of the Selçuk sub-basin (modified from Yazıcıgil et al, 2000a)

3.2. Climate

In the study area typical characteristics of Aegean (Mediterranean) climate is seen. It is rainy and mild in winter and dry and hot in summer. Meteorological stations in and around Küçük Menderes River Basin belonging to Turkish State Meteorological Service measure parameters such as precipitation, temperature, evaporation and relative humidity. There are 10 meteorological stations in Küçük Menderes River Basin including Selçuk meteorological station, which is located in the study area.

According to the meteorological measurements obtained from Selçuk meteorological station between the years of 1964 and 2009, averages of temperature, precipitation, evaporation and humidity values are 16.50 ^{o}C , 689.19 mm, 113.21 mm, 60.81 %, respectively.

Monthly average temperature values obtained from Selçuk station for the years of 1964-2009 are illustrated in Figure 3.2. The maximum average temperature value is observed in July, while the minimum average temperature is observed in January. Monthly average temperature values from May to September are above the annual mean value. Annual temperature distribution between 1964 and 2009 is shown in Figure 3.3. Temperature exhibits increasing and decreasing cycling patterns at each 5-8 year period. Average of temperature in Selçuk sub-basin is 16.5 ^{o}C. Since 1998, temperatures, which are above the average, have been observed.

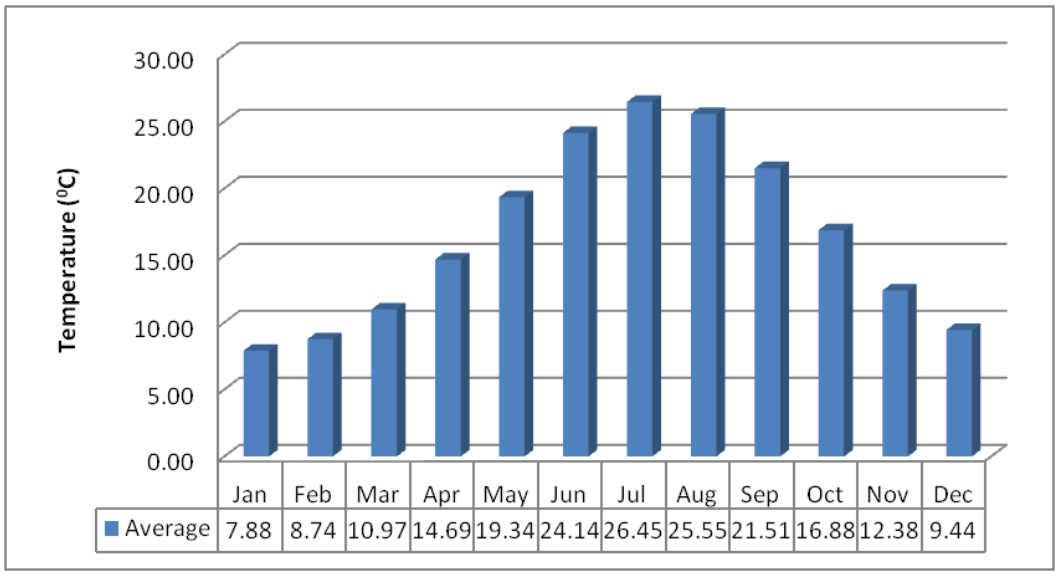

Figure 3. 2. Average (1964-2009) monthly temperature values in Selçuk station

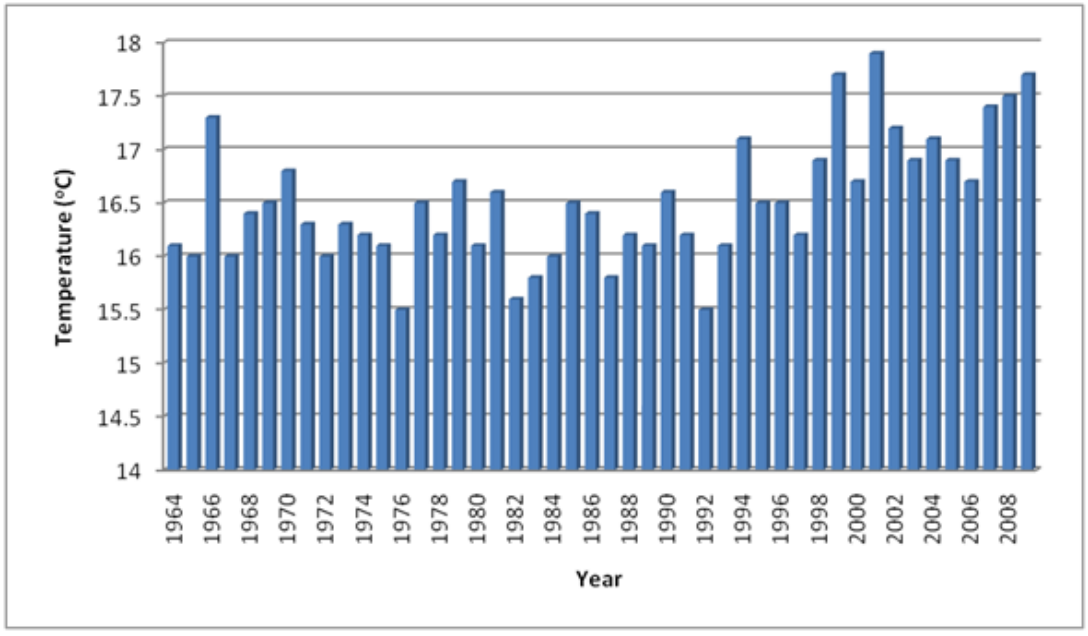

Figure 3. 3. Annual (1964-2009) temperature values in Selçuk station

Monthly average precipitation values obtained from Selçuk station for the years of 1964-2009 are illustrated in Figure 3.4. The maximum average precipitation value is observed in December, while the minimum average precipitation is observed in August. Monthly average precipitation values from November to March are above the annual mean value. Annual precipitation distribution between 1964 and 2009 is shown in Figure 3.5. Precipitation exhibits increasing and decreasing cycling patterns at each 6-8 year period. Average of precipitation in Selçuk sub-basin is 689.19 mm.

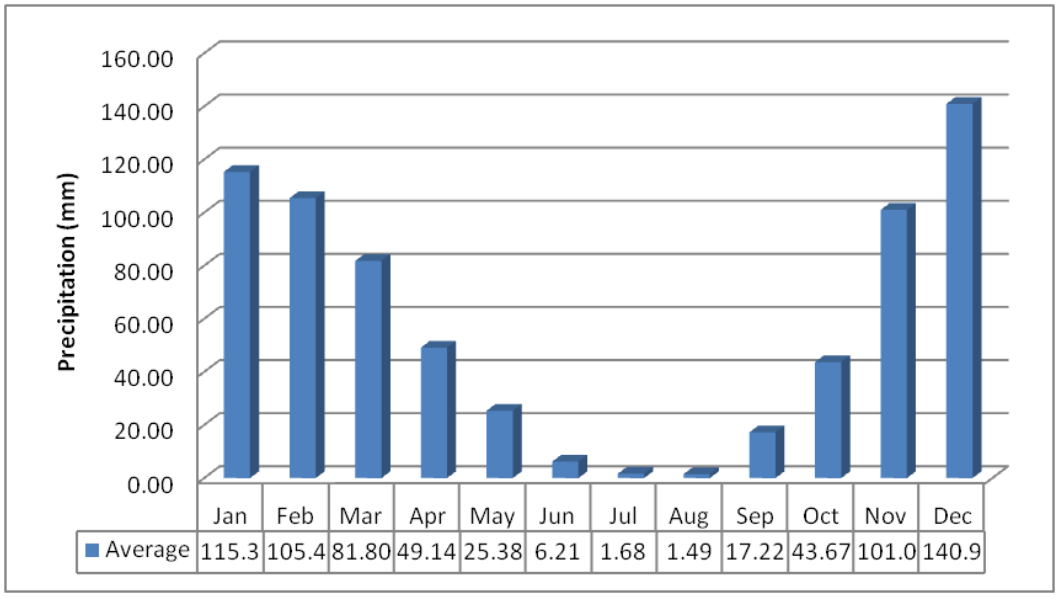

Figure 3. 4. Average (1964-2009) monthly precipitation values in Selçuk station

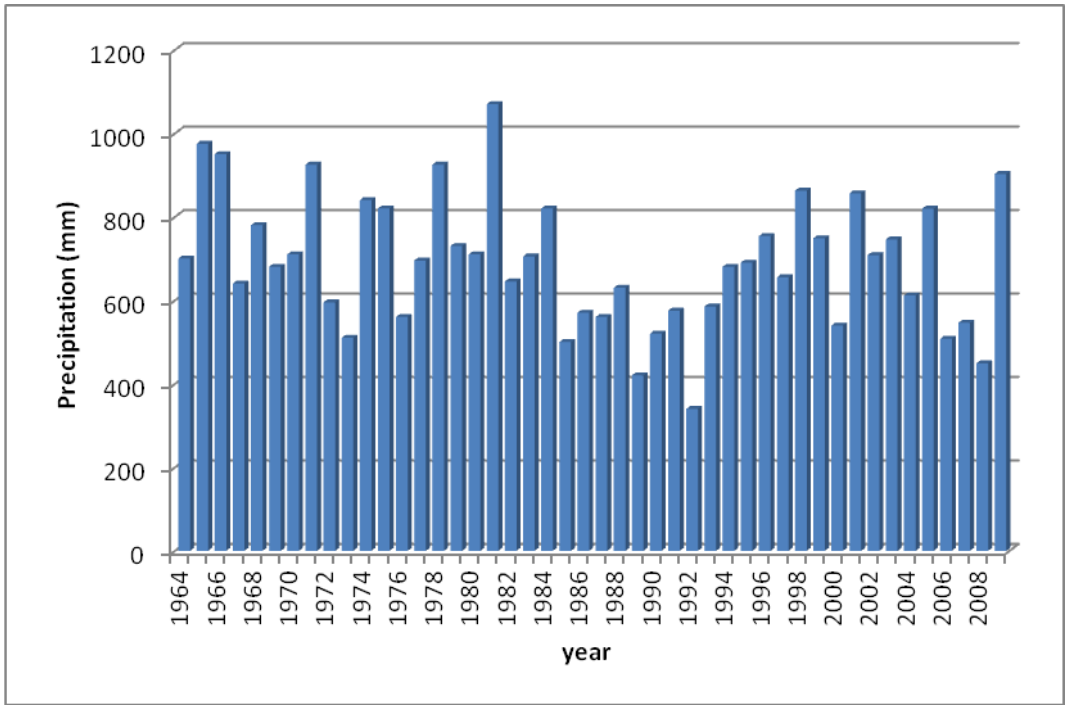

Figure 3. 5. Annual (1964-2009) precipitation values in Selçuk station

Monthly average evaporation values obtained from Selçuk station for the years of 1964-2009 are illustrated in Figure 3.6. The maximum average evaporation value is observed in July, while the minimum average evaporation is observed in January. Monthly average evaporation values from May to September are above the annual mean value. From January to March measurements cannot be performed due to freezing. Therefore, these missing data were obtained using the relationship between monthly average evaporation and temperature values measured in Selçuk meteorological station.

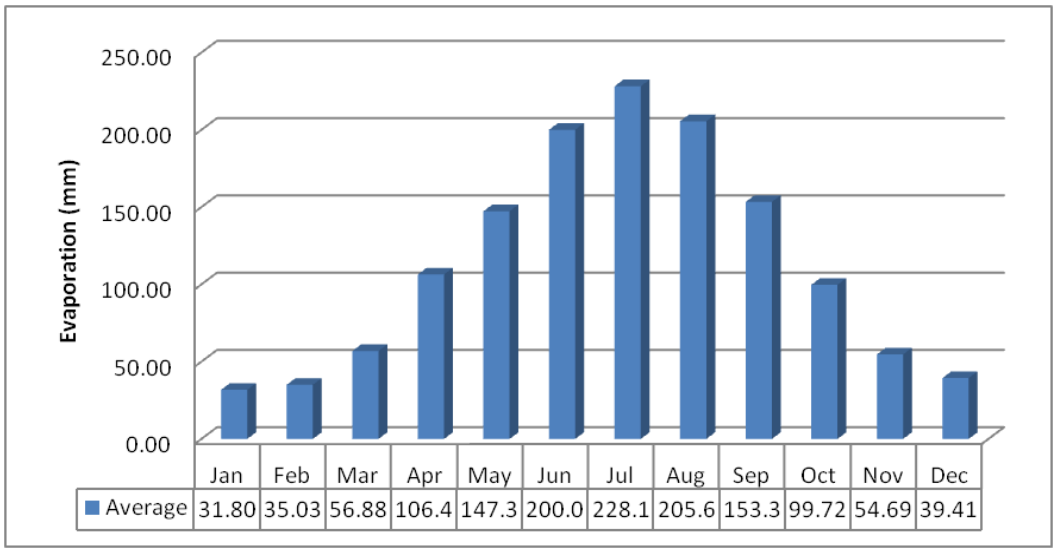

Figure 3. 6. Average (1964-2009) monthly evaporation values in Selçuk station

Monthly average relative humidity values obtained from Selçuk station for the years of 1964-2006 (available data period) are illustrated in Figure 3.7. The maximum average relative humidity value is observed in December, while the minimum relative humidity is observed in July. Monthly relative humidity values from May to September are below the annual mean value.

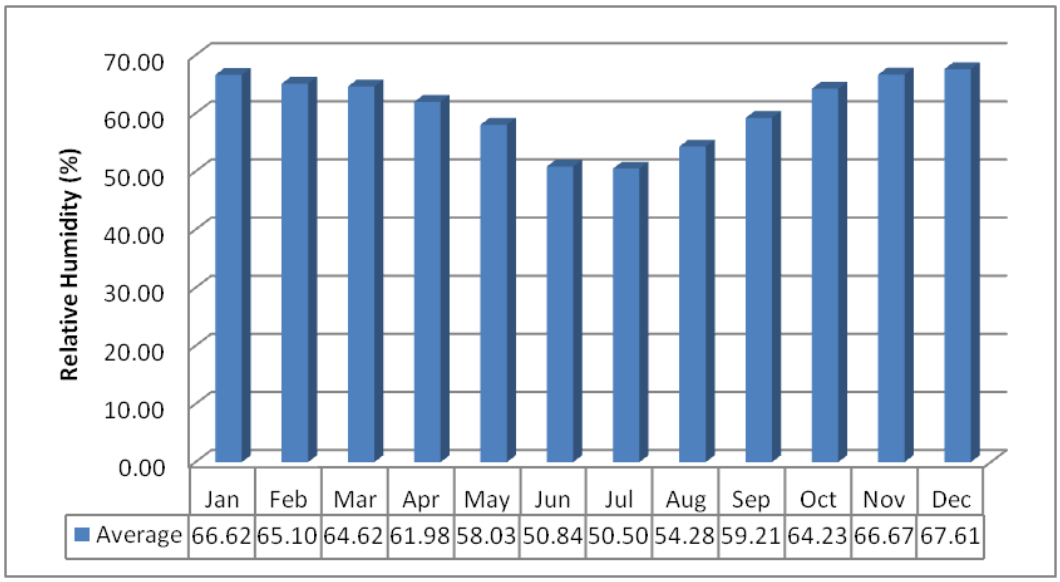

Figure 3. 7. Average (1964-2006) monthly relative humidity values in Selçuk station

3.3. Geomorphology

The alluviation of the Küçük Menderes River was reported by Kraft et al. (1977). Subsurface geological analyses were conducted in order to interpret archaeological settings and civilization according to the movement of the shoreline. The formation of the Küçük Menderes River Delta Complex is studied by Gökçen et al. (1990). It is stated that this delta complex, which is developed in Küçük Menderes Graben, is composed of four delta sequences. Each sequence is separated by a sea transgression surface. These transgressions occurred in 190000, 120000, 160000 and 130000 BC, respectively.

The gradual alluviation of the Selçuk Sub-basin is illustrated since ancient times by Gökçen et al. (Figure 3.8). Ancient shorelines since 1100 BC shown in Figure 3.8 were used in the modeling of the sea-regression period in this study.

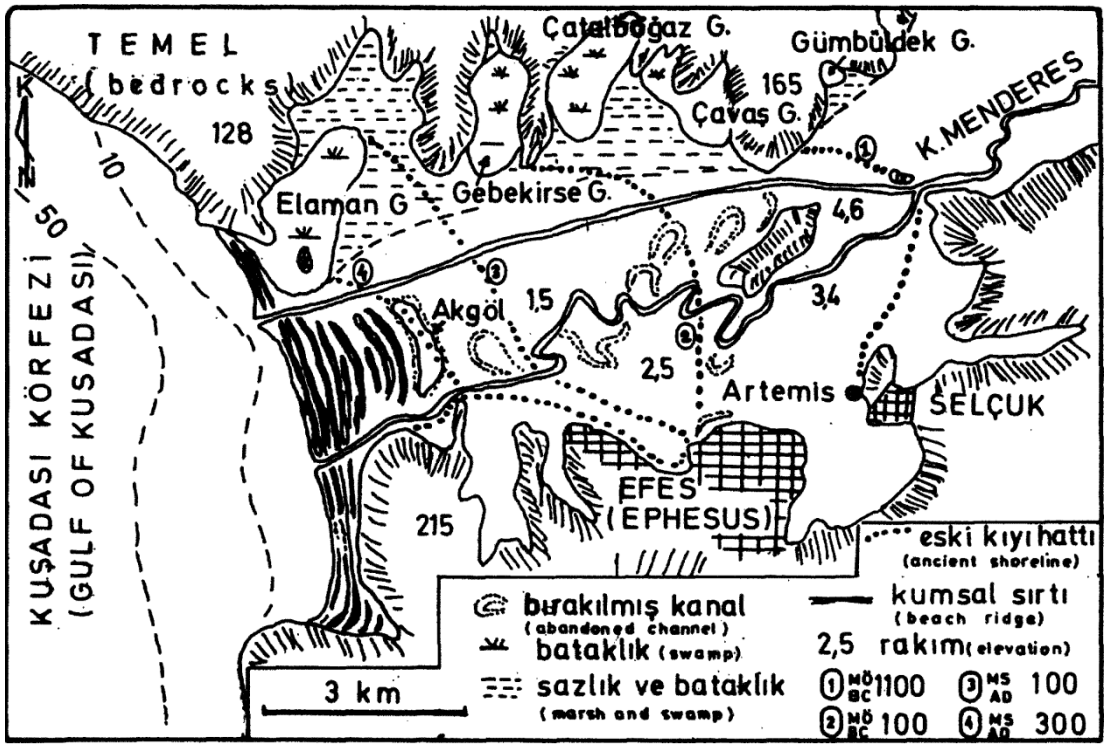

Figure 3. 8. Geomorphological map of the Küçük Menderes River delta (Gökçen et al., 1990)

3.4. Geology

Geological information about Küçük Menderes River Basin and study area given below is compiled from the final report of Yazıcıgil et al. (2000b).

3.4.1. Regional Geology

Küçük Menderes River Basin is one of the grabens formed in Western Anatolia. It is stretching along east-west direction and bounded by Gediz graben in north and Büyük Menderes graben in south.

Küçük Menderes River Basin includes metamorphic rocks of Menderes Massif as basement rock, Late Cretaceous- Paleocene aged Bornova flysch, Neogene units and Quaternary sediments (Figure 3.9). Generalized columnar section of Küçük Menderes River Basin after Yazıcıgil et al. (2000b) is illustrated in Figure 3.10.

Menderes massif metamorphics are bounded by İzmir-Ankara-Erzincan Suture Belt in north and Likya Nappes in south. It includes augen-gneiss, schist, phyllite and marble.

Bornova flysch is seen in western part of Küçük Menderes River Basin and northwest of Selçuk. It includes, from bottom to top, dark colored slate- greywacke and massive dolomitic limestone. The contact between Bornova flysch and Menderes Massif is an unconformity. Neogene units also overlay Bornova flysch unconformably.

Neogene units are represented by sediments including conglomerate, sandstone, mudstone and clayey limestone and volcanics. Volcanics are seen rarely and they are underlain by Quaternary alluvium and talus unconformably.

Plio-Quaternary units include Quaternary alluvium, alluvial cone, talus, peneplain, Plio-Quaternary river deposits and red pebbles. The contact between these units and underlying units is an angular unconformity. Alluvial fans are seen both in north and south part of the basin. They are mostly controlled by faults and erosions.

Faults in Küçük Menderes River Basin formed into two different directions. One of them is perpendicular to the longitudinal axis of the basin along north-south direction and the other one is parallel to the longitudinal axis of the basin passing through east-west direction. Analyses performed in the basin show presence of a syncline. The axis of the syncline is parallel to the longitudinal axis of the basin.

3.4.2. Local Geology

Selçuk sub-basin is located in the southwest of the Küçük Menderes River basin. North side of the sub-basin is represented by metamorphic rocks including marble (Figures 3.11 and 3.12). In two locations in the area Cretaceous units are mapped. Neogene units extending from east to west are also present.

In south part of the sub-basin marbles, schists and ophiolites of Menderes Massif are observed. They are extending in east-west direction. Marbles are massive upper parts of the sequence. In west and middle-south part of the sub-basin dissolution cavities are seen. Marbles are generally interbedded with schists. Neogene units outcropping in south part of the sub-basin is formed by continental sediments.

Units formed in east part of the sub-basin are the continuation of the units in the south. Most of the area of Selçuk sub-basin is covered by alluvial fills including alternation of clay, silt, sand and gravel. Black muds indicating swamp conditions are also important lithologies of alluvial fills.

In southern part of the area northwest-southeast oriented two faults are extending from the plain area to the highlands.

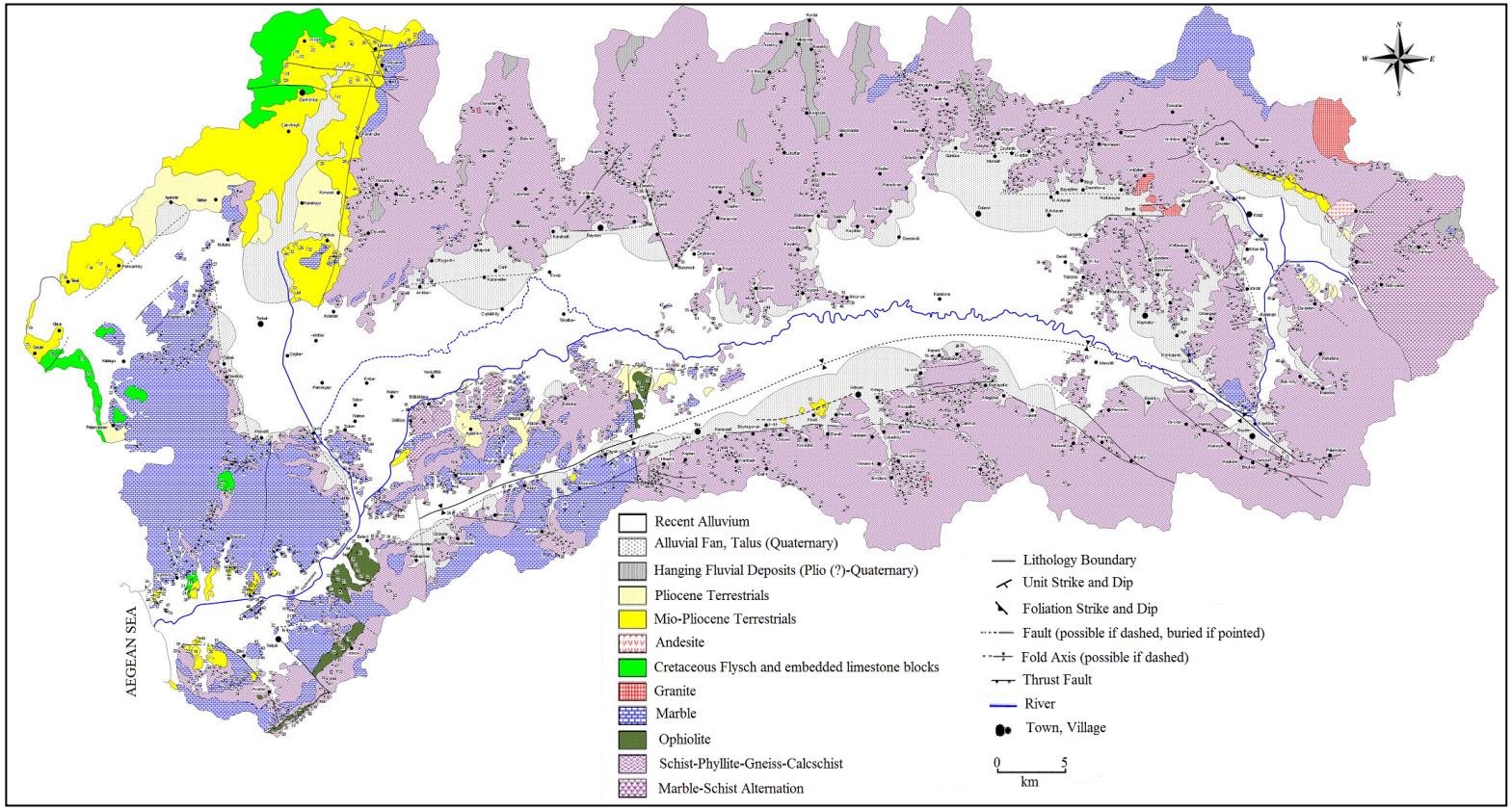

Figure 3. 9. Geological map of Küçük Menderes River Basin (Yazıcıgil et al.,2000b)

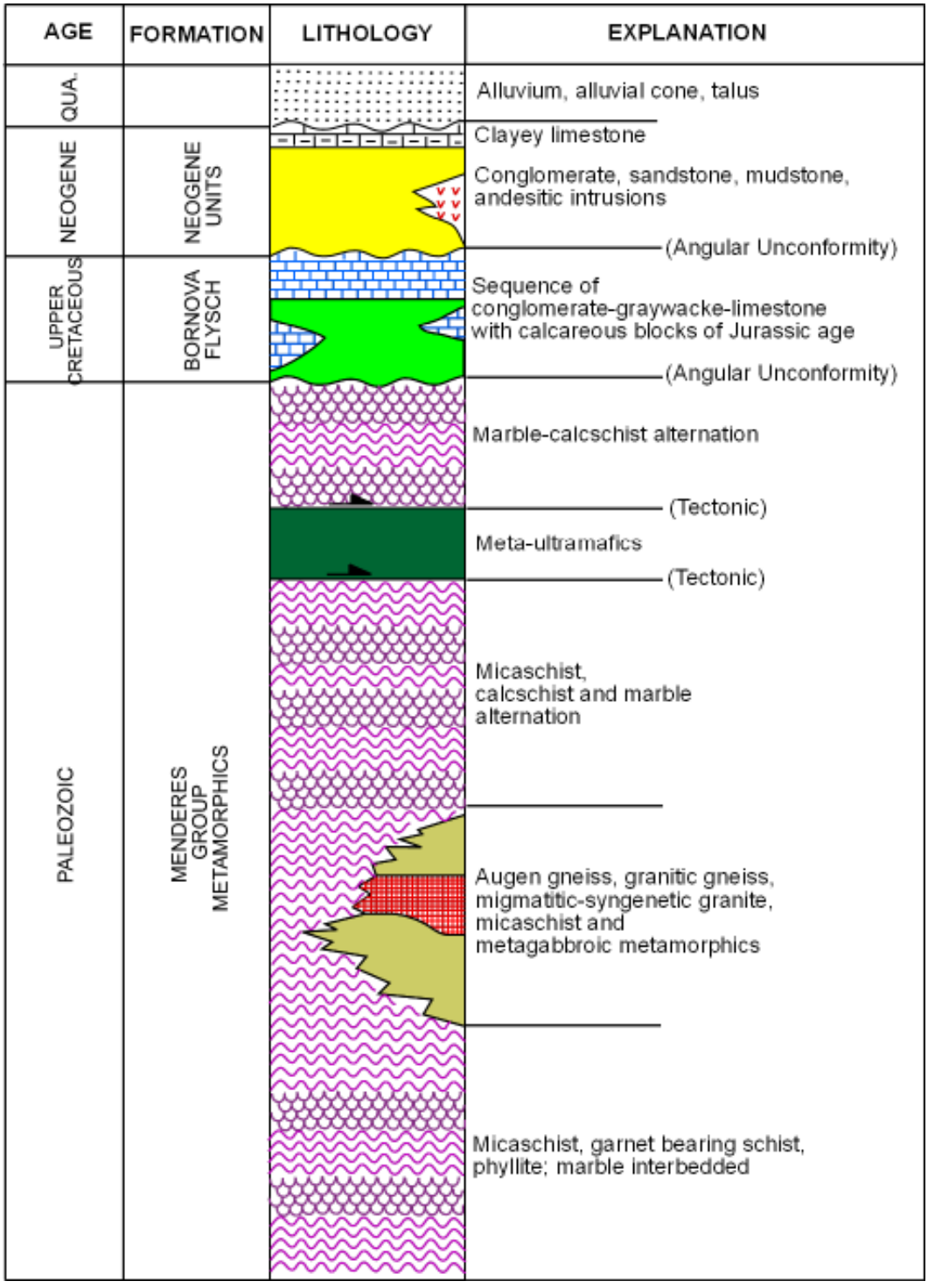

Figure 3. 10. Generalized columnar section of Küçük Menderes River Basin (after Yazıcıgil et al.,2000b)

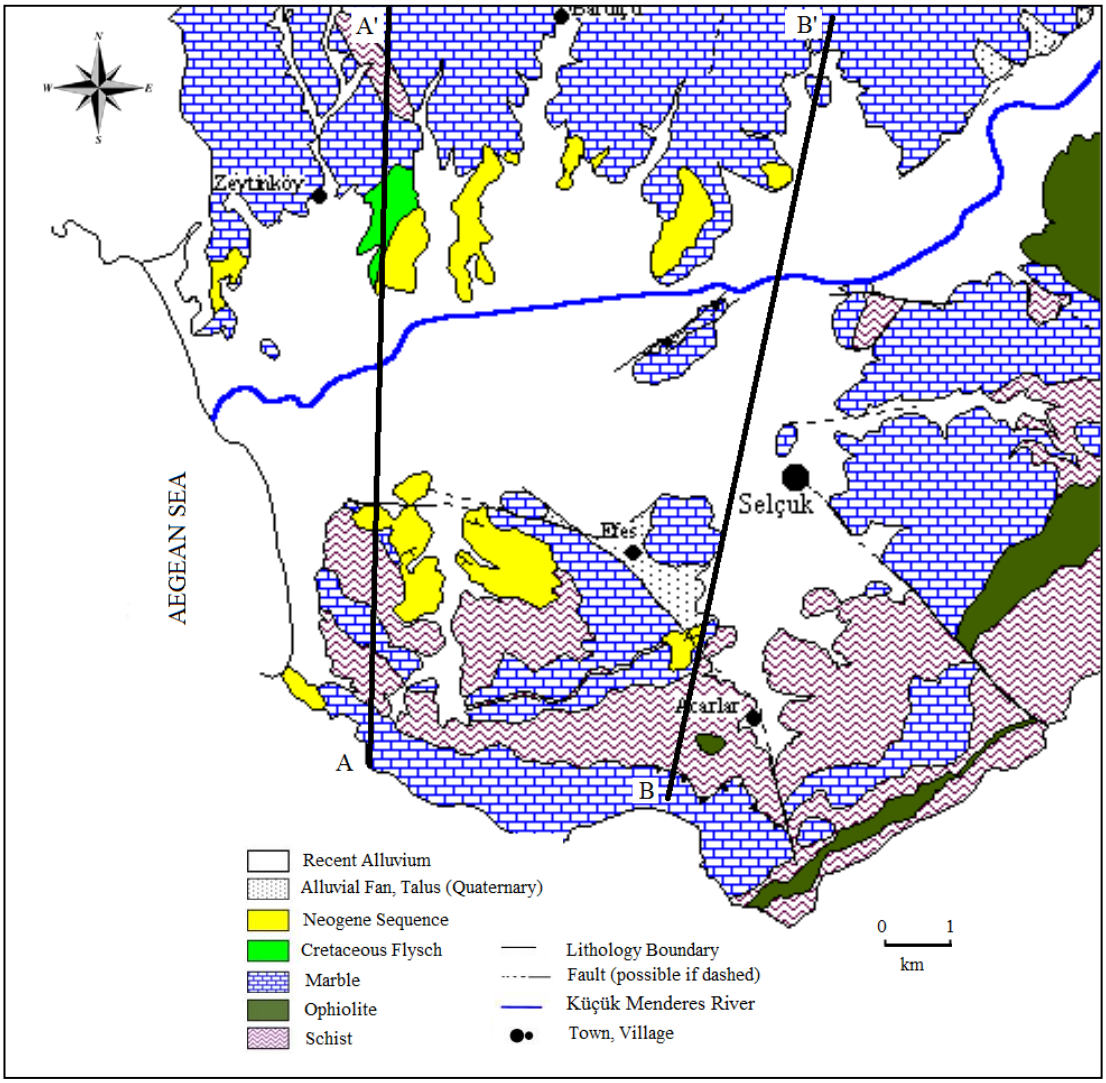

Figure 3. 11. Geological map of Selçuk Sub-basin (after Yazıcıgil et al.,2000b)

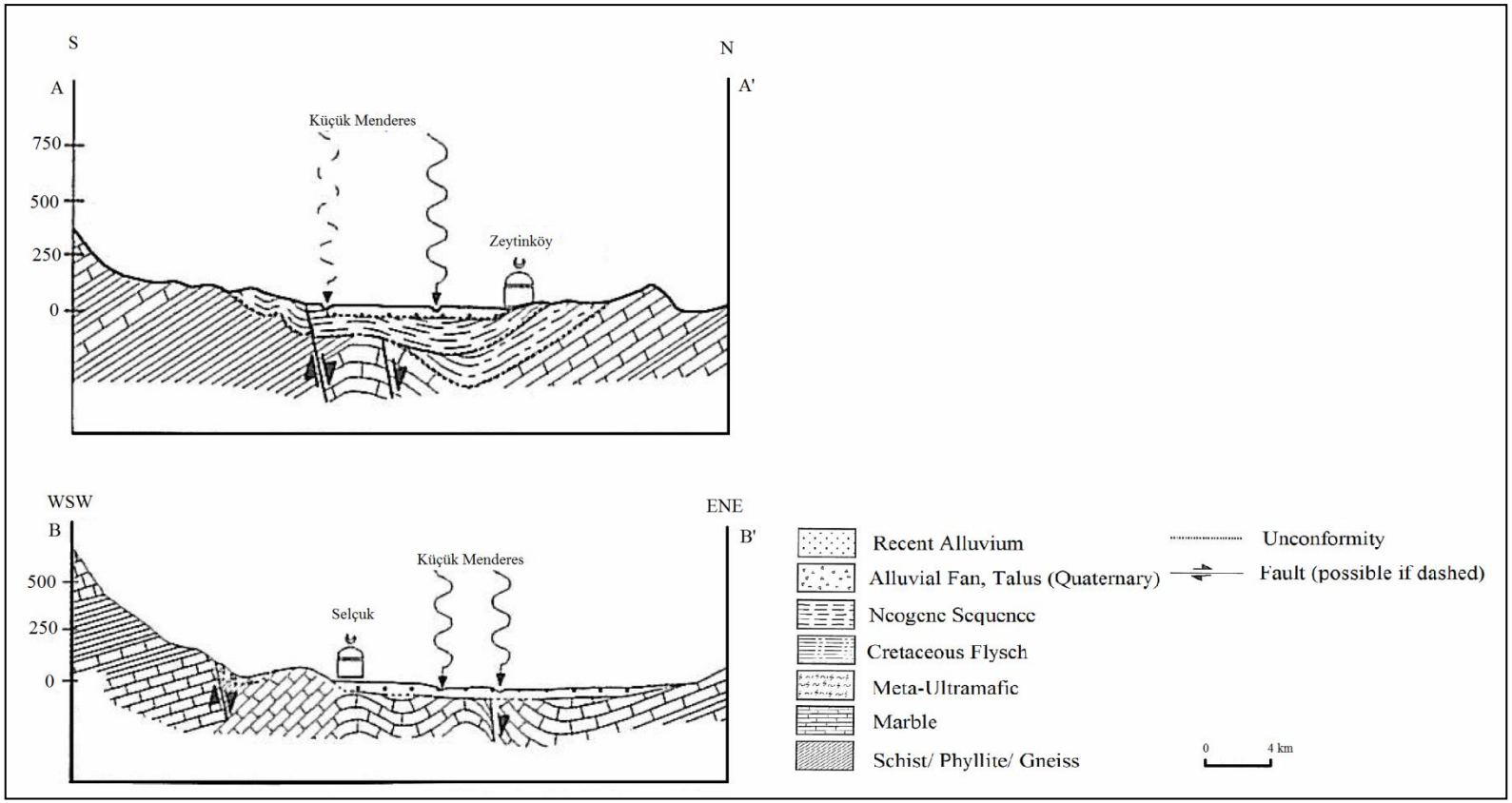

Figure 3. 12. Geological cross sections along A-A’ and B-B’ (after Yazıcıgil et al.,2000b)

3.5. Hydrogeology

Hydrogeological characteristics of the units in Selçuk sub-basin is obtained from the well logs of DSİ (State Hydraulic Work) and İller Bankası (Provinces Bank). There are 22 wells in the study area. Distribution of these wells is shown in Figure 3.13.

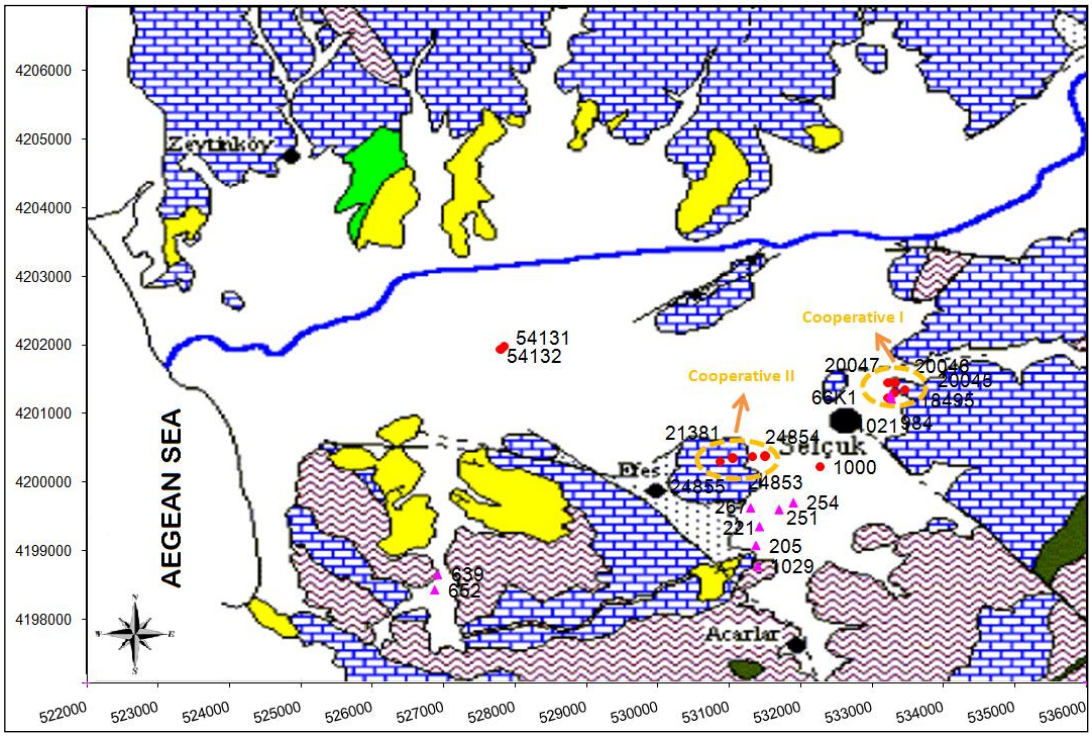

Figure 3. 13. Locations of the wells in Selçuk Sub-basin

3.5.1. Water Bearing Units

According to the studies carried out by Yazıcıgil et al. (2000c) not all the units observed in Selçuk sub-basin show aquifer characteristics. Schists, gneiss and ophiolites of Menderes Massif are impervious. However, marbles constituting upper part of the metamorphic sequence are productive aquifers in some places due to secondary porosities formed by dissolution cavities and fractures. Neogene sediments underlying alluvial fills shows aquifer characteristics. One well (no:

54132) in Selçuk sub-basin is penetrating this unit. The main aquifer system in the area is unconfined aquifer formed by alluvial fills that covers entire plain area. This unit is generally composed of alternation of gravel, sand, silt and clay deposits.

3.5.2. Hydraulic Parameters

Marble unit has the highest permeability among other permeable units in the sub-basin. However, it is permeable in few locations. Permeability of marble unit changes between 2.24 x 10^{-12} m^2 to 4.97 x 10^{-9} m^2. Average specific capacity of wells drilled in marble unit is 103 l/s/m. Storativity data is scarce for the sub-basin. According to available data it is 0.4 (Table 3.1).

Permeability and specific capacity of Neogene unit obtained from well no: 54132 are 0.37 x 10^{-11} m^2 and 4.6 l/s/m, respectively. Permeability of Küçük Menderes River Basin changes from 0.4 x 10^{-11} m^2 to 2.4 x 10^{-11} m^2. No storativity data is available for Neogene unit in sub-basin.

According to the wells located south of the Selçuk sub-basin permeability of alluvial fill is between 0.08 x 10^{-11} m^2 and 1.7 x 10^{-11} m^2. Permeability of the well no: 54131, which is the only well opened at the middle of the plain, is 0.38 x 10^{-11} m^2. This value is similar to the permeability of Neogene unit in the same location. Average specific capacity of alluvial fill is 5.1 l/s/m. Moreover, specific yield is 0.1 according to available data.

Table 3. 1. Well data of Selçuk Sub-basin

WELL NO	LITHOLOGY	SPEC. CAPACITY (l/s/m)	PERMEABILITY (m^2)	HYDRAULIC CONDUC. (m/day)	STORATIVITY
1000	Alluvium	0.3			
18495	Marble	106.78	1.31×10^{-09}	1107.5	0.4
20045	Marble	38.46	6.87×10^{-10}	582.6	
20046	Marble	70.99	1.49×10^{-09}	1261.8	
20047	Marble	263.15	3.88×10^{-09}	3291.7	
21381	Marble	56.52	1.06×10^{-09}	900.2	0.4
24853	Marble	153.85	4.97×10^{-09}	4213.3	
24854	Alluvium	6.13	8.73×10^{-12}	7.4	
24855	Marble	71.42	7.9×10^{-10}	669.6	
54131	Alluvium	13.9	3.78×10^{-12}	3.2	
54132	Neogene	4.6	3.66×10^{-12}	3.1	
35-0205	Alluvium+Marble	8.33	1.92×10^{-11}	16.3	0.1
35-0221	Alluvium+Marble	63.49	1.15×10^{-10}	97.7	0.15
35-0251	Alluvium	13.1	8.26×10^{-13}	0.7	0.1
35-0254	Alluvium	0.49	4.84×10^{-12}	4.1	0.1
35-0267	Marble	240	1.43×10^{-09}	1211.9	
35-0639	Alluvium+Marble	7.49	1.46×10^{-11}	12.4	
35-0652	Alluvium+Marble	0.46	1.06×10^{-12}	0.9	
35-0984	Marble				
35-1021	Marble	1.29	2.24×10^{-12}	1.9	
35-1029	Alluvium	5.41	1.71×10^{-11}	14.5	
66(K1)	Marble	26.05	5.06×10^{-11}	42.9	

3.5.3. Recharge

There is no artificial recharge in the sub-basin. According to studies performed by DSİ (1973) precipitation recharge to the Selçuk sub-basin was reported as 8 hm^3/year. Precipitation recharge to this aquifer was also studied by Gündoğdu (2000). Two methods were applied, namely water level fluctuation method and hydrologic budget method. In water level fluctuation method, recharge was deduced from water table fluctuations between October 1998 and March 1999 and it was founded to be 17 hm^3/year. According to hydrological budget method using data obtained between years 1970 and 1995, recharge was reported to be 14 hm^3/year. 8 hm^3 of this recharge belongs to 71.8 km^2 plain area.

There is also an additional inflow recharge affecting the sub-basin. This recharge occurs at the northeast part of the aquifer and moves from Bayındır-Torbalı sub-basin to Selçuk sub-basin. Groundwater flow flux was reported by Yazıcıgil et al. (2000c) as 5.57×10^{-3} m^3/day.

Moreover, the flow relation between Küçük Menderes River and Küçük Menderes River Basin was also reported by Yazıcıgil et al. (2000c). From November to June Küçük Menderes River is a losing river, but from July to October it is fed by the aquifer. However, there is no data about the flow relation between the river and the aquifer of Selçuk sub-basin. Further studies on head distributions in the study area show that equipotential lines are nearly perpendicular to the river flow direction. Therefore, Küçük Menderes River is assumed to be a neither gaining nor losing river in this study.

3.5.4. Discharge

Natural discharge in the sub-basin occurs to the Aegean Sea. Artificial discharge in Selçuk sub-basin was calculated using water need for irrigation and domestic water supply. Discharge of groundwater in this region has been proceeded since late 1970s.

Discharge for irrigation was calculated by Nippon (1996) using plant irrigation water need (Figure 3.14). Annual discharge per km^2 is 17.8 kg/s (0.56 hm^3 /year). Irrigation water need at south of the area is supplied from cooperative I wells since 1978. In 1989 cooperative II wells were added to this discharge. There are private wells whose discharge amounts are not known at the north of the sub-basin.

Discharge for domestic need of the sub-basin is stated to be 82.2 kg/s (2.59 hm^3 /year) for the year 1997 by Yazıcıgil et al. (2000c). Most of the water need is pumped in dry season.

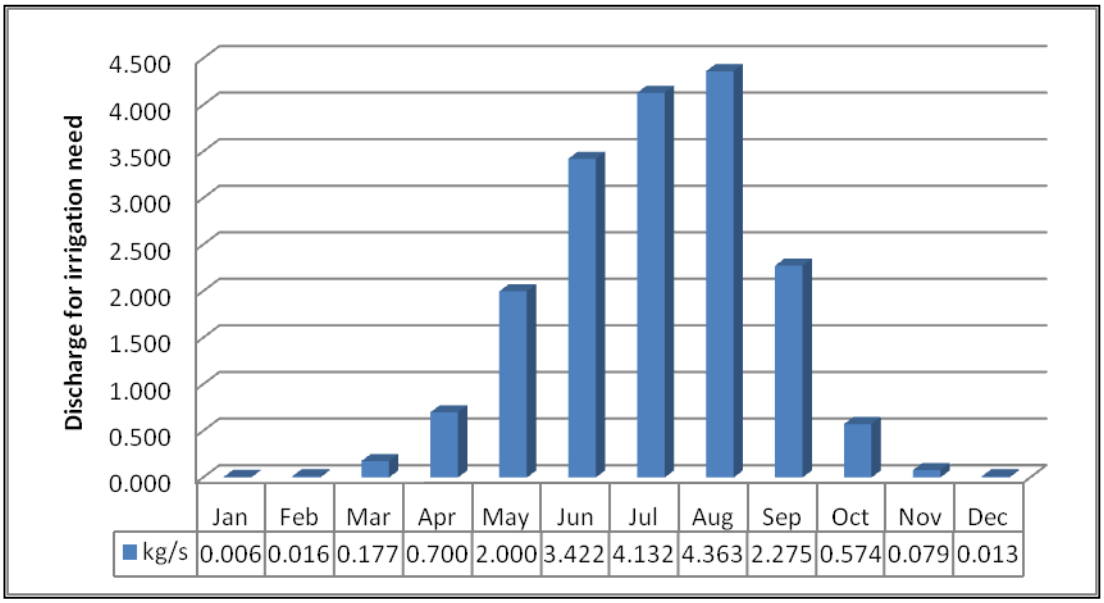

Figure 3. 14. Discharge for irrigation need per km^2 in Selçuk Sub-basin (Nippon, 1999)

3.6. Hydrochemistry

Hydrochemical measurements in the sub-basin waters between the years 1998 and 1999 were reported by Yazıcıgil et al. (2000a). These measurements suggested the existence of a salinity problem in the sub-basin aquifer. Hassan (2004) and Çamur et

al. (2005) have further studied this problem. Depthwise electrical conductivity (EC) measurements of the wells 54131 and 54132 by Hassan (2004) in 2002 indicate the existence of salt water intrusion (Figure 3.15). It can be easily seen from the figure that EC values increase as the depth increases. In well 54131 which penetrates alluvium unit, EC values increase from 2250 μS/cm to 37000 μS/cm up to the depth of 150 m. There is a sharp increase between the depths of 90 m and 115 m. These stepwise changes in EC measurements indicate heterogeneities and discontinuities in the aquifer properties. In well 54132, which filters Neogene unit groundwater between the depths of 160 m and 270 m, EC values increase from 10000 μS/cm to 38000 μS/cm.

Data of the hydrochemical analyses carried out in May 2002 were used to determine total dissolved solids (TDS) value of water in well 54131. Using relationship between EC and TDS, depthwise change in TDS was estimated for the year of 2002 (Figure 3.16). These TDS values for well 54131, which is the only well on the studied cross sectional area, were used for the calibration of pumping period cross sectional model parameters in Chapter 6.

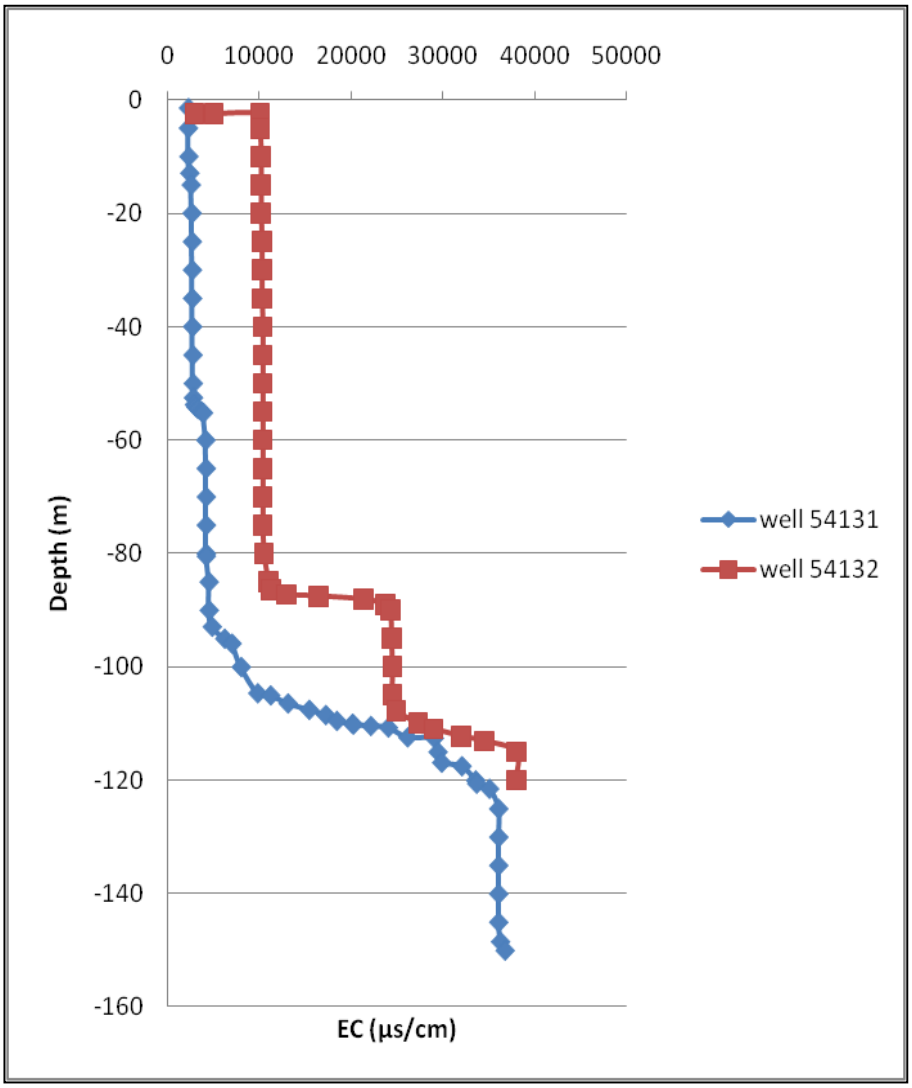

Figure 3. 15. Electrical conductivity (EC) measurements of 2002 in wells 54131 and 54132 (Hassan, 2004)

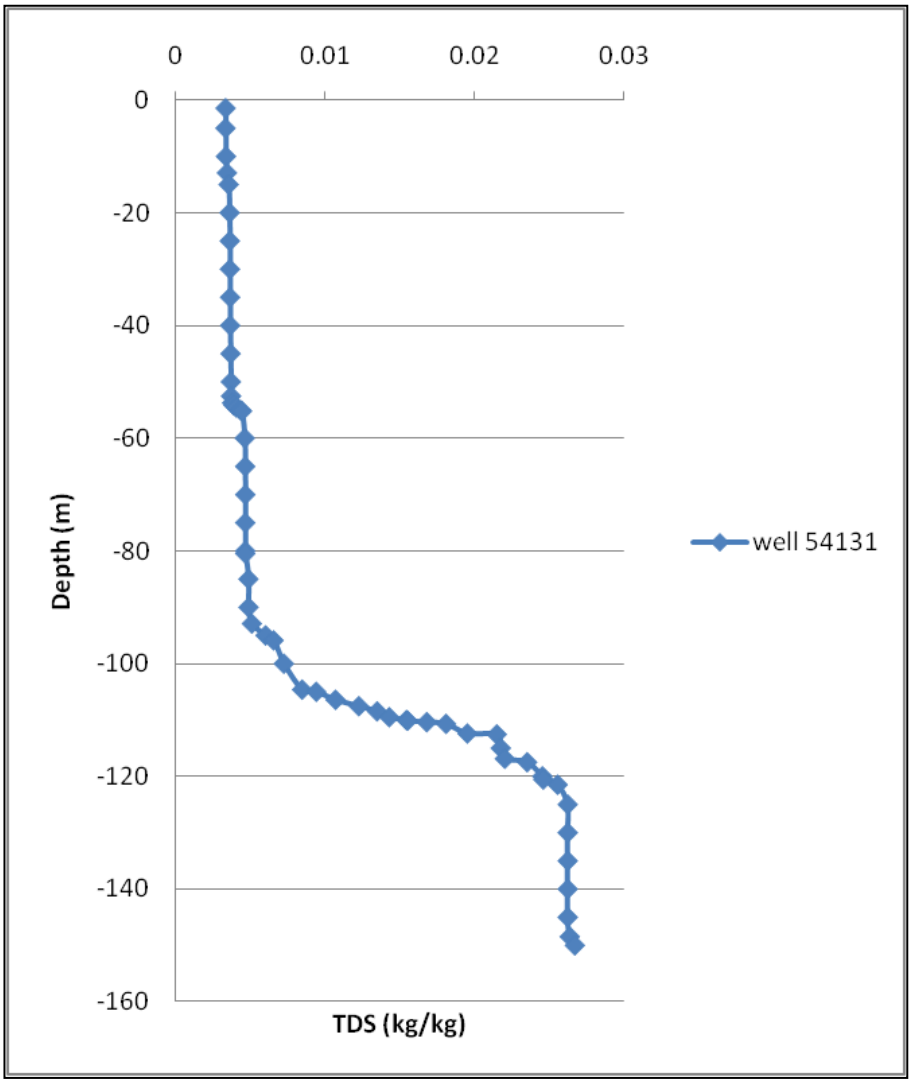

Figure 3. 16. Total dissolved solids (TDS) estimated from EC measurements of 2002 in well 54131

CHAPTER 4

MODELING AND METHODOLOGY

4.1. Modeling

4.1.1. Introduction

Model is a selected simplified representation of a real system and phenomena. It approximately simulates interested excitation-response relationships of the system (Bear and Cheng, 2010). In general, models describe physical systems using mathematical equations. The more closely the mathematical equation approximates the system, the more applicable the model is. Therefore, models cannot represent physical systems exactly.

Groundwater flow and fate and transport processes are expressed by the groundwater models using mathematical equations. These equations are based on some simplifying assumptions and uncertainties in the data, which are required by the model. Thus, a model must be assumed as an approximation of field conditions (Mandle, 2002).

The equations that are used to describe groundwater flow and fate and transport are solved by two types of models namely analytical model and numerical model.

Analytical models are exact solutions of these equations that are generally simplified. These simplifications are used to reduce three dimensional systems into one or two dimensional equations. Therefore, it is not possible to apply analytical models into field conditions that change with time or space.

However, numerical models are capable of solving more complex equations that describe multi-dimensional systems. Thus, they may give results more similar to the real system. Numerical models solve the equations using two major methods i.e. finite difference method and finite element method. Both of these approaches subdivide the area of interest into a number of smaller subareas (cells or elements) and the time of the simulation into time steps. The correctness of numerical model is dependent on several variables such as accuracy of the input data, space size, time discretization and the numerical methods used in order to solve model equation (Mandle, 2002).

4.1.2. Model Development Processes

Performing a groundwater model requires a detailed and comprehensive study to reach reliable results. Before starting modeling, purpose and scope of the study should be stated properly. This makes the steps of the modeling more clear and understandable. Purpose and scope of this study were mentioned in the Introduction Chapter.

After determining the purpose of model development, main components of modeling are performed. These components are listed as:

- Hydrogeologic characterization of the study area
- Model conceptualization
- Model selection
- Model design
- Model calibration
- Sensitivity analysis
- Presentation of results

4.1.2.1. Hydrogeologic Characterization

Hydrogeologic characterization of the site, which will be modeled, is important to understand the hydrogeologic and hydrogeochemical conditions dealt with during

modeling. This process requires compiling data from fieldworks, groundwater samples and laboratory analysis, and evaluating relevant data for the model. Typical data that are needed can be expressed as topographic, geologic and hydrogeologic maps, aquifer type, aquifer characteristics, boundary conditions, sources, sinks, water quality, contaminant, etc.

Determination of the hydrogeologic characteristics of the Selçuk sub-basin and obtained data were explained in Chapter 3 Study Area.

4.1.2.2. Model Conceptualization

The real system and its properties may be very complicated due to the amount of data and details of it. A conceptual model assembles data that describes the real system in a systematic way and reduces it to a simplified version in order to adjust it easily to the model.

The conceptual model aims to develop a better understanding of site conditions, characteristics of the aquifer system, groundwater flow and contaminant transport, to determine the modeling approach and to select a suitable model. Moreover, the conceptualization takes into account the objectives of the model, the schedule and resources to reach the objective.

Model conceptualization of Selçuk sub-basin was developed before starting each model mentioned in following chapters.

4.1.2.3. Model Selection

After conceptual model is developed, proper model can be selected. The selected model should be capable of simulating site conditions closer to the real system. As it is mentioned above, analytical models generally used to solve relatively simple groundwater flow or transport problems which do not change with time and space. In contrast to this, numerical models are used for more complex and multi-dimensional

groundwater flow and transport processes that varies with time and space. Therefore, numerical model was preferred in modeling of the study area.

Two types of numerical model, namely finite difference and finite element, are defined by finite pieces that subdivide the domain into smaller areas. Finite difference method uses rectangular grids, while finite element method offers flexibility for grids, which allows more similar boundaries for irregular shaped areas. In numerical modeling of Selçuk sub-basin finite element method was performed.

4.1.2.4. Model Design

Design of the model includes selecting the model domain, discretizing data in time and space, assigning boundary and initial conditions and inputting model data.

Model domain refers to the study area that is going to be modeled. It should be carefully defined to obtain accurate and reliable results. Choice of the domain also affects the physical and numerical resolution and level of effort of modeling.

Discretization is one of the important parts of the modeling. It means dividing the model domain or simulation time into small pieces. In terms of finite element method, discretized domain is defined as element. The shape of the element is flexible so that it can include the whole domain. Parameters for each element are assumed to be uniform. In order to get more precise results smaller elements should be used. Time discretization of the model depends on duration of the simulation and frequency of the results needed.

To obtain reliable model additional information about the physical state of the system is required. This information is obtained by boundary and initial conditions. While transferring a conceptual model to a groundwater model, the boundaries of the model must be defined with suitable conditions. There are three types of boundary conditions;

- *Specified head boundary* is a boundary condition along which measured and either constant or time-variant heads are applied.
- *Specified flux* is a boundary condition along which inflows or outflows are set.
- *Head dependent flux* is used as a boundary condition on the other sides of which flow into or out of the cell occurs depending on the head differences.

Initial conditions refer to the status of the system at the start of the simulation. They are needed for the solution of the transient equations. For most transient simulations, steady-state head distribution is taken as an initial condition.

After defining all of the conditions mentioned above, input data of the model is gathered and used in the model. Steps of the model design used in the modeling of the study area were expressed in following chapters in details.

4.1.2.5. Model Calibration

Calibration of the model refers to adjusting the input parameter until computed values match the field conditions. This process requires properly characterized field conditions. If there is a lack of field conditions or wrong data, the results of the model will not represent the real system. It is also reasonable to adjust the input data because input data are not perfectly known and there can be a certain range of data.

Calibration process includes both the calibration of steady state and transient state conditions. There is no change of data with time in steady state simulations in contrast to the transient ones. While calibrating the model it is important to minimize the difference between the simulation results and measured field conditions. It is obtained by trial and error method. However, in calibration process there is no guaranty that, input data found by trial and error is unique. There can be same results with different combinations of input values.

Calibrations of the models performed at the end of the simulations were mentioned in the following chapters for each modeling process.

4.1.2.6. Sensitivity Analysis

Sensitivity analysis is the process of observing the response of the model to the changes in uncertain input parameters. This process allows seeing the ranking of model input parameters in terms of their influence on the model simulation results. These analyses are also beneficial in determining parameters, which need more accurate data collection.

Sensitivity analyses of model results obtained for Selçuk sub-basin were performed in the following chapters in details.

4.1.2.7. Presentation of Results

Results of the model include obtained data after the all phases of the modeling procedure. This data can be in the form of graphics, tables, cross-sectional figures, vector illustrations, etc. Modeling results should be clear and concise.

Results of the models were demonstrated at the end of each simulation in the following chapters.

4.1.3. Numerical Modeling of Density Dependent Groundwater Flow and Solute Transport

In general, fluid properties (i.e. density, viscosity) are not affected by the transport of solute by groundwater flow. However, in some cases fluid density is strongly dependent upon concentration (Younes et al., 1999). As it is mentioned by Holzbecher (1998), if the flow pattern is influenced by density differences in the fluid system, this fluid flow is classified as density dependent. The important condition for this flow is changes in density from one location to another. This situation holds for steady state condition where the system does not change with time. If there is a transient flow, temporal changes of density is added to the system. Fluid density is influenced mainly by temperature and salinity. Pressure, which has minor importance, is the other dependency of density.

In modeling of a usual situation, flow and transport can be treated in separate steps. Transport is generally influenced by flow. It can be simulated in a second step, if the velocity field is given. This procedure is allowed since transport has no influence on the flow. The method becomes inappropriate when the interaction is in both directions. If there are density gradients in the system, flow will generally not be the same as in a constant-density situation. Large density variations make the problem of solute transport much more difficult to solve since it is highly nonlinear. In fact, when there is salt water in the system, it affects fluid density which changes local velocity field. This nonlinearity makes the solute distribution difficult to predict since recirculation regions may be formed. Therefore, for these problems there are no analytical models. Numerical models are used (Younes et al., 1999).

A finite element model, SUTRA (***S***aturated-***U***nsaturated ***Tra***nsport) developed by Voss (1984) has been applied to simulate the salt water intrusion in study area. SUTRA is a computer program that simulates fluid movement and the transport of either energy or dissolved substances in a subsurface environment (Voss, 1984). The code includes two- or three- dimensional finite-element and finite- difference methods to approximate the governing equations (Voss et al., 2010).

Density dependent saturated groundwater flow and solute transport equations used by SUTRA that were described by Voss et al. (2010) are as follows:

The groundwater fluid density may change depending on pressure and concentration. These essential variables are defined as follows:

p	$[M/(Ls^2)]$	fluid pressure
C	$[M_s/M]$	fluid solute mass fraction

(mass solute per mass total fluid)

Fluid density is a weak function of pressure and depends primarily on fluid solute concentration.

$$\rho = \rho(C) \cong \rho_0 + \frac{\partial \rho}{\partial C}(C - C_0) \quad (4.1)$$

where

ρ_0	$[M/L_f^3]$	base fluid density at $C=C_0$
C_0	$[M_s/M]$	base fluid solute concentration

The factor $\partial\rho/\partial C$ is a constant value of density change with concentration. For mixtures of sea water and fresh water at 20 ^{0}C, when C is the mass fraction of total dissolved solids, which is 0.0357 kg_{salt}/kg_{fluid}, C_0= 0 and ρ_0= 1000 [kg/m^3], then the factor, $\partial\rho/\partial C$, is approximately 700 [kg/m^3].

The density of the sea water is given by the linear fluid density expression used by SUTRA;

$$\rho = 1000 + 700 \times 0.0357 \quad (4.2)$$

$$= 1025 \ [kg/m^3]$$

For solute transport viscosity is taken to be constant. For example at 20 ^{0}C viscosity, $\mu(C)$, is 1.0×10^{-3} [kg/(m.s)].

The specific pressure storativity is stated as follows:

$$S_{op} = (1-\varepsilon)\alpha + \varepsilon\beta \quad (4.3)$$

where

S_{op}	$[M/(L.s^2)]^{-1}$	specific pressure storativity
ε	[unitless]	porosity (volume of voids per total volume)
β	$[M/(L.s^2)]^{-1}$	fluid compressibility
α	$[M/(L.s^2)]^{-1}$	porous matrix compressibility

The specific pressure storativity, S_{op}, is the volume of water released from saturated pore storage due to drop in fluid pressure per total solid matrix plus pore volume. The common specific storativity, S_o, is analogous to the specific pressure storativity used in SUTRA, except that specific storativity expresses the volume of water released from pore storage due to drop in hydraulic head. For pure water at 20 ^{0}C, $\beta \sim 4.47 \times 10^{-10}$ [kg/(m.s^2)]$^{-1}$. Factor α changes from 10^{-10} [kg/(m.s^2)]$^{-1}$ for sound bedrock to about 10^{-7} [kg/(m.s^2)]$^{-1}$ for clay (Freeze and Cherry, 1979).

The fluid mass balance equation implemented in Sutra by employing Darcy's law is:

$$\left(S_w \rho S_{op} + \varepsilon \rho \frac{\partial S_w}{\partial p}\right)\frac{\partial p}{\partial t} + \left(\varepsilon S_w \frac{\partial \rho}{\partial C}\right)\frac{\partial C}{\partial t} - \nabla.\left[\left(\frac{k\rho}{\mu}\right).(\nabla p - \rho g)\right] = Q_p \qquad (4.4)$$

where

Q_p	[M/L^3.s)]	fluid mass source (including pure water mass plus solute mass dissolved in source water)
k	[L^2]	solid matrix permeability
g	[L/s^2)]	gravitational acceleration
S_w	[unitless]	water saturation

The solute mass balance per unit aquifer volume at point (x,z) in an aquifer with variable-density fluid is given by Voss (1984):

$$\varepsilon \rho \frac{\boldsymbol{\partial C}}{\boldsymbol{\partial t}} + \varepsilon \rho v.\Delta C - \Delta.[\varepsilon \rho (D_m I + D).\Delta C] = Q_p(C^* - C) \qquad (4.5)$$

where

v	[L/T]	fluid velocity
C*	[M$_s$/M]	concentration of solute as a mass fraction in fluid
D_m	[L^2/T]	molecular diffusivity of solute in pure fluid

D	$[L^2/T]$	dispersion tensor
I		identity tensor

For modeling of the study area SUTRA GUI (***G***raphical ***U***ser ***I***nterface) was used by integrating it within the Argus ONE (**O**pen ***N***umerical ***E***nvironment) modeling environment. It allows the user to graphically input all GIS data, run SUTRA and visualize the results from Argus ONE.

4.2. Methodology

Steps of the modeling methodology to reach the purpose are listed below:

- pre-pumping period areal modeling (covering the years of pre 1976)
- pre-pumping period cross sectional modeling (covering the years of pre 1976)
- pumping period cross sectional modeling (covering the years of 1976-2009)
- sea-regression period cross sectional modeling (covering the years of 1100 BC to 1976)
- climate controlled future period cross sectional modeling (covering the years of 2010-2099)

4.2.1. Pre-Pumping Period Areal Model

The areal model was performed in order to obtain the distribution of steady state head values in the plain area. These values were used for the calibration of pre-pumping period model, because for this purpose there are not enough wells along the cross sectional line, through which the domain of the cross sectional model passes. Recharge and permeability parameters were calibrated using the head values. These calibrated head values were utilized as observation data to calibrate the head values of the pre-pumping period cross sectional model.

4.2.2. Pre-Pumping Period Cross Sectional Model

The pre-pumping period cross sectional model represents the conditions before 1976 when there were no intensive discharge wells in the area that can disturb steady state flow conditions. The purpose of establishing this model is to obtain initial head and concentration values for the pumping period cross sectional model. Pre-pumping period model recharge and permeability parameters were calibrated using the head values of the areal model.

4.2.3. Pumping Period Cross Sectional Model

The pumping period cross sectional model represents the movement of the salt water-fresh water interface from 1976 to 2009 considering variations in the artificial discharge amount. The aim of this model is to determine head and concentration distributions in 2009 by calibrating dispersivity values. The related calibration values were used in the sea-regression period and in the future period cross-sectional models.

4.2.4. Sea-Regression Period Cross Sectional Model

The sea-regression period cross-sectional model aims to observe movement of the salt water-fresh water interface from 1100 BC to 1976 using calibrated aquifer parameters. Model results at the end of simulation indicate the position of the interface for conditions that values of aquifer parameters and recharge amounts in the past were similar to present. These results were compared with those of the pre-pumping period which retrieved by back calculations using the calibrated pumping period model.

4.2.5. Climate Controlled Future Period Cross Sectional Model

The future period cross sectional model covering the years of 2010-2099 is performed to see the future change of head values and the interface position under the influences of climate and domestic water and agricultural water needs related artificial discharges. Calibrated aquifer parameters obtained from the pumping period

model are used in this model. Recharge and discharge values were changed according to the variations in temperature, precipitation and population.

CHAPTER 5

AREAL FLOW MODEL

The areal saturated flow simulation was performed in order to obtain steady state head values of the plain area. These head values were used to calibrate the pre-pumping period density dependent cross sectional model because there is no monitoring well data along the cross sectional line, through which the domain of the cross sectional model passes.

5.1. Conceptual Model

The domain of the areal model covers plain area of the Selçuk sub-basin. Alluvium, Neogene and Marble units included in this area were treated as a single aquifer having different hydrogeologic properties. The model domain is under the influence of precipitation recharge. It is also affected by the influx from the neighboring Bayındır-Torbalı sub-basin. There is no flow from the impermeable marble units located at the north and south of the model domain. Moreover, it is assumed that there is no flow relationship between the aquifer and Küçük Menderes River. Steady state flow conditions were applied.

5.2. Discretization and Boundary Conditions

Two dimensional irregular quadrilateral finite element mesh was created to discretize the model domain. 1157 elements and 1386 nodes were used (Figure 5.1).

Three types of boundary conditions were applied to represent the model domain (Figure 5.1);

- Constant pressure boundary along the shore line
- Constant flux boundary along northeastern boundary where there is an influx from Bayındır-Torbalı sub-basin
- No flow boundary along north and south of the plain

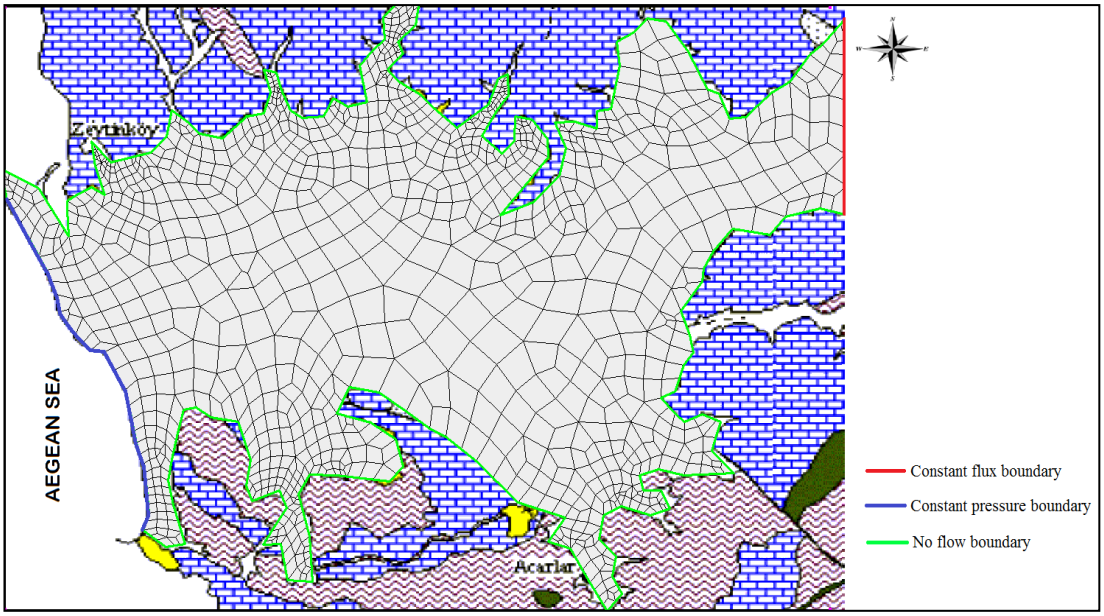

Figure 5. 1. Discretization and boundary conditions of the areal model

5.3. Model Parameters

Porosity of the areal model changes between 20-30 %. Intrinsic permeability changes in the range of 1.49×10^{-9} m^2 and 7×10^{-11} m^2. Total recharge applied to the model is 103 kg/s including influx from Bayındır-Torbalı sub-basin, which is located at east of the Selçuk sub-basin.

5.4. Calibration and Results

Calibration of the areal model was performed manually using data from the observation wells 18495 and 21381. These wells are located in the domain area and

they are the only available wells that have groundwater level measurements for the pre-pumping period. Pressure distribution of the steady state areal model is shown in Figure 5.2. Results of the model obtained as pressure are converted to head values in order to simplify the comparison. Simulated head values are compared with the observed head values in Table 5.1. The difference between them is in well acceptable limits.

Groundwater levels obtained from the areal model were used to calibrate the head values in the pre-pumping period cross sectional model.

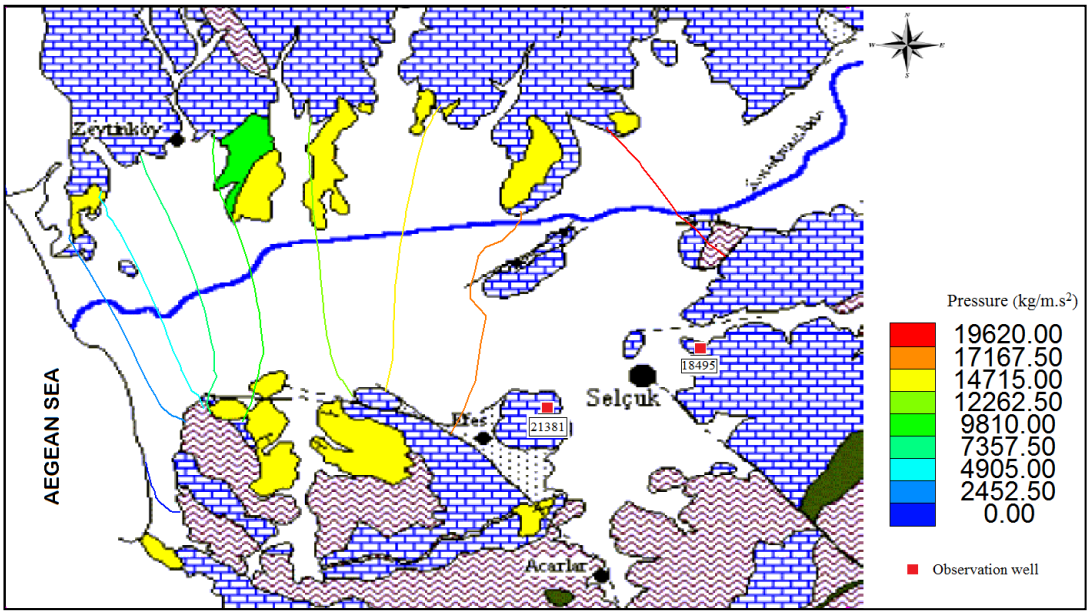

Figure 5. 2. Steady state groundwater pressure distribution in the study area

Table 5. 1. Observed and simulated head values of the areal model

Well No	Observed Head (m)	Simulated Head (m)
18495	1.83	1.81
21381	1.74	1.80

CHAPTER 6

CROSS SECTIONAL SATURATED FLOW MODELS

Density dependent saturated cross sectional models were simulated to predict the relationship between salt water and fresh groundwater. The cross section is passing from Aegean Sea at southwest towards Bayındır-Torbalı sub-basin at northeast (Figure 6.1).

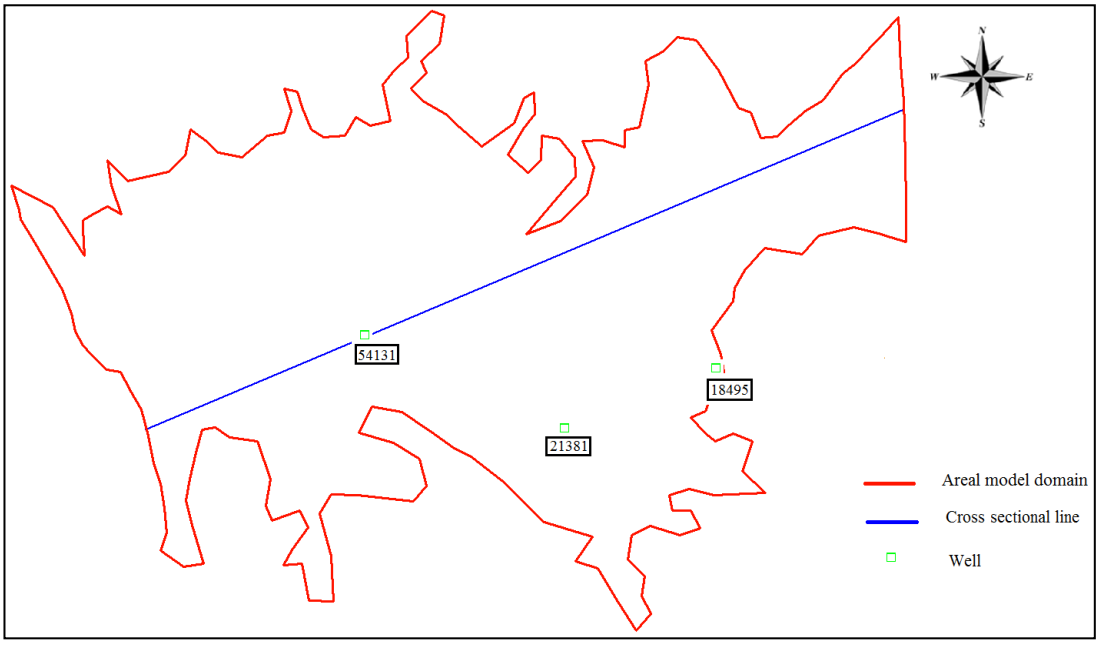

Figure 6. 1. Position of the cross sectional line

Four sets of cross sectional models were established;

- pre-pumping period cross sectional model (covering the years of pre 1976)
- pumping period cross sectional model (covering the years of 1976-2009)
- sea-regression period cross sectional model (covering the years of 1100BC-1976)
- climate controlled future period cross sectional model (covering the years of 2010-2099)

At first the pre-pumping period model was carried out in order to get the distribution of initial head and concentration values for the pumping period. Secondly, the pumping period runs were carried out between the years 1976 and 2009 in order to obtain the distribution of present head and concentration values. Thirdly, the sea-regression (historical) period runs were performed from 1100 BC to 1976 to determine the movement of the interface and position of the interface in 1976 under constant precipitation recharge conditions. Lastly, future (2010-2099) position of the interface was predicted according to the changes occur in recharge and discharge conditions under the influence of both climatic and artificial discharge effects.

Conceptual model, discretization, boundary conditions and aquifer parameters which were the same for all cross sectional models are explained below. The differences in each model are denoted separately in related sections.

6.1. Conceptual Model

The model domain covers a cross sectional area passing through the Selçuk sub-basin along SW-NE direction. Length of the section is 13600 m from seaward to landward direction. It covers Alluvium and Neogene units which were treated as a single aquifer having similar hydrogeologic properties. Depth of the model is determined as 270 m with respect to the sea level according to the data obtained from the wells 54131 and 54132, which are the only wells located on the cross sectional line. Lateral extent of the model is obtained from width of the plain area.

The model domain is under the influence of recharge through precipitation. Recharge was applied to the top section of the domain. Moreover, influx form Bayındır-Torbalı sub-basin was applied along the right boundary of the domain.

Because discharge wells are located at the southeastern boundary of the aquifer (Figure 3.13), away from the cross sectional line, discharge amounts could not be pumped out in the model from depths where well filters are present. The cross sectional line could not also be drawn passing through these wells because in this case both the observation well data location of 54131 used for the calibration would not be covered and the cross sectional line would not intersect either sea boundary or the Bayındır-Torbalı boundary where influx recharge to the aquifer occurs. Discharge values were applied to the models by projecting the locations of the discharge wells onto the cross sectional line. For this purpose top section of the model were divided into four segments (Figure 6.2). The first segment extends from Aegean Sea to the discharge area of the Cooperative II wells. In this first segment no artificial discharge occurs. The second segment covers discharge area of the Cooperative II wells. The third segment includes discharge area of the Cooperative I wells. The fourth one extends along the rest of the section from the Cooperative I wells to Bayındır-Torbalı sub-basin boundary. In this last segment also no artificial discharge occurs. Where discharge occurs, total discharge amount corresponding to that segment was subtracted from the recharge value of the segment in the models.

6.2. Discretization and Boundary Conditions

Two dimensional regular fishnet mesh, which is composed of quadrilateral finite elements, (137x31) was used to discretize the domain. 4247 nodes and 4080 elements were applied (Figure 6.2).

Four types of boundary conditions were implemented (Figure 6.2):

- Constant pressure boundary along the left vertical extend of the domain where the pressure is zero at sea level and increases with depth

- Constant flux boundary along the right vertical boundary where influx from Bayındır-Torbalı sub-basin is present
- No flow boundary along the bottom of the domain
- Variable pressure boundary due to recharge and discharge along the top of the domain

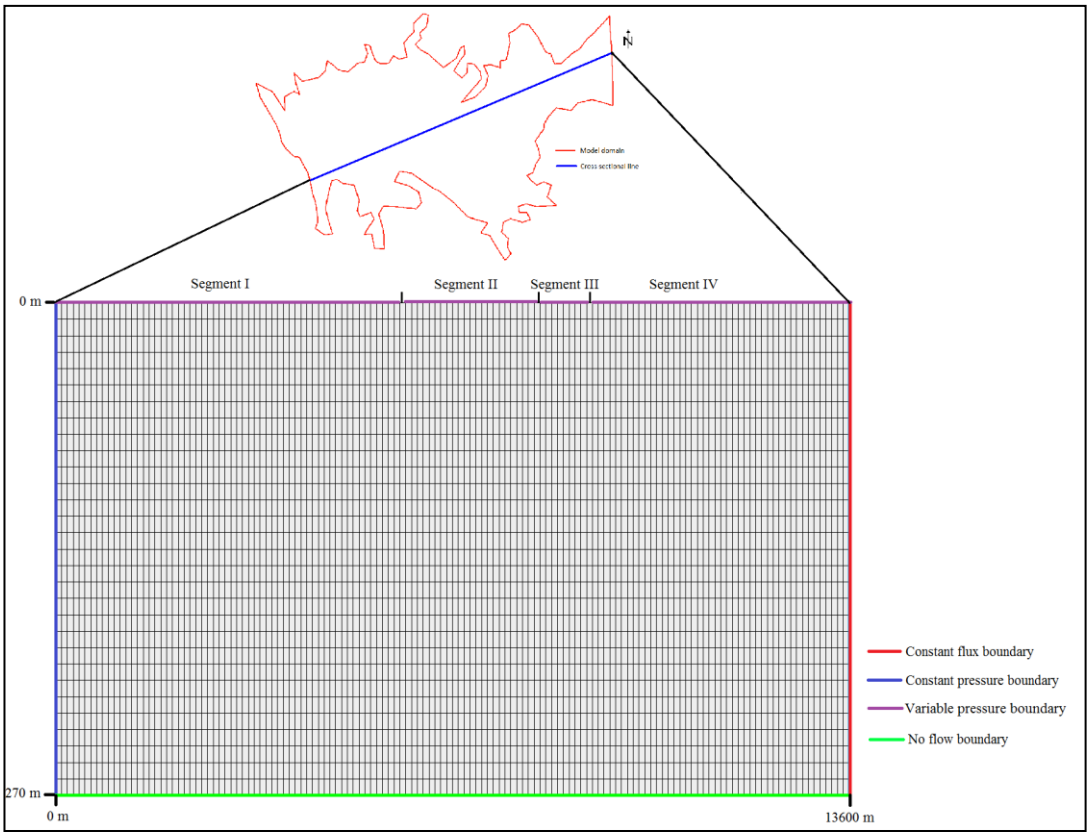

Figure 6. 2. Discretization and boundary conditions of cross sectional model

6.3. Model Parameters

The aquifer was assumed as homogeneous according to the data obtained from well 54131 and 54132, which are the only wells located on the cross sectional line.

Porosity, permeability, total recharge including recharge due to precipitation and recharge from Bayındır-Torbalı sub-basin, longitudinal and transverse dispersivities, which were chosen as minimum possible values that give stable solution, solid matrix compressibility, water compressibility, density of sea water and molecular diffusion coefficient values used in the cross sectional models is given in Table 6.1. Total recharge value of 90.2 kg/s (2.84 hm^3/year) is adapted for the period of 2003-2009 due to relatively dry conditions that occurred in the area in this period. The value was estimated based on the calibrated recharge value and precipitation relationship (for further explanation see section 6.7.1.1).

Table 6. 1. Parameters used in cross sectional models

Parameters	Value	Unit
Porosity	30	%
Permeability	$3.7x10^{-11}$	m^2
Dispersivity (longitudinal)	15	m
Dispersivity (transverse)	1.5	m
Total recharge*	103 (3.25)	kg/s (hm^3/year)
Water compressibility	$4.47x10^{-10}$	$1/kg/ms^2$
Solid matrix compressibility	$7.0x10^{-8}$	m^2/N
Molecular diffusion coefficient	$7.0x10^{-10}$	kg/m^3
Density of salt water	1025	kg/m^3

* Recharge values of the climate controlled future period model are different and given in related section.

6.4. Pre-Pumping Period Cross Sectional Model

The pre-pumping period model refers to the conditions (salt water-fresh water interface) before 1976 when there are no discharge wells that can disturb steady state conditions. The purpose of performing this model is obtaining initial head and concentration values for the pumping period cross sectional model.

Aquifer parameters mentioned above were applied to the pre-pumping period model. Transient flow run was carried out.

6.4.1. Initial conditions

In the pre-pumping period model, initial pressure and concentration were assumed as zero.

6.4.2. Calibration

Two observation wells, well no 18495 and 21381, were used for the calibration. Because there are no observation wells on the cross sectional line, observation wells of 18495 and 21381 were projected to the line considering their calibrated pressure values in the areal model. Calibrated and observed pressure and head values above sea level are given in Table 6.2.

Table 6. 2. Calibrated and observed pressure and head values

Well No	Observed Pressure (kg/ms^2)	Observed Head (m)	Calculated Pressure (kg/ms^2)	Calculated Head (m)
18495	17658	1.8	21980.13	2.2
21381	17756.1	1.81	24245.67	2.4

The pre-pumping period pressure calibration checks were also performed according to the pressure data obtained from the simulation of the areal model. Head values along the cross section, determined using the areal model, are compared with those of the pre-pumping cross sectional model in Figure 6.3. The observation wells having higher head values seen in the figure are located along the Bayındır-Torbalı sub-basin side of the cross section. Head values have an increasing trend from Aegean Sea to Bayındır-Torbalı sub-basin. Root Mean Squared Error (RMSE),

which is the square root of average of the squared differences in observed and simulated heads, was calculated for the goodness of fit.

$$RMSE = \left[\frac{1}{n}\sum_{i=1}^{n}(h_m - h_s)_i^2\right]^{0.5} \quad (6.1)$$

where;

h_m is measured (observed) head

h_s is simulated head

n is number of observations

Root Mean Squared Error determined using these data is 0.92 m. The correlation coefficient is 0.91.

The calibration of the concentration values could not be performed during pre-pumping period model runs, because there is no observation data about the concentration value in this period. Its calibration is carried out in the pumping period when data are available.

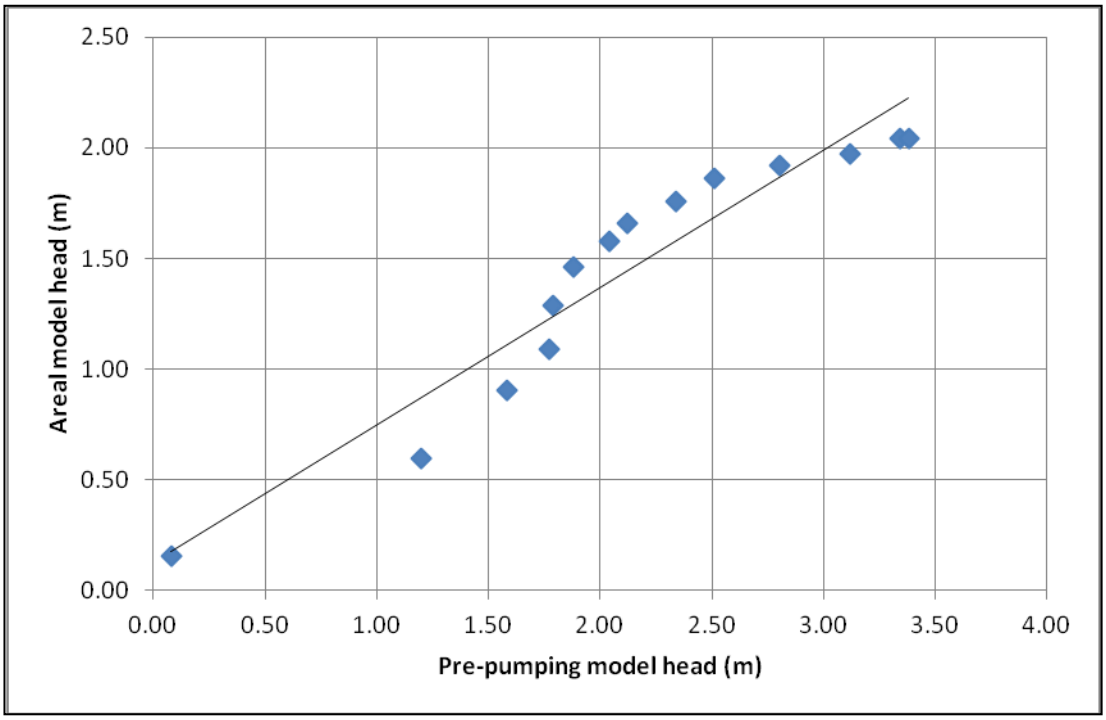

Figure 6. 3. Comparison of the areal and pre-pumping model head values along the cross section line

6.4.3. Results

Because the system is subjected to constant recharge condition, pressure and concentration changes in the system after series of continuous transient runs were found to be negligible. Pressure and concentration distributions representing steady state conditions are shown in Figures 6.4 and 6.5, respectively. The concentration distribution shown in Figure 6.5 was obtained by back calculation using the pumping period model results explained in the next section.

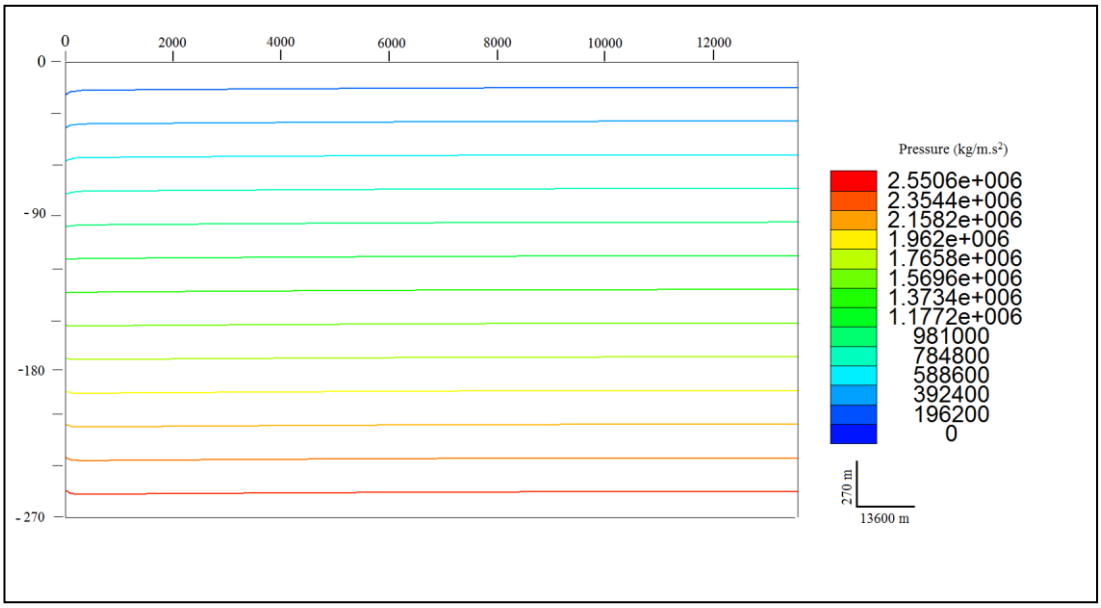

Figure 6. 4. Pressure distribution in the pre-pumping period

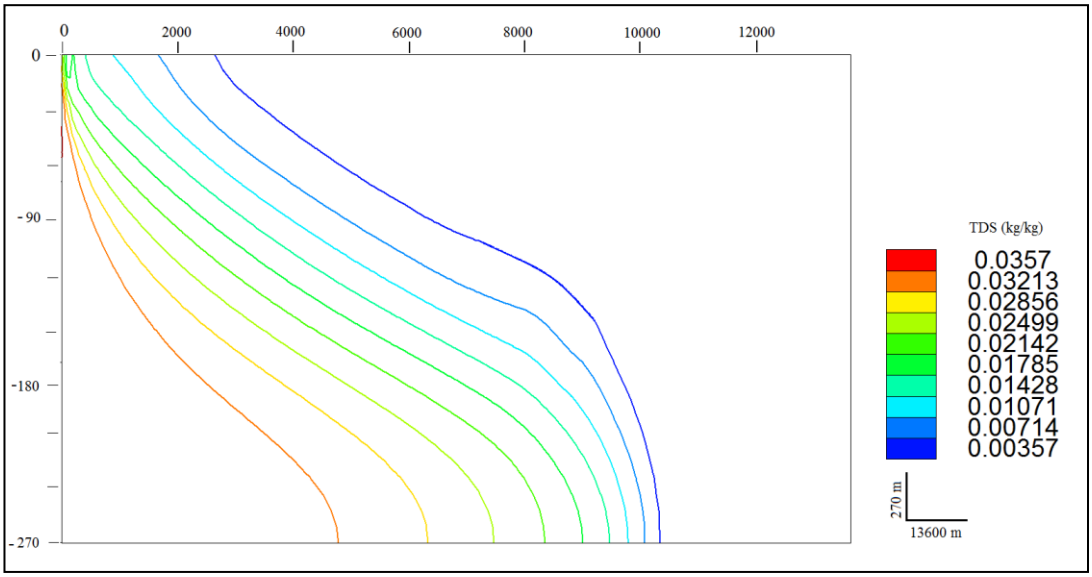

Figure 6. 5. Concentration distribution in the pre-pumping period

6.5. Pumping Period Cross Sectional Model

The pumping period cross sectional model represents the movement of the salt water-fresh water interface from 1976 to 2009 considering variations in discharge amounts. The purpose of this model is to determine pressure changes and the position of the interface at present by obtaining calibrated dispersivity values using concentration values of the observation well measured in 2002. These calibrated values and the previously determined ones (see Table 6.1) were used in the sea-regression period and future period cross sectional models. Transient flow runs were carried out.

In the pumping period simulations aquifer parameters listed in Table 6.1 were applied to the model. Discharge values used in this period were determined based on irrigation and domestic water needs supplied from two groups of wells called Cooperative I and Cooperative II where municipality wells are also present. Domestic needs were obtained from approximations based on population versus municipality discharge data in 1997 and the rate is extrapolated to the modeled years. Segment II and Segment III of the cross sectional model are subjected to the discharges from Cooperative II and Cooperative I wells, respectively. Moreover, discharge values change in different time periods. Therefore, the pumping period model was divided into five time periods. Discharge values in these periods are given in Table 6.3. These discharge values were applied to the related segments. Simulations were performed according to the discharge periods between 1976 and 2009 in monthly increments.

Table 6. 3. Discharge values in different time periods

Time Period		Discharge (kg/s)	Discharge (hm^3/year)
1st period:	1976 – 1977	42.7	1.4
2nd period:	1978 – 1988	97.7	3.1
3rd period:	1989 – 1990	143	4.5
4th period:	1991 – 2002	156.5	4.9
5th period:	2003 – 2009	172.6	5.4

6.5.1. Initial Conditions

Initial conditions for pressure and concentration were obtained from the pre-pumping period simulation results. These results were exported for each node as numerical values and imported into the 1st time period of the pumping period model. Pressure and concentration simulation results of this time period were used as initial condition for the 2nd time period. Similarly, initial conditions for the 3rd, 4th and 5th time periods were also obtained from the results of the related previous time period runs. Initial concentrations for the 1st time period were refined after each complete (covering all time periods) run until the concentration calibration was achieved.

6.5.2. Calibration

The pumping period calibrations were carried out using observation well data of 2002. Calibration of the groundwater level is performed by comparing observed and calculated values in well 54131, which is the only monitoring well in the plain area, and well 21381. Observed versus calculated pressure and head values above sea level at the end of 4th period were given in Table 6.4.

Table 6. 4. Observed and calculated head and pressure values in 2002 of the pumping period

Well No	Observed Pressure (kg/ms^2)	Observed Head (m)	Calculated Pressure (kg/ms^2)	Calculated Head (m)
54131	12262.50	1.25	18388.10	1.64
21381	14813.10	1.51	19458.20	1.56

Concentration values were calibrated using TDS values obtained from well 54131 (Figure 3.16). This well is located 4000 m inland from the sea boundary, in the first segment of the cross section. EC records of this well are converted to TDS values to perform the comparison. Figure 6.6 illustrates observed and simulated TDS values. The stepwise increase in observed TDS values was ignored due to the lack of data about aquifer parameters. The parameters were obtained from the wells 54131 and 54132, which are the only wells along the cross sectional line. Root Mean Squared Error (RMSE) determined using these data is 0.004 kg/kg. The correlation coefficient is 0.86.

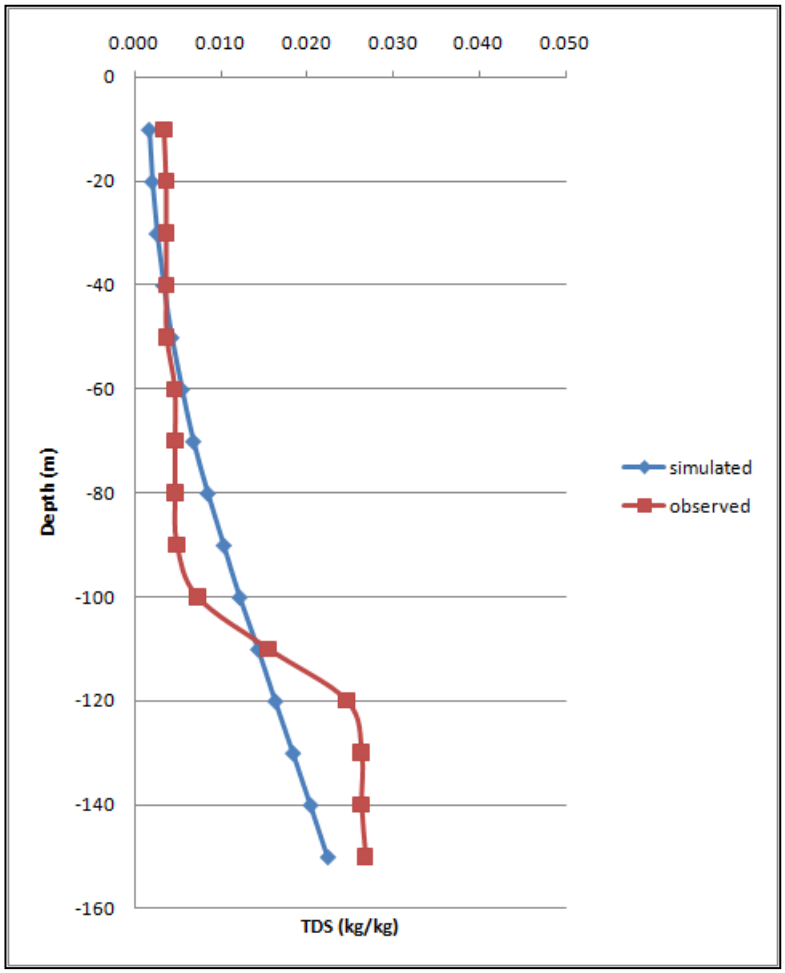

Figure 6. 6. Observed versus simulated concentrations in well 54131 for the year of 2002 in the pumping period

6.5.3. Results

Head values of the steady state condition are compared with the 2009 values in Table 6.5 for 13 observation points along the cross sectional line. These values indicate that head values decreased to 0.72 m on the average. Groundwater level in the area corresponding to Cooperative I projection in the cross section decreased from 2.47 m to 1.35 m. The value decrease is about 0.76 m for the Cooperative II projection.

Table 6. 5. Head values of steady state and 2009 in meters.

Observations	**O1**	**O2**	**O3**	**O4**	**O5**	**O6**	**O7**	**O8**	**O9**	**O10**	**O11**	**O12**	**O13**
Distance sea to landward (x 1000m)	1	2	3	4	5	6	7	8	9	10	11	12	13
Steady state	1.2	1.58	1.77	1.79	1.88	2.04	2.12	2.34	2.51	2.8	3.12	3.34	3.38
2009	0.97	1.27	1.47	1.56	1.59	1.57	1.51	1.42	1.5	1.83	1.91	1.94	1.95

Concentration distributions of five time periods are illustrated in Figure 6.7 and 6.8. TDS concentration of salt water which is 0.0357 kg/kg taken as 100 % and each concentration line in the figures was drawn using 10 % increment of TDS values. As it can seen from the figures, there is a continuous movement in the salt water-fresh water interface landward, salt water intrusion, during the pumping period. TDS value in the area corresponding to Cooperative I projection in the cross section increased from 0.0027 kg/kg to 0.0032 kg/kg at a depth of -85 m, which is the deepest well depth in the area. The value increase is 0.0003 kg/kg for the Cooperative II projection at a same depth.

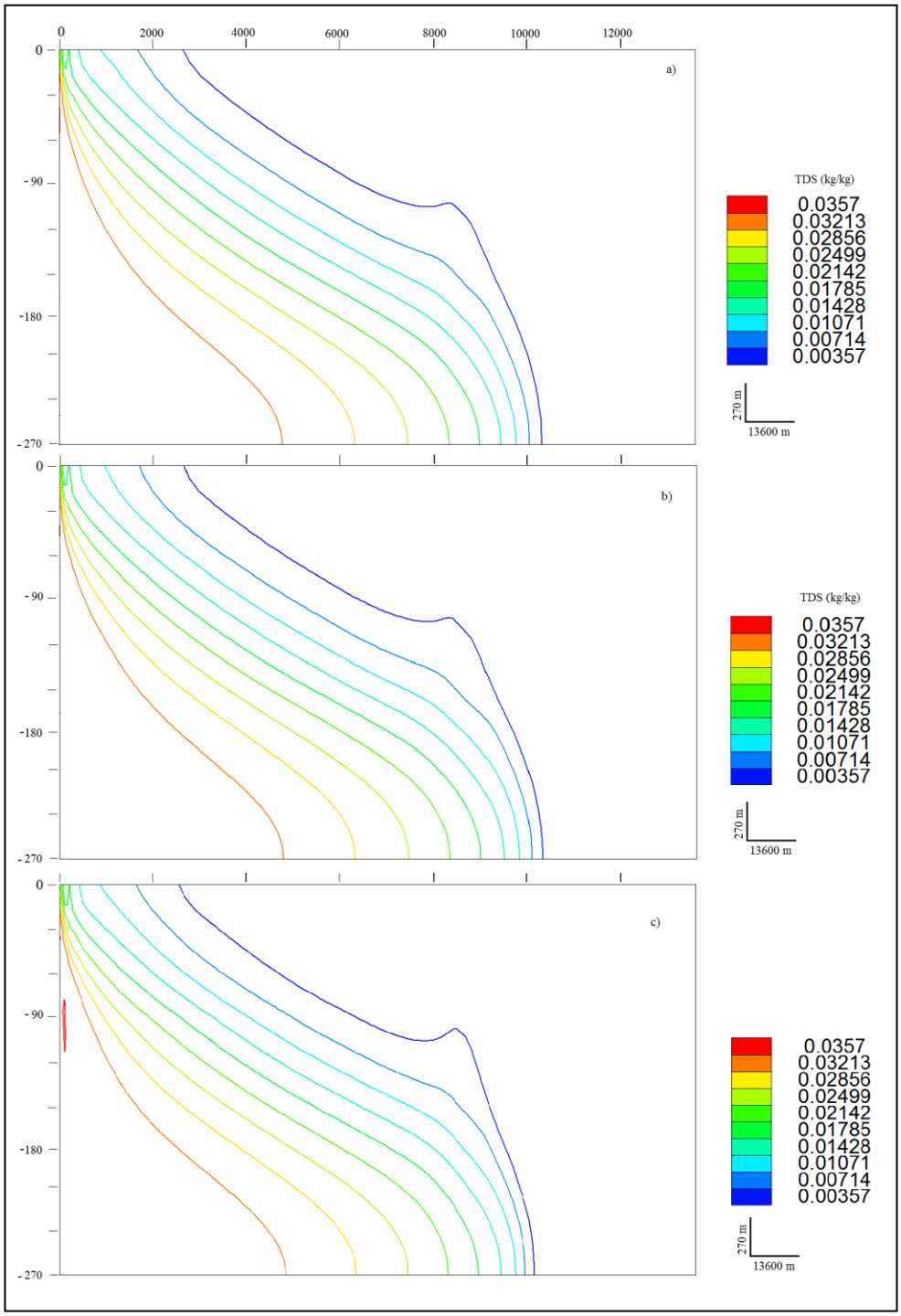

Figure 6. 7. Concentration distribution of the pumping period from 1976 to 1990 [a) 1976-1977, b) 1978-1988, c) 1989-1990]

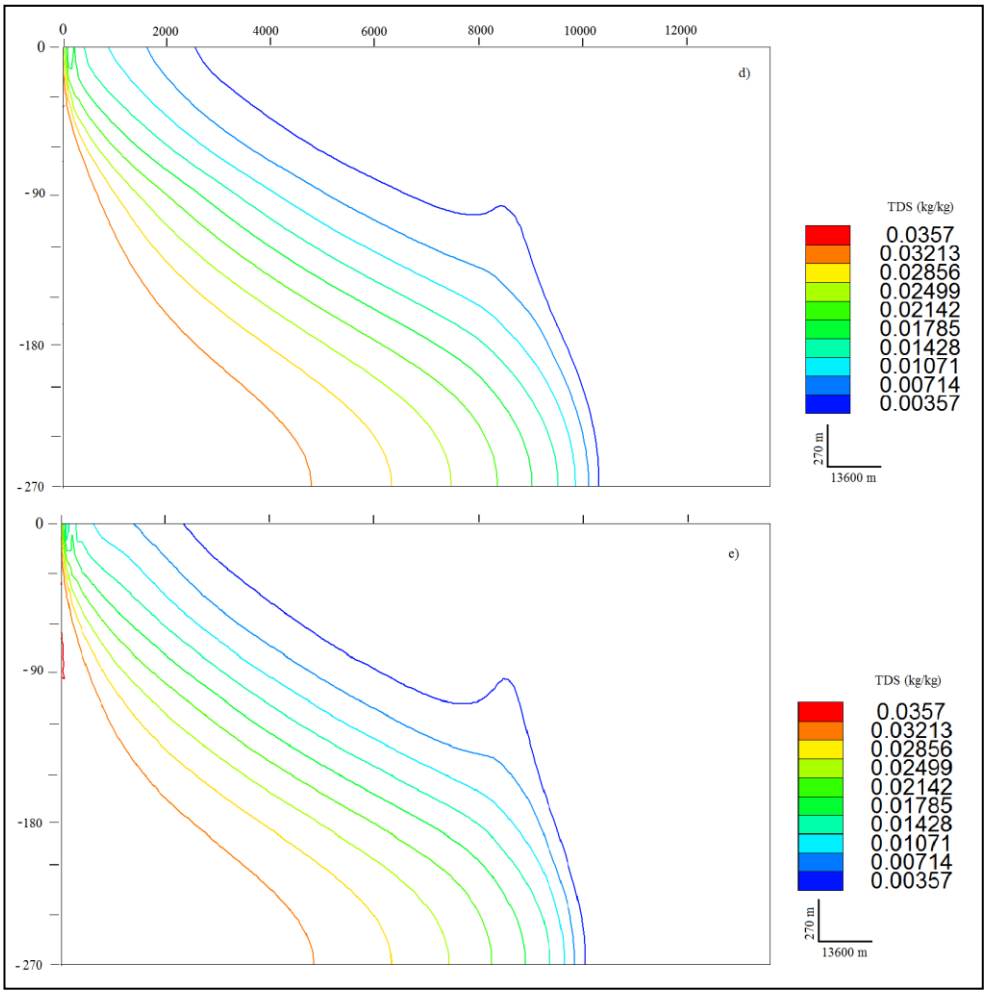

Figure 6. 8. Concentration distribution of the pumping period from 1991 to 2009 [d) 1991-2002 and e) 2003-2009]

6.6. Sea-Regression Period Cross Sectional Model

The aim of the sea-regression period cross sectional modeling is to determine the progradation of salt water-fresh water interface since 1100 BC using calibrated steady state precipitation recharge data. In other words, this model is established to predict what would be the position of the interface, if aquifer parameters and the recharge were the same as calibrated steady state conditions during the regression of sea. Position of the interface determined at the end of sea-regression period cross sectional model allows interpreting historical precipitation recharge amount to the aquifer, which is one of the controlling factors of the interface movement.

During modeling transient state flow runs were applied. The model runs were performed in five periods according to the movement data of the shoreline (Figure 6.9).

- pre-1100 BC
- from 1100 BC to 100 BC
- from 100 BC to 100 AD
- from 100 AD to 300 AD
- from 300 AD to 1976

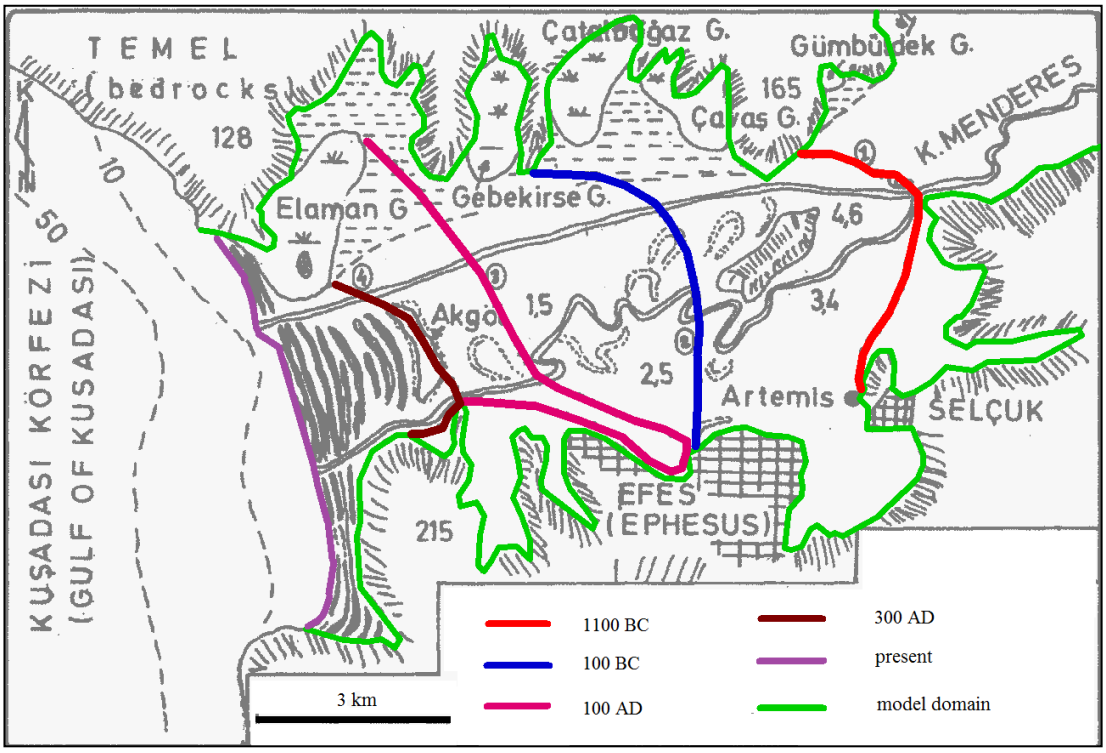

Figure 6. 9. Locations of the shorelines used in the sea-regression period model runs (modified from Gökçen et al.,1990)

6.6.1. Model Parameters

Current parameters of the aquifer that were calibrated in the previous models were used in the sea-regression period. Total recharge amount was distributed according to model domains that were applied in different periods of the sea-regression model (Table 6.6).

Table 6. 6. Precipitation recharge amounts for the sea-regression period models (for domain see Figure 6.9)

Model periods	Recharge (kg/s)	Recharge (hm^3/year)
pre-1100 BC	18.9	0.6
from 1100 BC to 100 BC	48.6	1.5
from 100 BC to 100 AD	72.9	2.3
from 100 AD to 300 AD	86.4	2.7
from 300 AD to 1976	100.0	3.2

6.6.2. Discretization and Boundary Conditions

For each sea-regression period the same spatially discretized cross sectional model domain, prepared in the pre-pumping model, was used. However, location of the constant pressure boundary was shifted according to the domain. Distances from the present shoreline to the past ones were measured and superimposed onto the cross sectional area as constant pressure boundary for a given period. In other words, sea boundary (constant pressure boundary) moved to the locations of the historical shorelines (Figure 6.10). Constant flux boundary, which represents flux from Bayındır-Torbalı sub-basin was maintained in all periods.

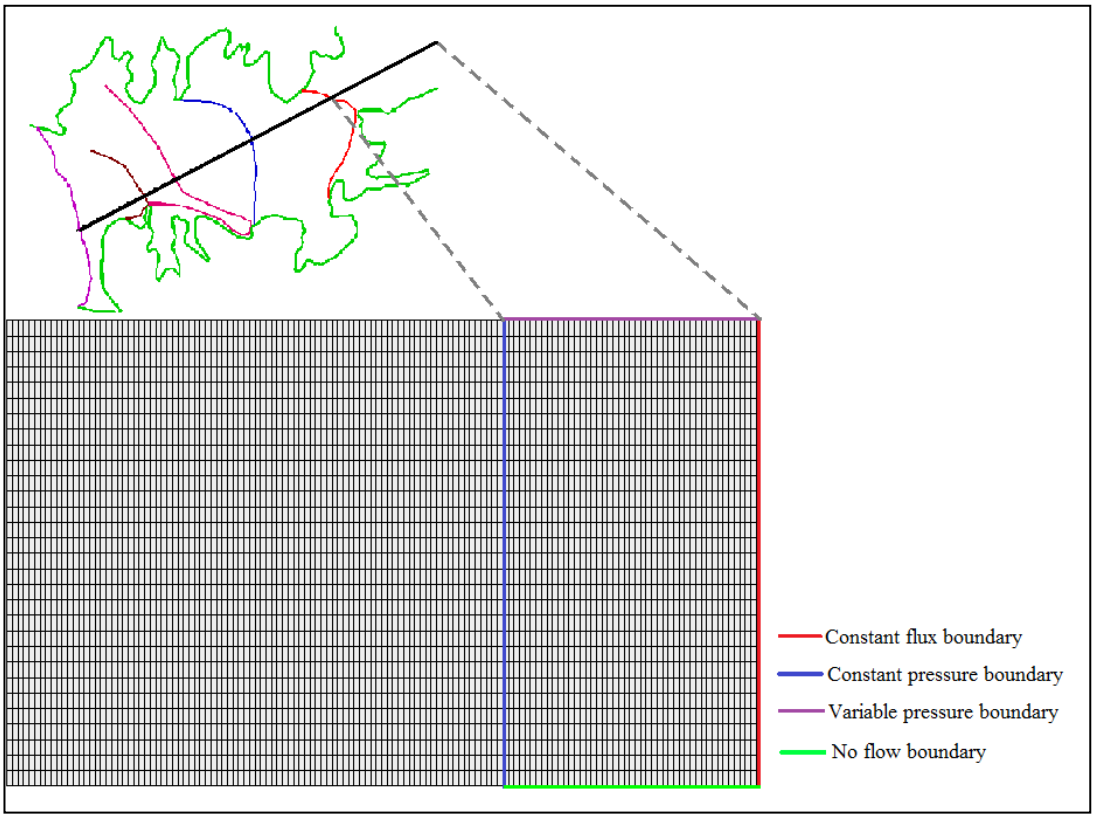

Figure 6. 10. Boundary conditions for the period of pre-1100 BC

6.6.3. Initial Conditions

Initial pressure and concentration data of each sea-regression period was obtained from simulation results of the previous ones except for the period of pre-1100 BC. For this period, the maximum possible intrusion condition (concentration distribution) was obtained by transient simulation of the model. The simulation terminated when the concentration distribution remained constant. Simulations were performed using 100 years time increment. Progradation velocity of the shoreline for each period was calculated and location of the shoreline for each 100 years time period was determined (Table 6.7).

Table 6. 7. Average progradation velocity of shoreline for each period

Period	Progradation velocity (m/year)
1100 BC - 100 BC	2.93
100 BC - 100 AD	13.55
100 AD - 300 AD	5.65
300 AD - 1976	1.29

6.6.4. Results

Head values predicted at the end of last period are compared with those of steady state (pre-pumping model results) in Table 6.8. These results suggest higher head values at the end of the sea-regression period indicating that applied recharge value to the model is high to reach the pre-pumping model results. Therefore recharge amount into the aquifer must have been less in the sea-regression period on the average.

Table 6. 8. Head values of pre-pumping period and sea-regression period in meters

Observations	O1	O2	O3	O4	O5	O6	O7	O8	O9	O10	O11	O12	O13
Distance sea to landward (x 1000m)	1	2	3	4	5	6	7	8	9	10	11	12	13
Pre-pumping	1.2	1.58	1.77	1.79	1.88	2.04	2.12	2.34	2.51	2.8	3.12	3.34	3.38
Regression	2.03	2.83	3.39	3.81	4.13	4.38	4.58	4.74	4.87	4.95	5.02	5.06	5.08

Concentration distribution predicted at the end of each period of historical runs is shown in Figure 6.11 and 6.12. The results indicate the progressive movement of the interface as a function of time. TDS values obtained at the end of the period 300 AD-1976 were compared with the pre-pumping period model concentration results at the

location of well 54131 (Figure 6.13). The results indicate that TDS values obtained after the sea-regression period model runs are less than those that are determined at the end of pre-pumping period model runs. This suggest that salt water-fresh water interface of sea-regression model should move farther inland to reach the similar position. This could be possible if less recharge amount is applied to the system as also suggested by the groundwater level results. Assuming recharge is the only possible major variable that could be subject to change in the system in the past, it could be stated that overall recharge amount in the period of 1100 BC to 1976 must have been less than that of determined (calibrated) value.

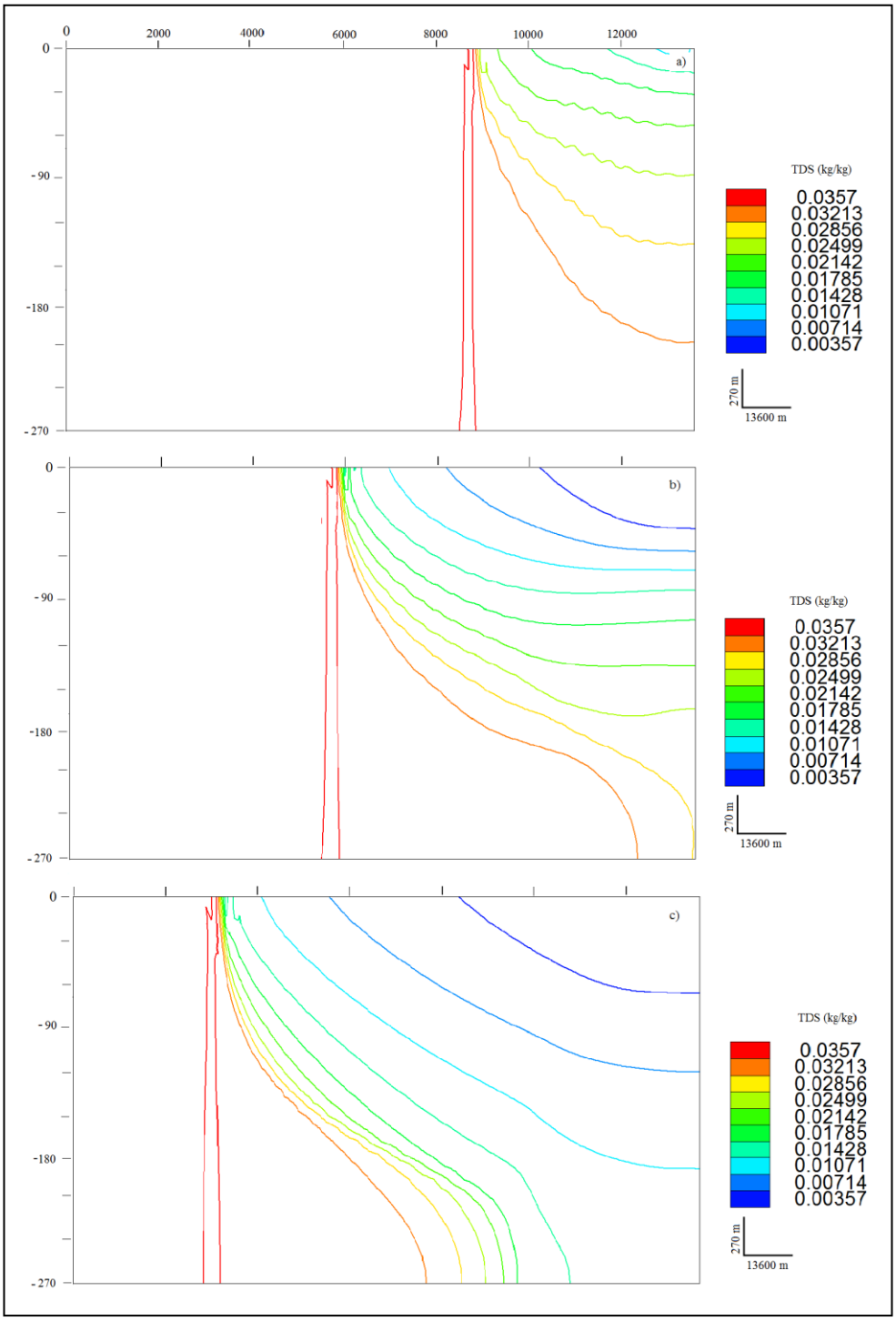

Figure 6. 11. Salt water-fresh water interface change from 1100 BC to 100 AD [a) pre-1100 BC, b) 1100 BC-100 BC, c) 100 BC-100 AD]

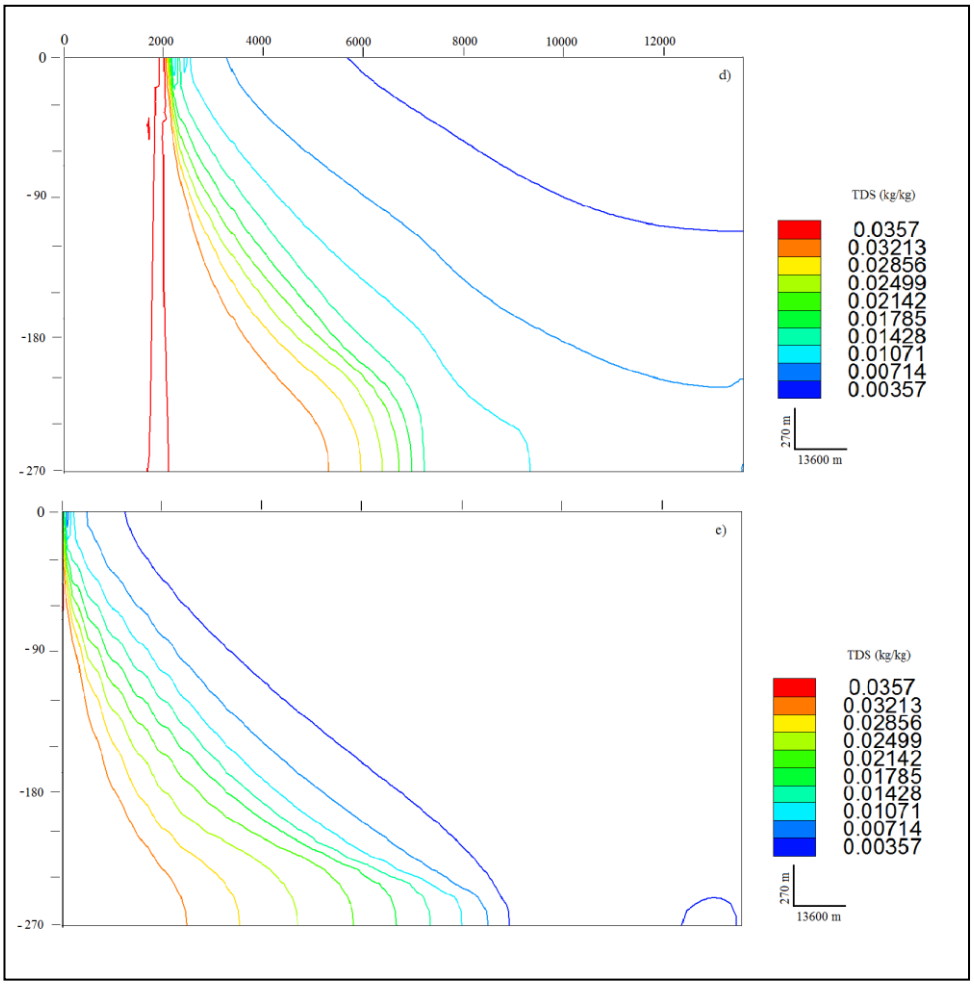

Figure 6. 12. Salt water-fresh water interface change from 100 AD to 1976 [d) 100 AD-300 AD and e) 300 AD- 1976]

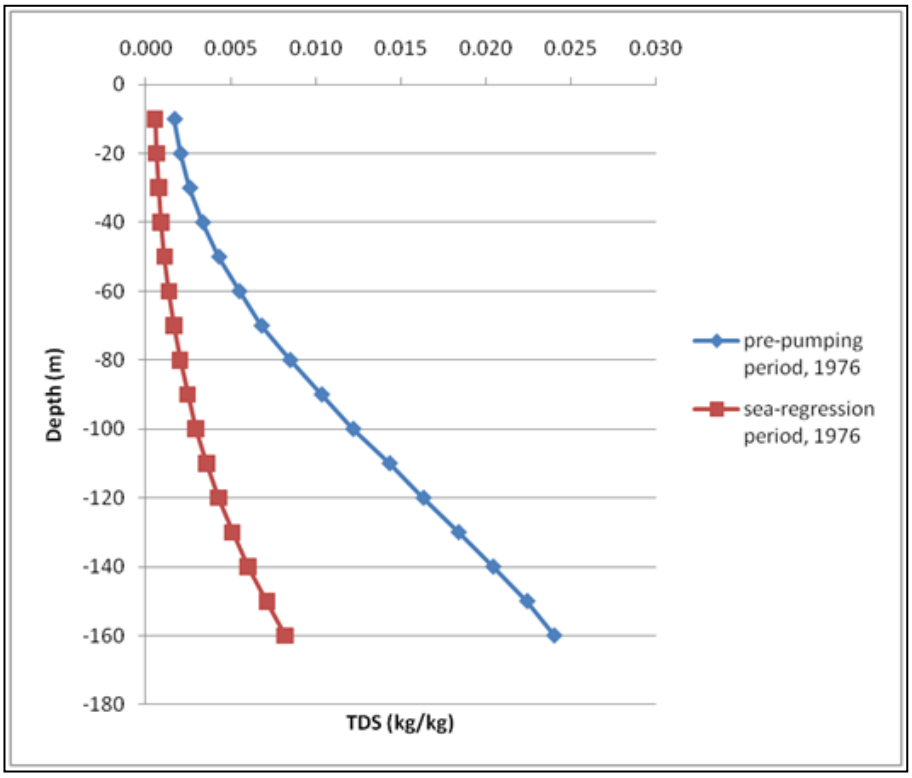

Figure 6. 13. Comparison of TDS values obtained from the sea-regression and pre-pumping period runs at the location of well 54131

6.6.5. Sensitivity Analysis

Sensitivity analysis was performed to observe the response of the model to the changes in recharge and permeability and hence, to check the reliability of the sea-regression period simulation results in terms of these calibrated values. For this purpose, sea-regression period simulations were repeated using minimum and maximum range of recharge and permeability data obtained in Selçuk sub-basin. Minimum recharge data was obtained using DSİ budget method and maximum one was determined applying hydraulic budget method (Yazıcıgil et al., 2000c). Permeability data range for alluvium and Neogene units were obtained from well log data of Selçuk sub-basin (Table 6.9).

Table 6. 9. Minimum and maximum values of permeability and recharge in Selçuk sub-basin.

	Permeability (m^2)	**Recharge (kg/s)**
Minimum	0.40E-11	145
Maximum	2.40E-11	254

Four cases were simulated by changing recharge and permeability values:

- Case I-Minimum recharge and minimum permeability
- Case II-Minimum recharge and maximum permeability
- Case III-Maximum recharge and minimum permeability
- Case IV-Maximum recharge and maximum permeability

For each case initially areal and pre-pumping models were run separately to examine if the calibration is feasible or not. Big differences between the simulated and observed head values in Case I and Case III prevent meaningful calibration (Table 6.10). The differences in the results of Case II and Case IV are relatively small and could be subject to possible further calibration procedures. Therefore, these cases were tested for the sensitivity analyses.

Table 6. 10. Observed and calculated head values (meter) for Cases I, II, III and IV.

Well No	Observed	Simulated Min. Recharge & Min. Permeability CASE I	Simulated Min. Recharge & Max. Permeability CASE II	Simulated Max. Recharge & Min. Permeability CASE III	Simulated Max. Recharge & Max. Permeability CASE IV
21381	1.80	19.74	**3.58**	32.82	**5.96**
18495	1.81	20.83	**3.77**	34.76	**6.29**

Backward approach was carried out for Cases II and IV to acquire concentration distribution in 1976 under given recharge and permeability conditions. For the application the last run pressure and concentration results of the pumping period model were used as initial values and recharge and permeability values of each Case were applied to the pumping period model. The model was run backward in time with associated discharge changes. The pre-pumping (1976) pressure and concentration distributions were determined for each Case. The sea-regression period simulations were repeated using Case II and Case IV parameters.

Sea-regression sensitivity simulation results of the Cases are shown in Figures 6.14 and 6.16. As it can be deduced from the figures that the model results are sensitive to the changes in permeability and recharge values. Salt water intrusion is greater in Case II conditions (min recharge-max permeability) in comparison to Case IV conditions (max recharge-max permeability). TDS values predicted in each case with sea-regression sensitivity runs in well location of 54131 are compared with the results of backward simulations in the same location (Figures 6.15 and 6.17). The sea-regression period TDS values are much less than those of the backward predictions in 1976 for both cases. These sensitivity run results support the deductions derived from the calibrated model runs earlier and suggesting that model results are valid in the range of maximum and minimum recharge and permeability values detected in the study area.

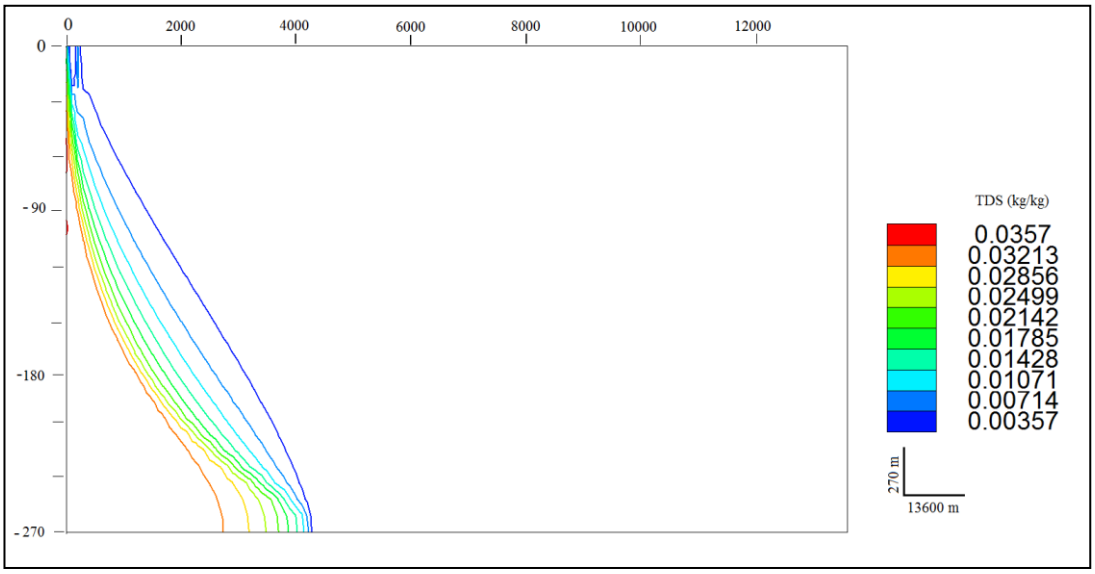

Figure 6. 14. Sea-regression period result in 1976 for Case II (min recharge-max permeability)

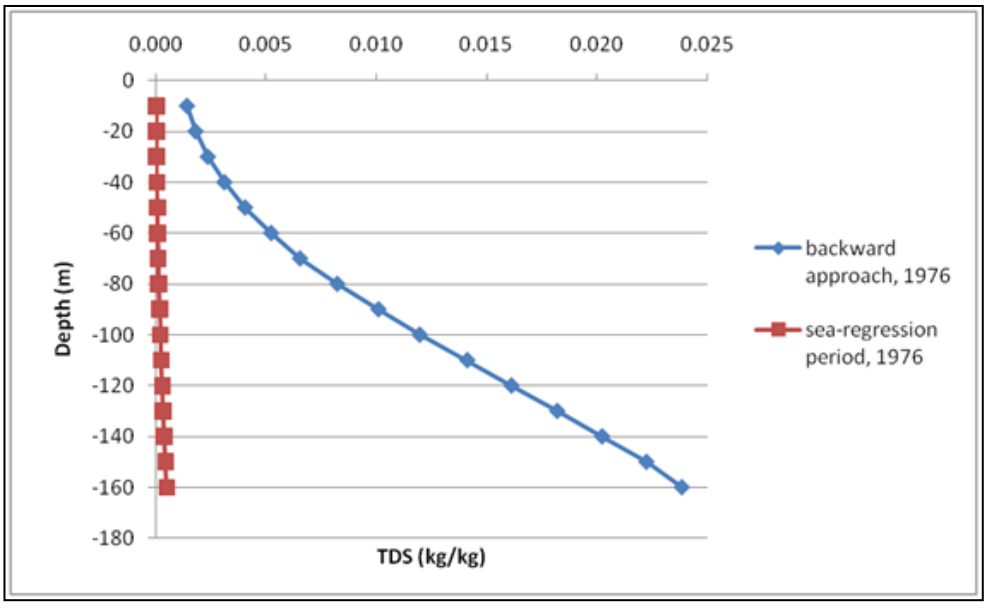

Figure 6. 15. Comparison of TDS values of Case II with those of estimated in 1976 at the location of well 54131.

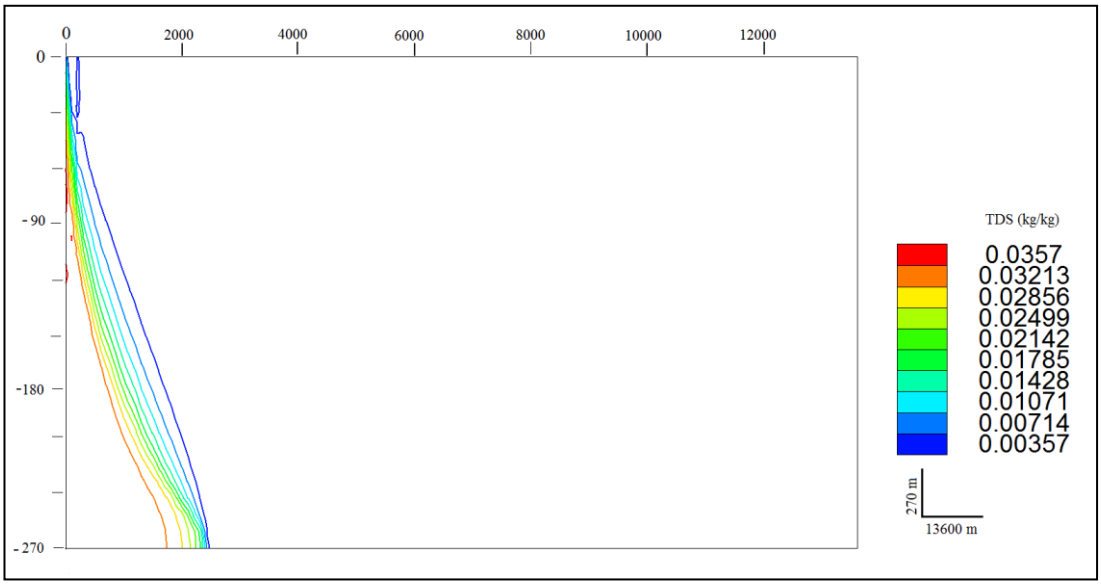

Figure 6. 16. Sea-regression period result in 1976 for Case IV (max recharge-max permeability)

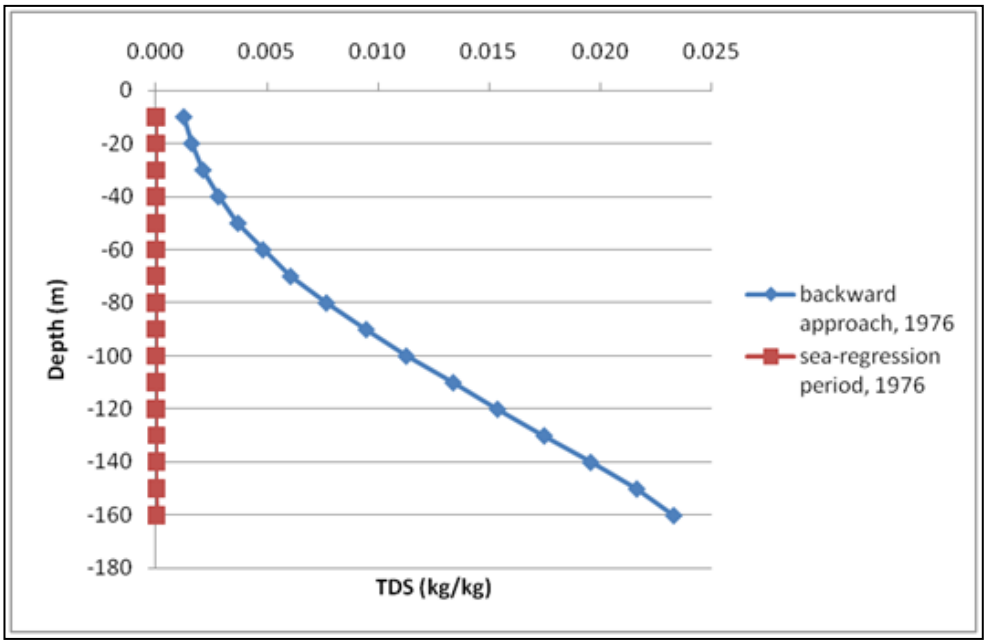

Figure 6. 17. Comparison of TDS values of Case IV with those of estimated in 1976 at the location of well 54131

6.7. Climate-Controlled Future Period Cross Sectional Model

The future period cross sectional model was established to determine head change and the future position of the interface in the aquifer under the influences of changes in climate and artificial discharges. To achieve this, estimated temperature and precipitation values published in IPCC report 2007 was used (Cruz et al., 2007). This report provides data of projections on possible increase in surface air temperature and percent change in precipitation, which are area-averaged and seasonal, for the seven sub-regions of Asia with respect to the baseline period 1961 to 1990 (Cruz, R.V., 2007). Two different models were reported by SRES (Special Report on Emission Scenarios): 1) A1FI (high future emission trajectory) and 2) B1 (low future emission trajectory). These models include pathways for three time periods, namely 2010-2039, 2040-2069 and 2070-2099 (Table 6.11). Values in the table are for the west Asia. According to these models, temperature increases continuously. As a general trend, precipitation amounts increase in autumn and summer but decrease in winter and spring in considered time duration.

Table 6. 11. Prediction of the IPCC models for future changes in temperature and precipitation (D,J,F,M,A,M,J,J,A,S,O and N refer to the first letters of the months) (see also Table 2.1)

	2010 to 2039				**2040 to 2069**				**2070 to 2099**			
Season	Temperature ^{0}C		Precipitation %		Temperature ^{0}C		Precipitation %		Temperature ^{0}C		Precipitation %	
	A1FI	B1	A1FI	B1	A1FI	B1	A1FI	B1	A1FI	B1	A1FI	B1
DJF	1.26	1.06	-3	-4	3.1	2	-3	-5	5.1	2.8	-11	-4
MAM	1.29	1.24	-3	-8	3.2	2.2	-8	-9	5.6	3	-25	-11
JJA	1.55	1.53	13	5	3.7	2.5	13	20	6.3	2.7	32	13
SON	1.48	1.35	18	13	3.6	2.2	27	29	5.7	3.2	52	25

In order to simulate climate controlled future location of the salt water-fresh water interface in the study area, three periods were studied using transient state flow runs;

- from 2010 to 2039
- from 2040 to 2069
- from 2070 to 2099

Possible sea level rise conditions in the study area are not included in the model.

6.7.1. Model Parameters

6.7.1.1. Recharge

The baseline temperature and precipitation averages of the sub-basin were determined using the data of 1964-1990 to be consistent with the IPCC data range (Figure 6.18). These baseline values were then decreased or increased according to the predictions in IPCC report for each period for the calculation of future temperature and precipitation amounts in the study area (Tables 6.12 and 6.13). The estimated future temperature and precipitation values were used for the future recharge determinations.

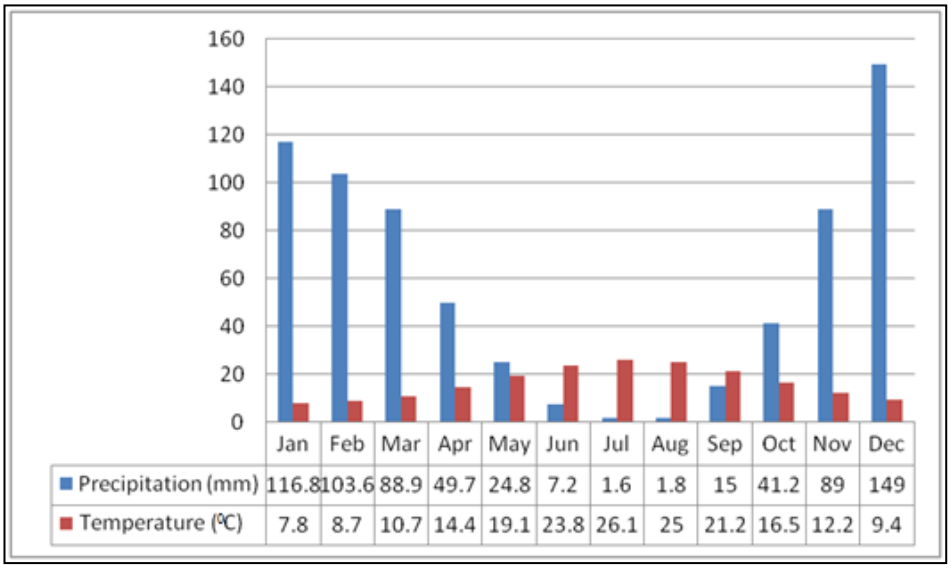

Figure 6. 18. Average (1964-1990) precipitation and temperature data of Selçuk Sub-basin.

Table 6. 12. Estimated mean future precipitation and temperature values for A1FI model

	Jan	Feb	Mar	Apr	May	Jun	Jul	Aug	Sep	Oct	Nov	Dec
Precipitation (mm)												
2010-2039	113.3	100.5	87.1	48.7	24.3	8.1	1.8	2.0	17.7	48.6	105.0	145.0
2040-2069	113.3	100.5	81.8	45.7	22.8	8.1	1.8	2.0	19.1	52.3	113.0	145.0
2070-2099	104.0	92.2	66.7	37.3	18.6	9.5	2.1	2.4	22.8	62.6	135.3	133.0
Temperature (^{0}C)												
2010-2039	9.1	10.0	12.0	15.7	20.4	25.4	27.7	26.6	22.7	18.0	13.7	10.7
2040-2069	10.9	11.8	13.9	17.6	22.3	27.5	29.8	28.7	24.8	20.1	15.8	12.5
2070-2099	12.9	13.8	16.3	20.0	24.7	30.1	32.4	31.3	26.9	22.2	17.9	14.5

Table 6. 13. Estimated mean future precipitation and temperature values for B1 model

	Jan	Feb	Mar	Apr	May	Jun	Jul	Aug	Sep	Oct	Nov	Dec
Precipitation (mm)												
2010-2039	112.1	99.5	81.8	45.7	22.8	7.6	1.7	1.9	17.0	46.6	100.6	143.0
2040-2069	111.0	98.4	80.9	45.2	22.6	8.6	1.9	2.2	19.4	53.1	114.8	141.6
2070-2099	112.1	99.5	79.1	44.2	22.1	8.1	1.8	2.0	18.8	51.5	111.3	143.0
Temperature (^{0}C)												
2010-2039	8.9	9.8	11.9	15.6	20.3	25.3	27.6	26.5	22.6	17.9	13.6	10.5
2040-2069	9.8	10.7	12.9	16.6	21.3	26.3	28.6	27.5	23.4	18.7	14.4	11.4
2070-2099	10.6	11.5	13.7	17.4	22.1	26.5	28.8	27.7	24.4	19.7	15.4	12.2

A computer program was developed to calculate annual recharge values considering the changes in temperature and precipitation between the years of 2010 and 2099. The recharge calculations were performed using Thornthwaite method where soil moisture storage and surface runoff coefficient were taken respectively as 100 mm and 0.1 representing sandy soil flat areas (Haan et al., 1994). The recharge which was estimated in millimeters was converted to kg/s using the model area of 71.8 km^2

for the considered periods. Because calculated values with this method were unexpectedly high, the ratio (6.4) between the calculated 2002 recharge value (using above methodology) and the model calibrated 2002 recharge value was used to estimate the future period recharges from the calculated values. Precipitation recharge value estimations are listed in Table 6.14.

Table 6. 14. Annual recharge values for three future time periods

	2010-2039 Recharge (hm^3/year)	**2040-2069 Recharge (hm^3/year)**	**2070-2099 Recharge (hm^3/year)**
A1FI	3.12	3.01	2.63
B1	2.98	3.02	2.91

6.7.1.2. Discharge

Future discharge from the aquifer was calculated by considering the increase in population. Population increase was determined for each modeling period using population projection method of TÜİK (Turkish Statistical Institute). Water usage per person ($1.1x\ 10^{-4}$ hm^3/year) was taken similar to the pumping period calculations. Water need for the irrigation was assumed to be constant (Table 6.15).

Table 6. 15. Discharge value for time periods

	2010-2039	**2040-2069**	**2070-2099**
Discharge (hm^3/year)	5.86	6.54	7.35

The aquifer parameters were those that estimated and used in the pumping period model. The boundary conditions are the same as those of the pumping period model as well.

6.7.2. Initial Conditions

Each model initial pressure and concentration values were those that were obtained from the previous period runs.

6.7.3. Results

Comparison of head values obtained at the end of last time period with those of 2009 indicates that the values decreased about 0.85 m on the average (Table 6.16). According to these values maximum head change is seen in A1FI model. Groundwater level in the area corresponding to Cooperative I projection in the cross section decreased from 1.35 m to -0.02 m according to A1FI model. The maximum value decrease is 1.18 m for the Cooperative II projection.

Table 6. 16. Comparison of head values in 2009 and in 2099 for both A1FI and B1 models (in meters).

Observations	**O1**	**O2**	**O3**	**O4**	**O5**	**O6**	**O7**	**O8**	**O9**	**O10**	**O11**	**O12**	**O13**
Distance sea to landward (x 1000m)	1	2	3	4	5	6	7	8	9	10	11	12	13
Pumping-2009	0.97	1.27	1.47	1.56	1.59	1.57	1.51	1.42	1.5	1.83	1.91	1.94	1.95
A1FI - 2099	0.69	0.86	0.91	0.88	0.78	0.61	0.42	0.19	0.19	0.61	0.80	0.85	0.86
B1 - 2099	0.72	0.92	0.99	0.97	0.89	0.73	0.55	0.33	0.34	0.76	0.95	1.00	1.02

Concentration distributions in the salt water-fresh water interface predicted according to B1 and A1FI climatic model results for each period are shown in Figures 6.19, 6.20 and 6.21. Concentration results of B1 and A1FI model prediction inputs show similar distributions in a given period. The results suggest that salt water-fresh water interface moves landward. However this movement is mostly due to increasing discharge amount rather than that of climatic changes because overall average recharge decrease is 5.6 % for B1 model and 7.6 % for A1FI model but discharge increase is about 20.9 % in the next 90 years.

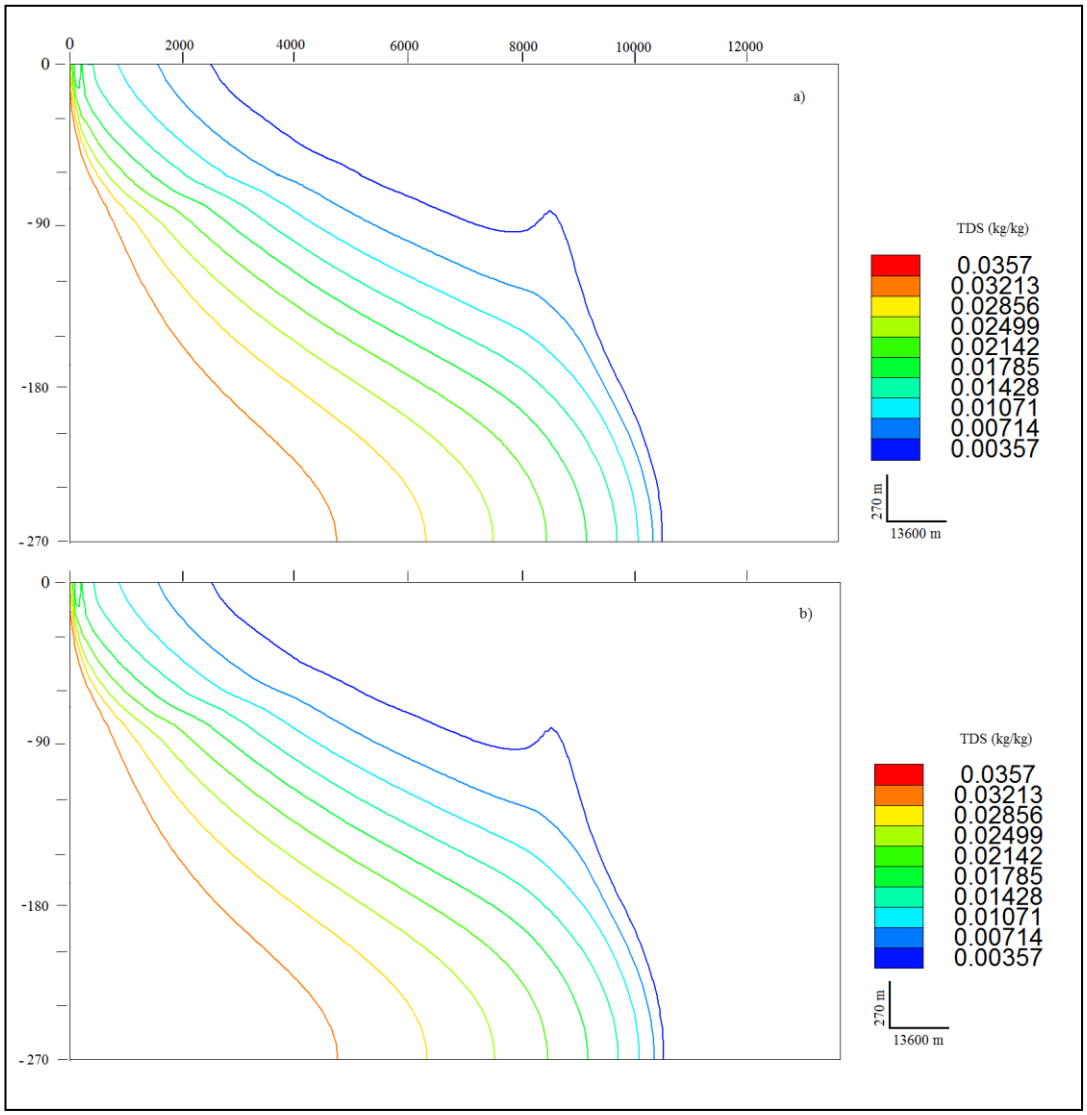

Figure 6. 19. Concentration distribution at the end of the period 2010-2039 [a) A1FI model and b) B1 model]

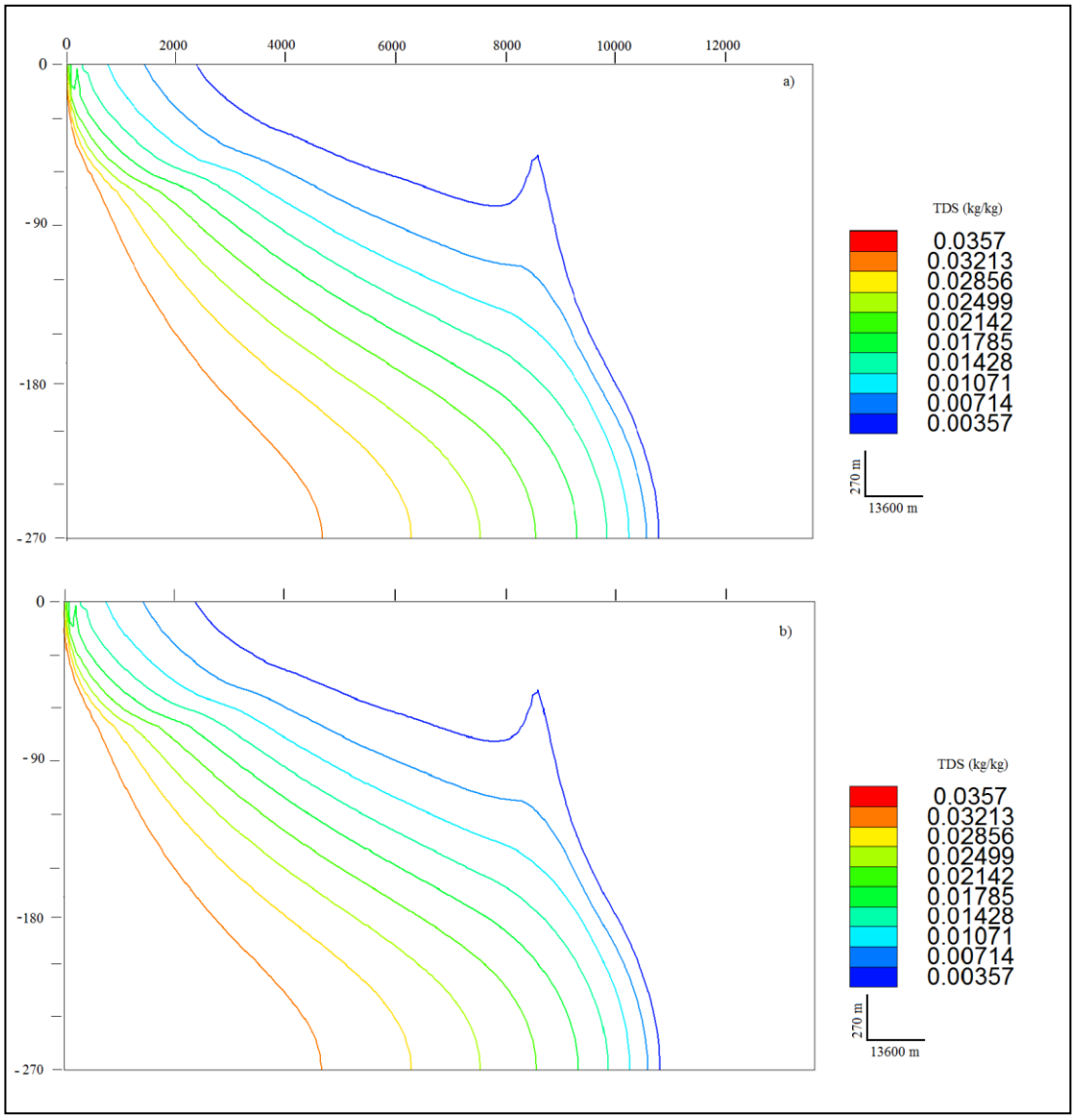

Figure 6. 20. Concentration distribution at the end of the period 2039-2069 [a) A1FI model and b) B1 model]

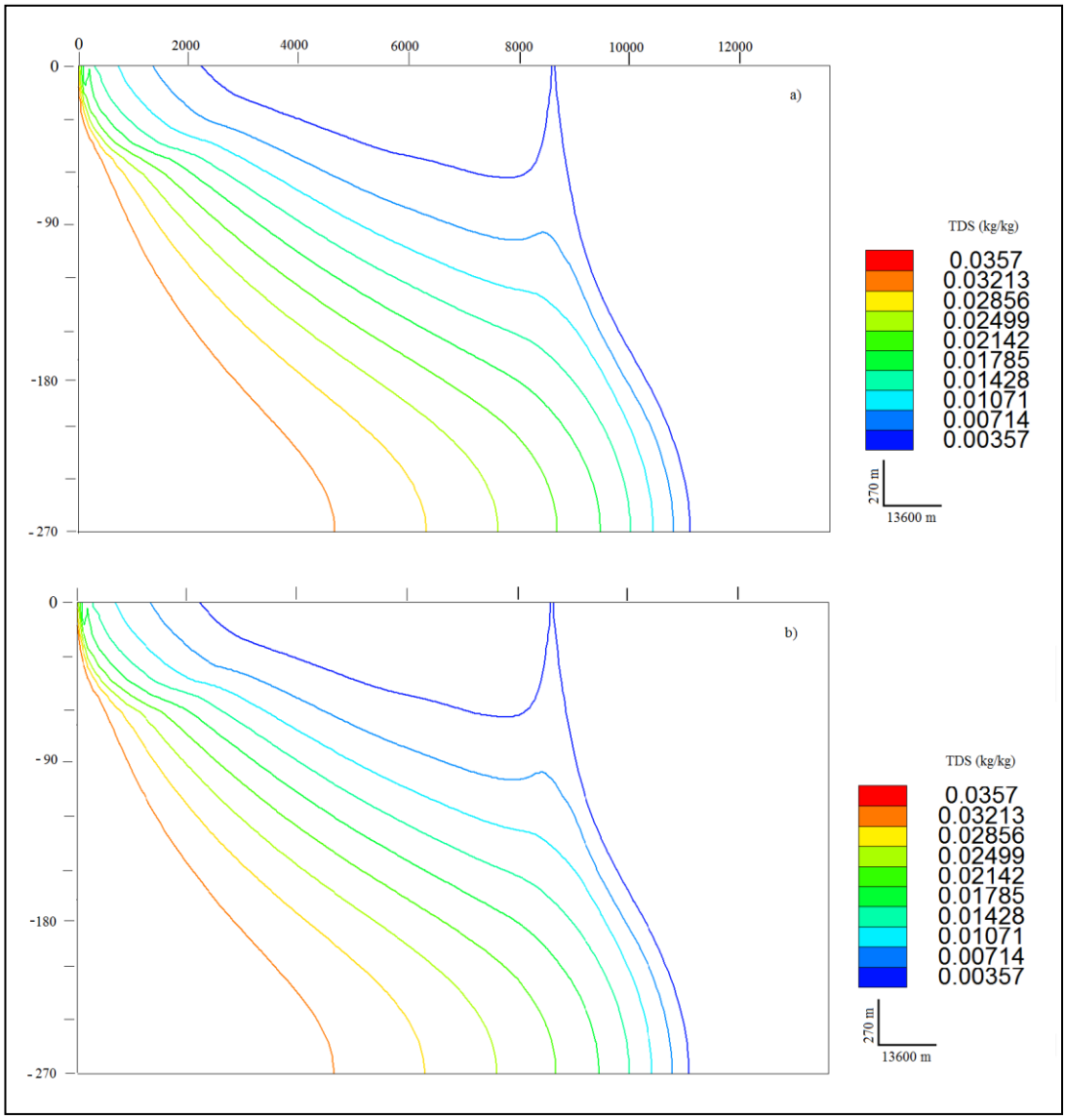

Figure 6. 21. Concentration distribution at the end of the period 2069-2099 [a) A1FI model and b) B1 model]

Concentration results of the future period model based on B1 and A1FI climatic inputs were contoured in Figure 6.22 and Figure 6.23, respectively, as a function of depth and time for the areas corresponding to the projections of the Cooperative I and II wells on the cross sectional line. Concentrations increase as a function of increasing time due to farther salt water intrusion in the areas of irrigation and domestic water supply wells. TDS value in the area corresponding to Cooperative I projection in the cross section increased from 0.0032 kg/kg to 0.0061 kg/kg at a depth of -85 m, which is the deepest well depth in the area. The value increase is 0.0037 kg/kg for the Cooperative II projection.

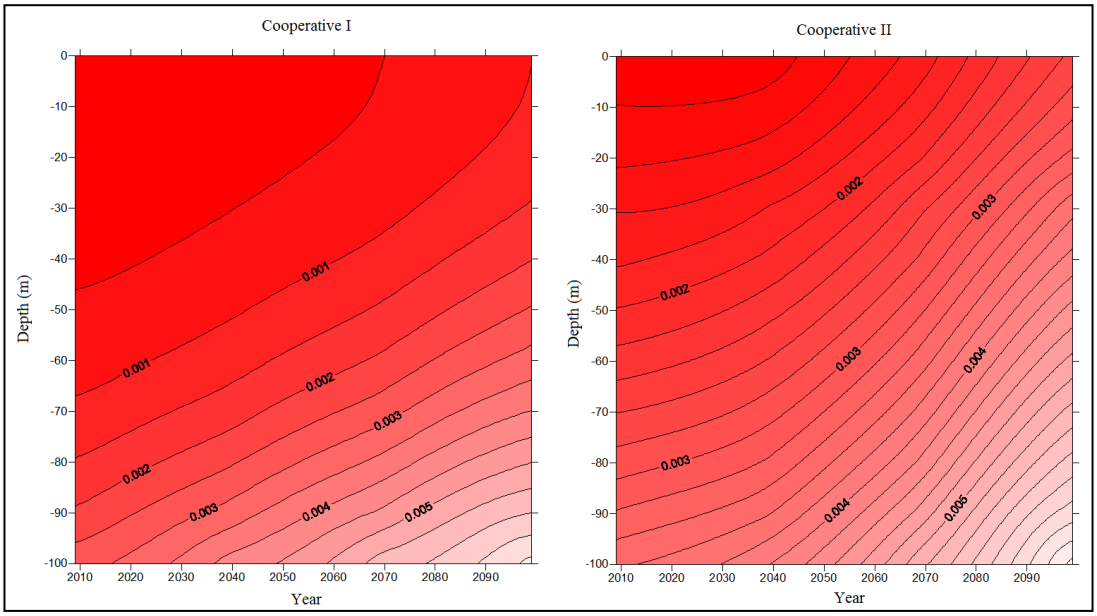

Figure 6. 22. Concentration (kg/kg) distribution in pumping areas of Cooperative I and II according to A1FI model

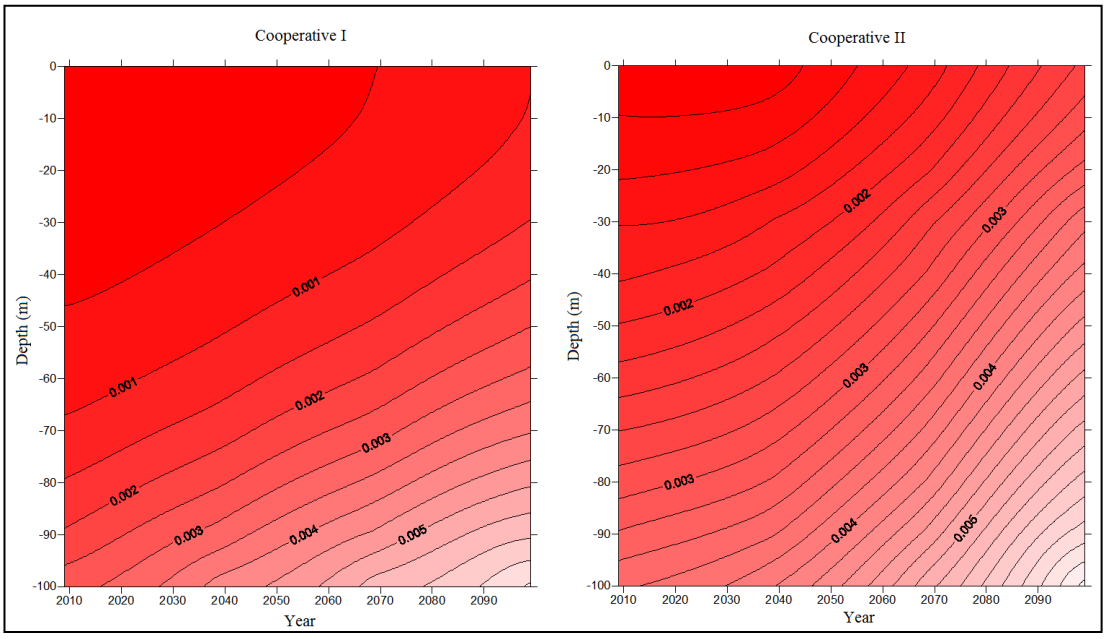

Figure 6. 23. Concentration (kg/kg) distribution in pumping areas of Cooperative I and II according to B1 model

CHAPTER 7

RESULTS AND DISCUSSION

After calibrating hydraulic properties of the aquifer, pressure and concentration distributions of the steady state and present conditions were successfully simulated in Selçuk sub-basin using the density dependent cross sectional groundwater flow with solute transport models. Groundwater level in the area corresponding to Cooperative I projection in the cross section decreased from 2.47 m to 1.35 m from steady state to the present time. The value decrease is 0.76 m for the Cooperative II projection. TDS value in the area corresponding to Cooperative I projection in the cross section increased from 0.0027 kg/kg to 0.0032 kg/kg at a depth of -85 m, which is the deepest well depth in the area. The value increase is 0.0003 kg/kg for the Cooperative II projection. These simulations are based on the following assumptions. Alluvium and Neogene units are treated as a single aquifer with uniform hydraulic properties. This assumption is justified by one available well data which penetrates both of these units. Bottom elevation of the aquifer (-270 m) is also based on this single well data. Head values of only two available observation wells were used for the pressure calibration in the cross sectional model. In addition, concentration results were calibrated using data of one well, which is the only well having depth related EC measurements. Because density of Aegean Sea is slightly less than 1025 kg/m^3, it should be kept in mind that slightly greater intrusion conditions were simulated in the model results. But this is believed to be within acceptable error limits associated with the model parameters in general. As a matter of fact, the difference between the calibrated head results of Çamur and Yazıcıgil (2005), who used 1016 kg/m^3 of density in their three dimensional model, and those of this study

is about 60 cm for the pre-pumping period and 12 cm for the pumping period. Calibrated concentration distribution pattern of 2002 at the observation point in both models are comparable. These comparisons also validate the discharge application procedure applied in the model.

Stepwise historical sea-regression model simulations (1100 BC-1976) based on 1976 values predicted less degree of salt water intrusion than that of currently detected in the area. Because only possible major controlling factor that could be different in the past to affect the position of the interface is precipitation recharge amount, it is interpreted that overall recharge amount in the last 3076 years must have been less than that of the calibrated pre-pumping period. How could this result be related to the past climatic conditions?

Precipitation, evaporation, soil moisture and surface runoff are the major factors that control precipitation recharge. Groundwater recharge would decrease due to the exceeded infiltration capacity of soil under high rainfall conditions in humid areas. However in semi-arid and arid areas increased rainfall may increase recharge because only high-intensity rainfalls can infiltrate fast enough before evaporating. Higher temperatures will cause higher evaporation and plant transpiration rate and thus, soils will dry. This will lead to higher losses of soil moisture and groundwater recharge in hot and arid areas (BGR, 2008). Alluvial aquifers may mainly recharged by floods in semi-arid areas (Al-Sefry et al., 2004). Therefore, in a given area, precipitation amount/regime and temperature are the two main controlling agents of precipitation recharge. In order to obtain information about precipitation and temperature conditions in the past in comparison to pre-pumping period, progradation rate data and climatic indications are need to be evaluated.

Progradation rates in the sub-basin indicate that the rate of 1100 BC-100 BC period was increased sharply from about 3 m/year to 14 m/year between 100 BC and 100 AD. Then, it was decreased to 6 m/year in the period of 100 AD-300 AD and to 1.3 m/year between 300 AD and 1976 AD. As stated by Eisma (1978), the rate changes

could have caused by 1) fluctuations in relative sea-level driven either by eustatic sea-level changes or by tectonic movements; 2) historical changes in regional climate and/or soil erosion either of which could bring the valley infill as well as the subsequent erosion; and 3) local circumstances: the delta while growing seawards, gradually reached deeper and more exposed open water, with stronger currents and waves, which may have slowed down delta-progression. The sub-basin subsidence associated with faults in the graben would create greater gradient conditions hence could increase the rate. However, there is no sufficient data to show that this is the main rate controlling factor in the area. Rapid acceleration of the rate corresponds to the period of relatively extensive colonization. Therefore, decreasing delta growth rate could be an after-effect of soil erosion: when most of the available soil has been removed, there is little left on the nearly bare slopes to be transported, while the process of soil formation is far too slow to supply as much sediment as was transported when the soils were being eroded. Eisma (1978) also suggest that local factors also played a role during Middle Ages when the river has reached deeper and more open waters. In summary, tectonic events, vegetation removal driven soil erosion and local factors or combination of these in addition to historical changes in climatic conditions are the effects that caused progradation rate changes in the sub-basin. Therefore, the progradation rate data cannot be used to obtain historical changes in climatic conditions of the sub-basin due to limited data.

There is no basin-specific data about historical changes in climatic conditions. On the basis of vegetation, human activity, lake levels, sea levels, drainage, dendroclimatological and meteorological data following relatively dry and wet periods are reported for Minor Asia by several workers (Gassner and Christiansen-Weniger 1948; Butzer 1958; Butzer 1959; Beug, 1967; Eisma 1978; Erinç 1978): Drier periods; 2400 BC-850 BC, early 900 AD, 1770-73 AD, 1779-82 AD, 1799-1803 AD, 1819-22 AD, 1845 AD, 1853 AD, 1873-74 AD, 1882 AD, 1890-92 AD, 1894 AD, 1898-1900 AD, 1916-18 AD, 1927-30 AD. Moister cold periods; 800 AD-1000 AD, 950 AD-1400 AD, 1600 AD-1680 AD, 1720 AD, 1740 AD, 1800 AD,

1810 AD, 1850 AD and 1875 AD-1880 AD. There is no comprehensive tree ring-based data about the study area. The results of tree ring-based reconstruction of central European precipitation (April-May-June) and temperature (June-July-August) variability over past 2500 years by Büntgen et al. (2011) is shown in Figure 7.1. In general, April-May-June precipitation exhibits increasing trends in the periods of 300 BC-100 BC, 300 AD-450 AD and 550 AD-750 AD and decreasing trends in the periods of 100 BC-300 AD, 450 AD-550 AD. The precipitation change is about 50 mm in the range from 250 mm to 150 mm. The precipitations are nearly constant at about 200 mm in the oscillation range between 1000 AD and 2000 AD. Overall, 550 years of increase, 500 years of decrease and 1000 years of steady conditions are indicated for precipitation. Summer temperatures are slightly high in the period of 500 BC-300 AD and low in the period of 650 AD-1980 AD. There is sharp decrease between 300 AD and 550 AD and sharp increase since 1980. The temperature change is about +/- 1.5^{o}C on the average, excluding the period of 300 AD-550 AD. Overall, 800 years of high and 1330 years of low conditions are indicated for temperature. Because latitude of the central Europe (about 50^{o}) is higher than that of Selçuk sub-basin (38^{o}) and the basin is bordered by sea on the contrary to the Central Europe, it is highly questionable to extrapolate the results of historical precipitation and temperature conditions of Central Europe to the sub-basin. In any case, the results suggest that in the last 1000 years precipitation and temperature values are nearly steady within the oscillation range except that there is a sharp increase in temperature in the last 30 years.

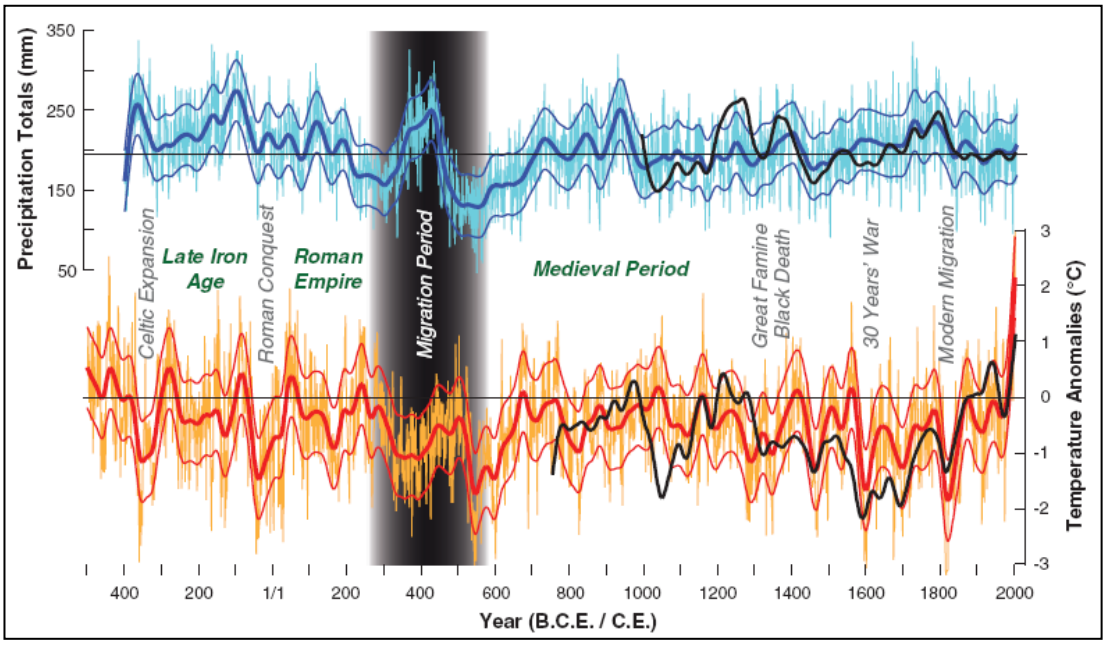

Figure 7. 1. Reconstructed April-June precipitation totals and June-August temperature anomalies. (Black lines show independent precipitation and temperature reconstructions from Germany and Switzerland. Bold lines are 60-year low-pass filters.) (Büntgen et al., 2011)

The data about historical climatic changes in the study area are insufficient to come to any definite conclusions in terms of precipitation and temperature distributions. If dominantly humid climatic conditions existed in the sub-basin in the past, relatively higher precipitation and cooler temperature conditions could have decreased the groundwater recharge at steeper gradient areas of the sub-basin due to the exceeded infiltration capacity of soil. Surface runoffs would be directed toward relatively flat alluvial areas. This would prepare greater recharge conditions for the alluvial aquifer. On the other hand, if dominantly semi-arid climatic conditions existed, relatively lower precipitation and higher temperature conditions in the past could have decreased the groundwater recharge as implied by the results of historical sea-regression model simulations. Available data in general indicate that drier climatic conditions were operative at longer period of time in Asia Minor in the past. However there is no in-depth data to support or rebut this deduction.

In addition to these, it should be kept in mind that during sea-regression period possible permeability changes are ignored because of unavailable data. Furthermore, it was assumed that the Küçük Menderes River had no flow relation with the aquifer during the sea-regression period.

Future model simulations (2010-2099) based on changing climatic scenarios indicate that salt water-fresh water interface moves farther landward. However this movement is mostly due to increasing discharge amount rather than that of climatic changes because overall average recharge decrease is in the range of 5.6% - 7.6 % but discharge increase is about 20.9 % in the next 90 years. Nevertheless, head values decrease 0.85 m with respect to present levels. Maximum head change is seen in A1FI model. Groundwater level in the area corresponding to Cooperative I projection in the cross section decreased from 1.35 m to – 0.02 m according to A1FI model. The value decrease is 1.18 m for the Cooperative II projection. TDS value in the area corresponding to Cooperative I projection in the cross section increased from 0.0032 kg/kg to 0.0061 kg/kg at a depth of -85 m, which is the deepest well depth in the area. The value increase is 0.0037 kg/kg for the Cooperative II projection. Following assumptions are associated with the results of future model. Because no climate change prediction data were found for the Aegean Region, the data covering relatively large region (west Asia) including Aegean Region were used for the future model predictions. In addition, agricultural and industrial needs were hold constant. Moreover, potential seawater rise related transgression that could occur in the next 90 years was not incorporated into the model due to the lack of data. But none of these assumptions could have drastic effects on the deduced results. Potential effects of transgression would be farther movement of the interface landward and related aquifer contamination in the sub-basin. Increasing water need for agriculture and industry would decrease head values and the interface would move farther landward.

CHAPTER 8

CONCLUSIONS AND RECOMMENDATIONS

8.1. Conclusions

The pumping period (1976-2009) modeling;

- Groundwater level in the area corresponding to Cooperative I projection in the cross section decreased from 2.47 m to 1.35 m from steady state to the present time.
- The head value decrease for the Cooperative II projection is 0.76 m.
- TDS value in the area corresponding to Cooperative I projection in the cross section increased from 0.0027 kg/kg to 0.0032 kg/kg at a depth of -85 m, which is the deepest well depth in the area.
- The increase in TDS value for the Cooperative II projection is 0.0003 kg/kg.

The historical sea-regression period (1100 BC-1976) modeling;

- Head values predicted at the end of last period are 1.92 m higher than those of steady state (pre-pumping model) results on the average indicating that less precipitation recharge conditions must have existed in the past.
- TDS values obtained after the sea-regression period model runs are less than those that are determined at the end of pre-pumping period model runs, suggesting less degree of salt water intrusion than that of detected for 1976 in the area. It also indicates that less precipitation recharge conditions must have existed in the past.

- Sea-regression period model results are sensitive to the changes in permeability and recharge values.
- The sensitivity run results support the deductions derived from the calibrated sea-regression period model runs.

The climate-controlled future period (2010 BC-2099) modeling;

- Maximum head change is seen in A1FI model.
- Groundwater level in the area corresponding to Cooperative I projection in the cross section decreased from 1.35 m to -0.02 m according to A1FI model.
- The head value decrease for the Cooperative II projection is 1.18 m.
- Concentrations increase as a function of increasing time due to farther salt water intrusion in the areas of irrigation and domestic water supply wells.
- TDS value in the area corresponding to Cooperative I projection in the cross section increased from 0.0032 kg/kg to 0.0061 kg/kg at a depth of -85 m, which is the deepest well depth in the area.
- TDS value increase for the Cooperative II projection is 0.0037 kg/kg.
- The results suggest that salt water-fresh water interface moves landward.
- Increasing discharge effects have greater control than climatic effects on the interface movement.

8.2. Recommendations

The progress of the study indicated that more researches should be done in the study area to get more data about the aquifer properties. Especially, more information about hydraulic conductivity and electrical conductivity along the cross sectional line was needed for the accuracy of the head and concentration calibrations.

Moreover, possible permeability changes and the flow relation between Küçük Menderes River and the aquifer during the regression of the sea should be studied in detail to analyze the sea-regression period better.

Furthermore, during the climate-controlled future period simulations, there should be more detailed climate change predictions for Aegean Region including Selçuk sub-basin. Possible variations in the location of the shoreline in the next 100 years should be known to get more accurate results about the position of the salt water-fresh water interface in the future. Besides, changes in the future water need for irrigation and industry can easily affect the model results.

In addition to these, results of the climate-controlled future period model indicate that salt water intrusion increases in the pumping areas. Therefore, locations of these wells should be moved to the east of the aquifer towards Bayındır-Torbalı sub-basin.

REFERENCES

Al-Sefry S.A., Al-Ghamdi S.A., Al-Ashi W.A., Al-Bardi W.A. (2004). Strategic ground water storage of Wadi Fatimah, Makkah region. Technical Report SGS-TR-2003-2. Saudi Geological Survey, p. 168

Bear J., Cheng A.H.-D. (2010). *Modeling groundwater flow and contaminant transport*. New York: Springer, p. 29

Bear J., Verruijt A. (1987). *Modeling groundwater flow and pollution: Theory and applications of transport in porous media*. Netherlands: D. Reidel Publishing Company, p.196

Behringer W. (2010). A Cultural History of Climate. Cambridge: Polity Press. p.15

Beug H. J. (1967) Contributions to the post glacial vegetational history of northern Turkey. Quaternary Paleoecology. Proc. VII Congress Int. Assoc. Quat. Res. 7, 349-356.

Bundesanstalt für Geowissenschaften und Rohstoffe (BGR) (2008). Groundwater and climate change: Challenges and possibilities. In: Hetzel F., Vaessen V., Himmelsbach T., Struckmeier W., Villholth K.G. (Eds.), p. 5

Butzer K. W. (1958) Quaternary stratigraphy and climate in the Near East. Bonner Geogr. Abh. Volume 24, 1-157

Butzer K. W. (1959) Contributions to the Pleistocene geology of the Nile valley. Erdkunde. Volume 13, 46-67

Büntgen U., Tegel W., Nicolussi K., McCormick, Frank D., Trouet V., Kaplan J.O., Herzig F., Heussner K.U., Wanner H., Luterbacher J., Esper J. (2011). 2500 years of European climate variability and human susceptibility. Science. Vol. 331, 578-582

Cooper H. H. (1959). A hypothesis concerning the dynamic balance of fresh water and salt water in a coastal aquifer. Journal of Geophysical Research. Vol. 64, No. 4, 461–467

Cruz R.V., Harasawa H., Lal M., Wu S., Anokhin Y., Punsalmaa B., Honda Y., Jafari M., Li C., Huu Ninh N. (2007). Asia. Climate change 2007: Impacts, adaptation and vulnerability, contribution of working group II to the fourth assessment report of the Intergovernmental Panel on Climate Change. In: Parry M.L., Canziani O.F. (Eds.) Cambridge, UK: Cambridge University Press, p. 24

Çamur M.Z., Yazıcıgil H. (2005). Effects of the planed Ephesus recreational canal on fresh water-sea water interface in the Selçuk sub-basin, İzmir-Turkey. Environmental Geology. Vol 48, 229-237

DSİ (1973). Küçük Menderes Ovası Hidrojeolojik Etüt Raporu, DSİ Genel Müdürlüğü, Jeoteknik Hizmetler ve Yeraltısuları Dairesi Başkanlığı, Ankara, 64 pp.

Eisma D. (1978) Stream deposition and erosion by the eastern shore of the Aegean. In: W.C. Brice (Ed.). London: Academic Press, 68-81

Erinç S. (1978). Changes in the physical environment in Turkey since the end of the last Glacial. The environment history of the Near and Middle East since the last Ice Age. In: W.C. Brice (Ed.). London: Academic Press, 87-110

Freeze R.A., Cherry J.A. (1979). Groundwater. Englewood Cliffs, N.J.: Prentice-Hall, 604 pp.

Garbrecht J.D., Piechota T.C. (2006). Water resources and climate. *Climate variations, climate change, and water resource engineering*. In: Garbrecht J.D., Piechota T.C. (Eds.). Virginia: American Society of Civil Engineers, p. 22

Gassner G., Christiansen-Weniger, F. (1948) Dendroclimatological studies on the annual growth rings of Anatolian pines. Orman Genel Müdürlüğü Yayınları, Ankara, pp. 58

Glover R.E. (1959). The pattern of fresh-water flow in coastal aquifer. Journal of Geophysical Research. Vol. 64, No. 4, 457-459

Gökçen S.L., Kazancı N., Yaşar D., Gökçen N., Bayhan E. (1990). Küçük Menderes delta kompleksi ve gelişiminde tektonizma etkileri. Türkiye Jeoloji Bülteni. Cilt:33, 15-29

Guo, W., and Langevin, C.D. (2002) User's guide to SEAWAT: A computer program for simulation of three-dimensional variable-density ground-water flow: Techniques of Water-Resources Investigations of the U.S. Geological Survey, Book 6, Chapter A7. Virginia: USGS.

Gündoğdu A., (2000). Groundwater recharge estimation for Küçük Menderes River Basin aquifer system. M.Sc. Thesis, January 2000. Middle East Technical University. 181 pp.

Haan C.T., Barfield B.J., Hayes J.C. (1994). *Design hydrology and sedimentology for small catchments.* California: Academic Press, Inc, p. 84

Hardy J.T. (2003). *Climate change: causes, effects, and solutions*. England: John Willey & Sons. Ltd, pp. 23, 77

Hassan A. (2004). Numerical modeling of seawater- fresh groundwater relationship in the Selçuk Sub-basin, İzmir-Turkey. M.Sc. Thesis, January 2004. Middle East Technical University, 67 pp.

Henry H.R. (1959). Salt intrusion into fresh-water aquifers. Journal of Geophysical Research. Vol. 64. No. 11, 1911-1919

Holzbecher E. (1998). *Modeling density-driven flow in porous media: principles, numerics, software*. Germany: Springer, 1-9

IPCC (1990). *Climate change: IPCC scientific assessment*. In: Houghton, J.T., Jenkins G.J. and Ephraums J.J. (Eds.). Cambridge, UK: Cambridge University Press, 365 pp.

IPCC. (2001). *Appendix I – Glossary*. *Climate change 2001: the scientific basis: contribution of Working Group I to the Third Assessment Report of the Intergovernmental Panel on Climate Change*. In: Houghton, J.T., Theodore J., (Eds.). Cambridge, UK: Cambridge University Press.

IPCC. (2001). *Technical Summary*. *Climate change 2001: the scientific basis: contribution of Working Group I to the Third Assessment Report of the Intergovernmental Panel on Climate Change*. In: Houghton, J.T., Theodore J. (Eds.) Cambridge, UK: Cambridge University Press, p. 24

Kiehl J. and Trenberth K. (1997). Earth's annual global mean energy budget. Bull. Am. Meteorol. Soc. Vol. 78, 197-206

Koch M. and Zhang G. (1998). Numerical modeling and management of saltwater seepage from coastal brackish canals in southeast Florida. In: Environmental Coastal Regions, Brebbia C.A. (Ed.) Southampton: WIT Press. 395-404

Kohout F.A. (1960). Cyclic flow of salt water in the Biscayne aquifer of southeastern Florida: Journal of Geophysical Research. Vol. 65, No. 7, 2133-2141

Kraft J.C., Aschenbrenner S.E., Rapp G. (1977). Paleogeographic reconstructions of coastal Aegean archaeological sites. Science, New Series. Vol. 195, No. 4282, 941-947

Mandle R.J. (2002). Groundwater modeling guidance. Groundwater modeling program. Michigan Department of Environmental Quality, 54 pp.

Merritt M.L. (1994). A rewetting approximation for a simulator of flow in a surficial aquifer overlain by seasonally inundated wetland: Ground Water, 32 (2), 286-292.

National Research Council. Board on Global Change. Commission on Geoscienses, Environment, and Resources (1994). *Solar influence on global change*. Washington D.C.: National Academy Press, p. 23

Nippon. (1996). The study on Küçük Menderes River Basin irrigation project in the Republic of Turkey, Final Report: Vol I: Main Report, Vol II: Annexes, Volume III: Drawings. Nippon Koei Con., Ltd.-Nippon Giken Inc.

Parliament of Australia, http://www.aph.gov.au/library/pubs/climatechange/whyclimate/naturalClimate/reflectivity.htm, last visited on February 2011.

Peck A.J., Allison G.B. (1988). Ground water and salinity response to climate change. *Greenhouse: planning and climate change*. In: Pearman G.I. (Ed.). Australia: CSIRO Publications, p. 241

Reilly T.E., Goodman A.S. (1985). Quantitative analysis of salt water-fresh water relationships in groundwater systems-a historical perspective. Journal of Hydrology. No.80, 125-160

Rosenzweig C.,Casassa G., Karoly D.J., Imenson I., Liu C., Menzel A.,Rawlins S., Root T.L., Seguin B., Tryjanowski P., (2007). Assessment of observed changes and responses in natural and management systems. *Climate Change: 2007: Adaptation and Vulnerability. Contribution of Working Group II to the Fourth Assesment Report of Intergovernmental Panel on Climate Change*. In: Parry M.L. (Ed.). Cambridge: Cambridge University Press, pp. 185, 480

Voss C.I. (1984). A finite element simulation model for saturated-unsaturated, fluid-density-dependent ground-water flow with energy transport or chemically-reactive single-species solute transport. Virginia: USGS

Voss A. and Koch M. (2001). Numerical simulations of topography-induced saltwater upconing in the state of Brandenburg, Germany. Physics and Chemistry of the Earth (B). 26. 353-359

Voss C.I., Provost A.M. (2010). SUTRA: A model for saturated-unsaturated, variable-density ground-water flow with solute or energy transport. Water Resources Investigation Report 02-4231. Virginia: USGS, p. 1

Yazıcıgil H. (2000a). *Revize hidrojeolojik etütler kapsamında Küçük Menderes Havzası yeraltısularının incelenmesi ve yönetimi. Cilt-I: Ana Rapor*. Ankara: Orta Doğu Teknik Üniversitesi

Yazıcıgil H., Toprak V., Rojay B., Süzen L.,Yılmaz K. (2000b). *Revize hidrojeolojik etütler kapsamında Küçük Menderes Havzası yeraltısularının incelenmesi ve yönetimi.* Cilt-III: Jeoloji. Ankara: Orta Doğu Teknik Üniversitesi

Yazıcıgil H., Karahanoğlu N., Yılmaz K., Gündoğdu A., Şakıyan J., Yeşilnacar E., Tuzcu B. (2000c). *Revize hidrojeolojik etütler kapsamında Küçük Menderes Havzası yeraltısularının incelenmesi ve yönetimi.* Cilt-IV: Hidrojeoloji. Ankara: Orta Doğu Teknik Üniversitesi

Younes A., Ackerer Ph., Mose R. (1999). Modeling variable density flow and solute transport in porous medium: 2. Re-evaluation of salt dome flow problem. Transport in Porous Media. No. 35. Netherlands: Kluwer Academic Publishers, 375-394